INFORMATION TO USERS

UNIVERSITY OF ALBERTA

**CRYOPRESERVATION
OF
PORCINE HEART VALVES**

By

GENE YEL CHAN

A thesis submitted to the Faculty of Graduate Studies and Research in partial

fulfillment of the requirements for the degree of Master of Science

In

Experimental Pathology

Department of Laboratory Medicine and Pathology

Edmonton, Alberta

Spring 2001

The author has granted a non-exclusive licence allowing the National Library of Canada to reproduce, loan, distribute or sell copies of this thesis in microform, paper or electronic formats.

The author retains ownership of the copyright in this thesis. Neither the thesis nor substantial extracts from it may be printed or otherwise reproduced without the author's permission.

L'auteur a accordé une licence non exclusive permettant à la Bibliothèque nationale du Canada de reproduire, prêter, distribuer ou vendre des copies de cette thèse sous la forme de microfiche/film, de reproduction sur papier ou sur format électronique.

L'auteur conserve la propriété du droit d'auteur qui protège cette thèse. Ni la thèse ni des extraits substantiels de celle-ci ne doivent être imprimés ou autrement reproduits sans son autorisation.

0-612-60420-9

Canada

UNIVERSITY OF ALBERTA

LIBRARY RELEASE FORM

Name of Author: **Gene Yel Chan**

Title of Thesis: **Cryopreservation of Porcine Heart Valves**

Degree: **Master of Science**

Year this Degree Granted: **2001**

Permission is hereby granted to the University of Alberta Library to reproduce single copies of this thesis and to lend or sell such copies for private, scholarly, or scientific research purposes only.

The author reserves all other publication and other rights associated with the copyright in the thesis, and except as herein before provided, neither the thesis nor any substantial portion thereof may be printed or otherwise reproduced in any material form whatever without the author's prior written permission.

Gene Yel Chan
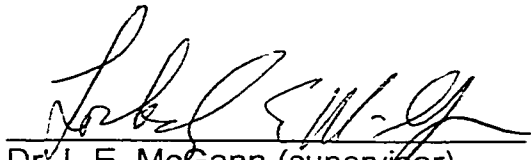
99 Armitage Close
Red Deer, Alberta
T4R 2K5

April 10, 2001

UNIVERSITY OF ALBERTA

FACULTY OF GRADUATE STUDIES AND RESEARCH

The undersigned certify that they have read, and recommend to the Faculty of Graduate Studies and Research for acceptance, a thesis entitled **Cryopreservation of Porcine Heart Valves** submitted by **Gene Yel Chan** in partial fulfillment of the requirements for the degree of **Master of Science in Experimental Pathology**.

Dr. L.E. McGann (supervisor)

Dr. J.R.T. Lakey

Dr. I. Rebeyka

Dr. J. Hugh

April 10, 2001

ABSTRACT

While still controversial, cryopreserved heart valves have demonstrated longer life-spans over fresh grafts once transplanted. Yet there remains room for improvement. This study examined the osmotic parameters that define the freezing response of endothelial cells and fibroblasts of heart valve leaflets during cryopreservation. The parameters were used in a simulation program devised to model cryopreservation procedures. Simulations were performed to examine cell response to different components of cryopreservation, as well as graded freezing simulations. Data from graded freezing experiments were compared to virtual graded freezing experiments to determine limits of cellular response. These observations were able to allow us to recommend changes to the current procedure that will improve the life-span of heart valves after cryopreservation and transplantation by reducing antigenicity and increasing fibroblast recovery. This investigation served practical purposes in clinical medicine as well as demonstrated the concepts of selective preservation and solute centralization in cryobiology.

ACKNOWLEDGEMENTS

TABLE OF CONTENTS

LIST OF TABLES

LIST OF FIGURES

LIST OF APPENDICES

LIST OF ABBREVIATIONS AND SYMBOLS

ABBREVIATIONS

CPA	cryoprotective agent
DMSO	dimethyl sulfoxide
EB	ethidium bromide
PBS	phosphate buffered saline
PG	propylene glycol

SYMBOLS

E_a	activation energy
L_p	hydraulic conductivity
P_s	solute permeability
V_b	osmotically inactive fraction
V_{iso}	isotonic volume
π	osmotic pressure
σ	reflection coefficient
μm	micron

CHAPTER 1

GENERAL INTRODUCTION

1.1. Cryobiology

Cellular Cryobiology

Whether we realize it or not, cryobiology affects most people in this world in one way or another. In the deep winters of Canada, the breadth of this evolving science is more apparent since animals need to find some way to cope with the chilling temperatures of the harsh winters. Frogs have been known to freeze completely and revive in spring with warmer temperatures (21) and arctic flounders live in sub-zero salt-water without freezing (27). Cryobiology however has greater applications. Every autumn, farms and orchards fear the damage to crops from frost. Millions of dollars can be lost each year. Tomatoes, oranges, grapes and other fruits and vegetables are sensitive to the effects of dropping temperatures. On the other hand, fruits and vegetables are also frozen for storage. By simply walking through the freezer aisle in the local grocery store, one will find frozen berries, potatoes, peas, carrots, etc. Food scientists research the effects of freezing and thawing on products to determine the food quality following the process.

Cryobiology as a natural system can be separated into two different forms. In the first instance, cryobiology can be used to cryopreserve biological matter. This includes plants, seeds, cells, tissues, and organs. The purpose of cryopreservation is to maximize the number of viable cells following freezing and thawing. In the second instance, cryobiology can be

1

used in cryosurgery. The purpose of the freeze-thaw process in this case is to kill cells. Cryosurgery has been researched mainly in the area of cancer treatment (3,6,14,16,18,34).

As a science, cryobiology is relatively young and Polge, Smith and Parkes (37) spurred the expansion of this field when they discovered that the addition of glycerol to spermatozoa in suspension could be frozen and thawed with high post-thaw motility of the spermatozoa. This initial discovery has expanded progressively by applying the same technique to numerous cell types. Red blood cells have been greatly used to establish some of the principles of cryobiology during its early years. Since then, experiments have dealt with stem cells, yeast, hamster cells and endothelial cells, just to name a few.

In general, as a cell is cooled slowly, there is normally a small degree of supercooling prior to an ice nucleation event. This event leads to the formation of extracellular ice. Water removal in the form of ice formation leads to an increase in extracellular solute concentration. As this concentration exceeds that of the intracellular solute concentration, an osmotic gradient is formed over the membrane and water passes out of the cell to compensate. The cell dehydrates, leading to the volumetric reduction.

Clearly cryopreservation has proven to be a complex interaction of a number of variables. Many debates still continue on the mechanism of cell injury due to the freeze-thaw cycle. Lovelock (29) in 1953 suggested that the major damage from freezing be caused by the concentration of electrolytes

2

within the cell and in the suspending medium. Through his studies with red blood cells, he determined the critical range of temperatures to be between $-3^\circ C$ and $-40^\circ C$, which coincides with the high salt concentrations. Mazur *et al.* (30) in 1973 introduced a two factor hypothesis, which states that cells are susceptible to damage in two ways. First, by the concentrating of solutes due to extracellular ice formation. Second, by intracellular ice formation and recrystallization during cooling and thawing respectively. According to Mazur *et al.* (30) the type of damage depends upon the rate of cooling. A low cooling rate exposes cells to high solute concentrations over long periods of time, while high cooling rates increase the likelihood of intracellular ice formation. Subsequently, a low warming rate again exposes the cells to high salt concentrations and increases the likelihood of recrystallization.

Meryman in 1967 (31) suggested that cell injury was a result of excessive cell shrinkage. Meryman described a "minimal critical volume" at which irreversible damage occurs. Steponkus *et al.* (40) extended Meryman's theory by proposing the concept of a 'tolerable surface area increment' (TSAI) in which cells can tolerate a limited change in surface area. The TSAI is a variable independent of the extent of contraction; it describes the maximum expansion of cell surface area.

Farrant and Morris (10) proposed that thermal and dilution shock as causes of freeze-thaw injury. The increase in intracellular and extracellular salt concentration renders the cell membrane susceptible to leakage upon

application of subsequent stress, such as cold shock upon cooling and dilution shock upon warming.

Lovelock, Mazur, Meryman, and Farrant have been major contributors to the evolution of concepts in cryobiology. Their ideas have sustained the interest in developing cryobiologists. However, these concepts have been applied only to cells in suspension. Extending these principles to attached cells and tissues adds another level of complexity.

Cryoprotection

So, how do we protect cells from freezing injury? The initial discovery of glycerol's protective property (36) has since lead to searches for newer and better cryoprotectants. Actions of the two classes of cryoprotectants (penetrating and nonpenetrating) have been outlined by McGann (30).

Penetrating cryoprotectants (e.g. dimethyl sulfoxide - DMSO, propylene glycol - PG) protect cells by increasing the intracellular solute concentration of the cell, hence decreasing the osmotic gradient across the plasma membrane during freezing. As a result, the volumetric contraction is less than those of cells without a penetrating cryoprotectant. The cells are then exposed to lower salt or electrolyte concentrations at any given sub-zero temperature. Consequently, cells are exposed to high salt concentrations at temperatures sufficiently low to minimize damage to the cell.

Nonpenetrating cryoprotectants (e.g. sucrose, hydroxyethyl starch - HES) on the other hand, perform the opposite role by dehydrating a cell. The increase in extracellular solute concentration leads to an osmotic gradient

4

across the membrane moving water out of the cell. The cell as a consequence contracts and although the cell is exposed to high salt concentrations, the minimal volume of water prevents intracellular ice formation (IIF).

In regards to the two-factor hypothesis, penetrating cryoprotectants protect cells during slow cooling by reducing the "solution" effects, while nonpenetrating cryoprotectants protect against damage from rapid cooling. The deleterious effects of ice formation have prompted others to examine the alternative of vitrification.

Vitrification

The purpose of vitrification is to avoid ice formation, either intracellular or extracellular. Vitrification can be defined as the amorphous formation of the glass state (9). Theoretically, this is possible and practically has been used in some systems. The limitation in this process is the high concentration of cryoprotectant necessary, which could be toxic and leads to osmotic stress. Hence special procedures for addition and removal of cryoprotectants is necessary.

With the increased understanding of low-temperature preservation (hypothermic, cryopreservation, and vitrification), banking of tissues and organs for the purpose of transplantation has become more feasible. Currently, tissues such as blood, skin, bone and embryonic stem cells are harvested from donors and stored for future use. Hypothermic storage is limited by short-term viability and vitrification has yet to be proven to be

effective. Cryopreservation is currently the most applicable procedure. It has been shown to be cost-effective while maintaining viability of cells in suspensions. However, the next progression is to improve cryopreservation of tissues and organs.

1.2. Heart Valve Replacement

Between the years of 1986 and 1995, there were 52 659 heart valve replacements performed in 47 718 patients in the United Kingdom alone (42). In a retrospective study of 43 301 patients from the United Kingdom Heart Valve Registry, 1051 (2.43%) underwent a second heart valve replacement operation (42). Of the 43 301 patients, 52.8% were males and 47.2% female; 73.4% under the age of 70 and 26.6% over 70. Of the heart valve replacements used, 67.9% were biological valves and 32.1% were mechanical valves. The incidence of heart valve replacement can be clearly shown to increase as 46.5% of replacements were performed within the first five years of the study and 53.5% in the latter five years (42). However, the data suggests that heart valve replacements are improving as 71.6% of second operations occurred in the first five years and only 28.4% occurred in the latter five years (42).

Heart valve disease can be of two major forms. Any of the four valves of the mammalian heart can become insufficient and/or regurgitant. One form of insufficiency arises due to a decrease in the diameter of the valve orifice. As a result, blood flow and pressure decreases in the subsequent chamber or vessel. The decrease in valve orifice diameter is a consequence of stenosis.

6

The leaflets of the valves in this case become calcified and the commisures and fissures usually become sealed thus decreasing the orifice size.

Regurgitant valves can also be stenotic, closing improperly and allowing blood to move back across the valve into the chamber. Prolapse may also cause regurgitation. With valve prolapse, the hinge of a leaflet(s) has weakened such that the increased pressure distally to the valve leads to an inversion of the leaflet and blood flow in the reverse direction.

Prior to the 1950's the focus of surgical procedures to remedy these problems in mitral valve stenosis by valvotomy and valvectomy (22) was typically unsuccessful. The resulting valvular insufficiency, which at the time was still regarded as safe and desirable, was in fact deleterious. The next evolution of surgical procedures was the development of valvular commisurotomy. Initially this was done by digital dilation; transatrial and transventricular dilator later advanced it. This was a more successful procedure.

In the early 1950s surgeons turned their focus to correcting mitral regurgitation. A number of materials were implanted into the valve to prevent regurgitation – ventricular lucite spheres, spindle-shaped baffles, mounted nylon leaflets, and autogenous tissue (22). However, these implants functioned inadequately, causing the propagation of thrombi or tissue degradation.

It wasn't until 1952 that Dr. Charles Hufnagel successfully treated valvular stenosis and prolapse (13). Using an acrylic caged-ball prosthetic

valve and fixation ring for implantation, a patient was treated for aortic regurgitation. The years to follow witnessed increase in use of artificial and tissue valves.

Artificial valves took two forms – ball and cage or tilting discs. Artificial valves failed in 10-15% of patients within 2 years (39). In general, ball valve complications included thromboemboli, ball variance and hemolysis. Disc valves had similar complications of thromboemboli, disc variance, and hemolysis as well as disc wear/grooving. In both cases, there was also the recurrence of regurgitation or stenosis and infective endocarditis. Although artificial valves encounter a number of possible complications, they are still used being used.

Tissue valves can also be of two types – graft or bioprosthetic valves. Grafts represent human or animal tissue, which replace the defective valve. In 1962, Ross and Barratt-Boyes were independently successful in the implantation of homograft valves (23). In 1965, Binet and Carpentier performed the first valve replacement utilizing a prepared porcine aortic valve xenograft (24). Binet reported a 68% failure rate after a 4-year period (4). In both homografts and xenografts, leaflets showed shrinkage, decreased tensile strength, prolapse, inflammatory cellular reaction and acellular patches (for homografts). In fixed, acellular grafts there were no indications of host fibroblast regeneration or infiltration (24).

By 1968, the xenograft was adapted and evolved into the bioprosthesis (24). A bioprosthesis is the combination of biological tissue and synthetic

materials. Initially, the porcine xenograft was treated with glutaraldehyde in order to introduce cross-linkages between the collagen fibres. Hancock adapted the bioprosthesis by fixing the valves with formaldehyde and mounting it on a Dacron-covered rigid metal stent. This stent was later replaced with a flexible stent comprised of a polypropylene support and a rigid Stellite ring. Bioprosthetic valves however also showed leaflet prolapse and heavy calcification in conjunction with tissue degradation (35). Fishbein *et al.*, after examining 23 explanted xenografts ranging from 1 month to 2.6 years, found focal calcification and thrombus confirming the surface is not inert (12).

Although bioprosthetic valves encounter complications, they do have one major advantage over artificial valves. In a study by Gabbay and Kresh, the hydrodynamics of artificial and bioprosthetic valves were tested (15). Bioprosthetic valves were shown to have much better hydrodynamics than that of artificial valves. The presence of either ball or disc interrupts any possibility of laminar flow, which in theory would indicate best flow through any tubular vessel.

It is apparent that the need for heart valve replacement is present. Valvular defects and disease leave surgeons with few options otherwise. However, history has shown that mechanical valves are inferior to biological valves based upon hemodynamic measurements (15). However, biological replacements face challenges as well. The issue at hand is how to create or maintain a structurally sound replacement that leads to the least complications.

1.3. Heart Valve Preservation

Hypothermic Storage

For short-term storage, the best available method is hypothermic storage. Refrigeration of tissues at 4°C can be extended for days with good viability of cells. Lockey *et al.* (28) stored 126 valves in one of two antibiotic solutions. The storage solution of gentamicin (4mg/ml), methicillin (10mg/ml), erythromycin-lactobionate (6mg/ml), and nystatim (2500 units/ml) in Hank's solution was able to sterilize all valves by 24 hours and remained sterile thereafter. Through this study, Lockey *et al.* also determined that the use of nutritive media rather than Hank's Solution could extend the duration of viability. Viability was assayed using autoradiography and tissue culture. With the proper antibiotics and solution, ~70% fibroblast viability can be maintained for 48-72 hours. Preservation in this fashion limits the time span of tissue viability and the possibility of surgical procedures. Based upon hypothermic storage only, it is not feasible to establish heart valve tissue banks for transplantation.

Cryopreservation

Cryopreservation is currently the most practical means of preserving tissue structure and cell viability for long-term function. Heart valve cryopreservation can be divided into 5 areas: (i) harvesting of the donor heart, (ii) valve preparation and antibiotic sterilization, (iii) control-rate freezing with cryoprotectants; (iv) storage of the processed valves, and (v) thawing/diluting and implantation. The typical cryopreservation protocol for heart valves has

been adapted from Smith's initial work with spermatozoa (36). In general, cryopreservation of heart valves uses a balanced salt solution, such as Hank's or a nutrient media, with 10% dimethyl sulfoxide (some formulae supplement with 10% fetal calf serum). Valves are then cooled at 1°C/min to at least –40°C before transferring to storage at temperatures below -135°C (1,5,17,26,34). Brockbank *et al.* (5) have determined that storage above – 80°C leads to a loss of cell viability and cracking of the tissue. Cryoprotectants are then removed in a step-wise dilution to minimize damage from rapid influx of water. Since cryobiology is a relatively new science, many of the procedures are empirically based. This protocol for cryopreserving heart valves is no different and although this protocol has been shown valid for cells in suspension, it can not be assumed to be valid or optimal for heart valves.

1.4. Previous Studies

Follow-up Studies

Numerous studies have been conducted concerning the viability and duration of viability when cryopreserved valves were used in valve replacement surgeries. Two major conclusions can be inferred from these studies. However, to draw conclusions about the use of cryopreserved valves in replacement surgeries, it is necessary to establish a base line of results of valve replacements using fresh valve allografts.

a) Fresh Valves

During the infancy of heart valve replacements, 16 implants were performed by Barrett-Boyes during 1962 and 1963 and 6 grafts were recovered during autopsy or second operation at intervals from 3.5 months to 8.5 years after implantation. Of the 6 valves recovered, 3 showed severe cusp shrinkage and prolapse; the graft recovered at 8.5 years was incompetent due to a large perforation (23).

In a later study by Barratt-Boyes *et al.* (2), a six-year review of valve replacements using antibiotic sterilized homograft valves included 121 patients (78 males and 43 males). Ages ranged from 11 to 74 years with 62% of patients over 50 years. An overall hospital mortality rate was 5.7%. Reoperation was required for incompetence in 11 patients. The most significant problem encountered was cusp rupture, occurring at a rate of 8%. The clinical data suggested that ruptures might be in part due to a rejection reaction.

Over the duration of 8 years (1969 to 1978), Thompson *et al.* performed valve replacements in 679 patients using fresh unstented homografts (41). There were 16 (3.9%) early deaths (before 30 days) and 43 (10.5%) late deaths (during follow-up between 3 and 102 months). Actuarial survival was 87% at 5 years and 81% at 8 years. In total valve failure occurred in 24 (3.5%) patients. The authors of this study judged homograft replacement of the aortic valve to be satisfactory.

b) Cryopreserved Valves

From the follow-up studies performed using cryopreserved valves for replacements, failure could be reduced to two forms. Early failure of valve replacements could be due to host to graft rejection. Typically, valve replacements are performed without HLA matching or immunosuppression post-operatively; this opens the possibility of rejection of the graft. Fischlein *et al.* (11) studied 41 patients who underwent aortic valve replacement, of which 33 received allograft valves (17 ABO-compatible and 16 ABO-incompatible), and 8 received commercially available xenografts. Those who received ABO-Incompatible valves showed greater cytoimmunologic reaction that ABO-compatible valves; activation index of 2.1±1.6 (n=16) versus 1.3±0.8 (n=17), respectively. Interestingly, the 8 patients with xenograft valve replacements showed no activation, indicating that exposed leaflets and conduit surfaces lacking cells do not elicit an immune response.

Other studies have also examined the role of immunologic response in the failure of implanted valves. Of note are studies by Ketheesan *et al.* (20) and Moustapha *et al.* (33). Both studies conducted utilised rat model systems. Ketheesan *et al.* determined no significant difference in immunogenicity between fresh and cryopreserved valves (cryopreserved with cooling rates of 1°C/min or 5°C/min). However, a significant reduction of immunogenicity was observed for valves cryopreserved at 10°C/min, 30°C/min, and >100°C/min. The study by Moustapha *et al.* showed typical cell-mediated rejection. Pathology of the cryopreserved allogeneic valves at

56 days after implantation indicate moderate to severe mononuclear cell infiltration, mainly lymphocytes and macrophages. In addition, diffuse intimal thickening enveloped the free leaflets forming 'leaflet ghosts'. Multiple acellular sites resulted from the immunological response. Ketheesan *et al.* and Moustapha *et al.* have demonstrated the important role the host immune system plays in short-term valve failure.

Long-term failure has been suggested to be a result of tissue deterioration (37). Although short-term failure is also due to tissue deterioration, the mechanism by which this occurs is different. In long-term failure, the tissue degenerates not by immune response but rather by mechanical stress and lack of viable fibroblasts (37). Since fibroblasts sustain the tissue in its structural integrity, a lack of fibroblasts leads to the loss of collagen matrix maintenance. For this reason, we speculate that a nonviable cryopreserved valve lasts no longer than an acellularized graft .

The failures of heart valve replacements in patients are expected but can they be prolonged or even prevented? Consider the cost of heart valve cryopreservation. The cost of procuring and cryopreserving a single heart valve at an on-site tissue bank was estimated by Lever *et al.* to be Can$1362.56 in 1990 (26). What if 5% of these valves fail when transplanted? Consider the cost of a second operation required for those patients, financially, physically, and emotionally. Consider an infant born with congenital valve defects and undergoing valve replacements every 15 years or less. To ensure the quality of the cryopreserved heart valve after thawing

an understanding of cellular responses during cryopreservation is critical. Ideally these studies would utilize human heart valve tissues. However, since healthy human tissues are in short supply and are valuable for transplantation purposes, these are not readily available for experimentation. Available human heart valve tissues are normally discards from surgical procedures, either as explants or non-ideal grafts. These tissues may have confounding variables, therefore an animal model is required.

The ultimate goal of these studies is to provide viable heart valve tissues for transplantation. Since early degeneration of heart valve replacements has been connected to rejection of the graft by the recipient (7,11,19,25,33) and later failure of valves due to lack of fibroblast cells (43), the viable heart valve after cryopreservation and thawing should have viable fibroblasts and reduced or eliminated immunogenecity.

Cochran and Kunzelman have shown that cryopreservation preserves the antigenicity of the heart valve (8). Studies by Moustapha *et al.* support this finding in the rat model (33). However, Moustapha *et al.* have also demonstrated that an acellularized leaflet initiates no immune response. We speculate endothelial cells to be initial sites of rejection. Elimination of endothelial cells may reduce and possibly prevent eliciting an immunological response. However, endothelial cells are critical to proper function. This can be overcome by reendothelialization of the leaflets by the recipient's own cells. Zavazava *et al.* have demonstrated this with porcine valves in human recipients (45).

1.5. Hypothesis

By understanding the osmotic parameters of cells in porcine heart valve leaflets and correlation to cell viability, cryopreservation protocols can be devised which allows differential selection of cells (i.e. eliminate endothelial cells and preserve fibroblasts) to potentially improve the life-span of heart valves after transplantation.

1.6. Rationale for Experiments

Porcine heart valves were selected for this study for several reasons. Porcine valves are an obvious second choice since porcine xenografts have already been used for heart valve replacements. More specifically, the dimensions of porcine valves are similar to that of human valves, so the kinetics of heat and mass transfer during cryopreservation will be similar. Studies reported in the literature (12,35) have used porcine heart valves in other experiments related to cryopreservation, which will be useful for comparing results. Local abattoirs provide a ready supply of porcine hearts from healthy animals with short warm ischaemic times. In these experiments, heart valves were excised and handled using the standard operating procedures for human heart valve transplantations.

The data gathered from porcine heart valves may be useful for human valves. We recognize that human and pigs are different species and this is one major limitation in this study. However, the establishment of procedures and techniques in the porcine model are valid and important, and can be transferred to human valves. Three studies have been designed to integrate

current knowledge and techniques to investigate the possibility of selective preservation. Each study examines an aspect of the cryopreservation procedure.

(A)   To examine and determine cellular response and parameters of porcine heart valve leaflet endothelial cells and fibroblasts to cryopreservation conditions.

A cell's plasma membrane differentiates the external and internal environment. It also responds chemically and physically with different stresses. During cryopreservation, a cell is exposed to high salt, low temperatures, physical disruption by ice formation, and dilution stress during thawing. Understanding how a cell reacts to these stresses is critical to formulating an optimal cryopreservation protocol.

Experiments will be conducted to investigate and quantify cellular response to these stresses. Cell response will be reduced to cell-specific parameters. These parameters are determined by measuring cell volume change by electronic particle size analyzer over the duration of cell exposure to hypertonic salt solutions and cryoprotectants. Comparisons can then be made to other cell types.

(B)   To investigate the damage to cells of intact porcine heart valve leaflets from solution effects versus intracellular ice formation by a graded freeze-thaw protocol.

The graded freeze-thaw protocol has been used previously to determine the effects of low cooling rates versus high cooling rates. *In situ*

17

analysis of leaflets will be done by coupling a dual fluorescence stain with confocal microscopy. Leaflets will be analyzed of varying depths and will provide measures of viability for endothelial cells and fibroblasts. This can be correlated to data from computer simulations of the graded freeze-thaw protocol. Correlating experimental with theoretical data may provide insight into the limits of these cells in order to maintain viability.

(C)   To use determined cell-specific parameters for porcine heart valve leaflet endothelial cells and fibroblasts to model aspects of cryopreservation by computer simulation.

Although previous computer simulations have been used to examine aspects of ice formation and water movement, none have specifically modeled cell response to cryopreservation. Factors such as cell volume, supercooling, intracellular and extracellular salt and solute concentrations provide vital information concerning cellular stresses. Aspects of cryopreservation to be investigated are: equilibration of cryoprotectant addition, cooling rates, and removal of cryoprotectants. Simulations will also be performed to model responses of cells in graded freezing. The difference in response between endothelial cells and fibroblasts may be important in designing an optimal cryopreservation protocol.

1.7. References

1.   Adam M, Fei Hu J, Lange P, and Wolfinbarger U. The effect of liquid nitrogen submersion on cryopreserved human heart valves. *Cryobiology.* 27: 605-614 (1990).

2.   Barratt-Boyes BG, Roche AFIG, and Whiflock RML. Six year review of the results of freehand aortic valve replacement using an antibiotic sterilized homograft valve. *Circulation* 55: 353-361 (1977).

3.   Benson JW.   Combined chemotherapy and cryosurgery for oral cancer. *Am J Surg.* 130: 596-600. (1975).

4.   Binet JP, Planche C, and Weiss M: Heterograft replacement of aortic valve. In Ionescu MI, Ross DN, and Wooler GH (eds): Biological tissue in heart valve replacement. London, Butterworth, 1971. pp. 409-444.

5.   Brockbank KG, Carpenter JF, and Dawson PE. Effects of storage temperature on viable bioprosthetic heart valves. *Cryobiology.* 29: 537-542 (1992).

6.   Brown NJ, Bayjoo P, and Reed MW.   Effect of cryosurgery on liver blood flow. *Br J Cancer.* 68: 10-12. (1993).

7.   Carpentier A, Robert L, and Dubost C. Biological factors affecting long-term results of valvular heterografts. *J Thorac Cardiovasc Surg* 58: 467-482 (1969).

8.   Cochran RP and Kunzelman KS.   Cryopreservation does not alter antigenic expression of aortic allografts. *Journal of Surgical Research.* 46: 597-599. (1989).

9.   Fahy GM, MacFarlane DR, Angell CA, and Meryman HT. Vitrification as an approach to cryopreservation. *Cryobiology.* 21: 407-426. (1984).

10.   Farrant J and Morris GJ.   Thermal shock and dilution shock as the causes of freezing injury. *Cryobiology.* 10: 134-140. (1973).

11. Fischlein T, Schutz A, Haushofer M, Frey R, Uhlig A, Detter C, and Reichart B. Immunologic reaction and viability of cryopreserved homografts. *Ann Thorac Surg*. 60: S122-S126 (1995).

12. Fishbein MC, Gissen SA, Collins JJ Jr, Barsamian EM, and Cohn LH. Pathology of cardiac valve replacement with glutaraldehyde-fixed porcine valves. *Am J Cardiol*. 40: 331. (1977).

13. Frankl WS: The evaluation of patients for prosthetic valve implantation. In Morse D, Steiner RM, and Fernandez J (eds): Guide to prosthetic cardiac valves.new York Springer-Verlag, 1985. pp. 5-51.

14. Fraunfelder FT, Farris HE Jr, and Wallace TR. Cryosurgery for ocular and periocular lesions. *J Dermatol Surg Oncol*. 3: 422-7. (1977).

15. Gabbay S and Kresh JY: Bioengineering of mechanical and biological heart valve substitutes. In Morse D, Steiner RM, and Fernandez J (eds): Guide to prosthetic cardiac valves. New York, Springer-Verlag, 1985. pp. 239-256.

16. Gage AA. Cryosurgery in the treatment of cancer. *Surg Gynacol Obstet*. 174: 73-92. (1992).

17. Goffin Y, Grandinougin D, and Van Hoeck B. Banking cryopreserved heart valves in Europe: assessment of a 5-year operation in an international tissue bank in Brussels. *Eur J Cardio-thorac Surg*. 10: 505-512 (1996).

18. Gould RS. Total cryosurgery of the prostate versus standard cryosurgery versus radical prostatectomy: comparison of early results

and the role of transurethral resection in cryosurgery. *J Urol.* 162: 1653-1657. (1999).

19.   Hogan P, Duplock L, Green M et al. Human aortic valve allografts elicit a donor-specific immune response. *J Thorac Cardiovasc Surg* 112: 1260-1267 (1996).

20.   Ketheesan N, Keamey J, and Ingham E. The effect of cryopreservation on the immunogenicity of allogeneic cardiac valves. *Cryobiology.* 33: 41-53 (1996).

21.   Layne Jr. JR. Freeze tolerance and cryoprotectant mobilization in the gray tree frog (Hyla versicolor). *J Exp Zool.* 283: 221-225. (1999).

22.   Lefrak EA and Starr A. Cardiac Valve Prostheses. (1979). London, UK. Prentice-Hall International, Inc. pp. 5-8.

23.   Lefrak EA and Starr A. Cardiac Valve Prostheses. (1979). London, UK. Prentice-Hall International, Inc. p. 274-279.

24.   Lefrak EA and Starr A. Cardiac Valve Prostheses. (1979). London, UK. Prentice-Hall International, Inc. pp. 301-303.

25.   Lehalle B, Geschier C, Fieve G, and Stoltz JF. Early rupture and degeneration of cryopreserved arterial allografts. *J Vasc Surg* 25: 751-752 (1997).

26.   Lever CG, Ross DB, Page LK, La Prairie A, Molyneaux M, and Murphy DA. Cost-effectiveness and efficacy of an on-site homograft heart-valve bank. *CJS.* 38: 492-496 (1995).

27. Lin Q, Ewart KV, Yang DS, and Hew CL. Studies of putative ice-binding motif in winter flounder skin-type anti-freeze polypeptide. *FEBS Lett.* 453: 331-334. (1999).

28. Lockey E, Al-Janabi N, Gonzalez-Lavin L, and Ross DN. A method of sterilizing and preserving fresh allograft heart valves. *Thorax* 27: 398-400 (1972).

29. Lovelock JE. The mechanism of the protective action of glycerol against haemolysis by freezing and thawing. *Biochima et Biophysica Acta.* 11: 28-36. (1953).

30. Mazur P, Liebo SP, and Chu EHY. Two-factor hypothesis of freezing injury. Exptl Cell Res. 71: 345-355. (1971).

31. McGann LE. Differing actions of penetrating and nonpenetrating cryoprotective agents. *Cryobiology.* 15: 382-390. (1978)

32. Meryman HT. Freezing injury and its prevention in living cells. *Ann Rev Biophys Bioeng.* 3: 341-363. (1974).

33. Moustapha A, Ross DB, Bittira B, Van-Velzen D, McAllister V, Lannon C, and Lee T. Aortic valve grafts in the rat: evidence for rejection. *J Thorac Cardiovasc Surg* 114: 891-902 (1997).

34. Neel HB 3d. Cryosurgery for the treatment of cancer. *Laryngoscope.* 90 (8 Pt 2): 1-48. (1980).

35. O'Brien MF, Stafford 0, Gardner M, Pohlner P, McGiffin D, Johnston N, Brosnan A, and Duffy P. The viable cryopreserved allograft aortic valve. *J Cardiac Surg* 2 [Suppl]: 153-167 (1987).

36.   Pipkin RD, Buck WS, and Fogarty TJ.   Evaluation of aortic valve replacement with a porcine xenograft without long-term anticoagulation. *J Thorac Cardiovasc Surg.* 71: 179-186. (1976)

37.   Polge C, Smith AU, Parkes AS. Revival of spermatozoa after vitrification and dehydration at low temperatures. *Nature.* 164: 666. (1949).

38.   Schoen FJ, Mitchell RN, and Jonas RA. Pathological consideration in cryopreserved allograft heart valves. *The Journal of Heart Valve Disease.* 4: S72-S 76 (1995).

39.   Song YC, Khirabadi BS, Lightfoot F, Brockbank KGM, and Taylor MJ. Vitreous cryopreservation maintains the function of vascular grafts. *Nature Biotechnology.* 18: 296-299. (2000).

40.   Steiner RM and Flicker S: The radiology of prosthetic heart valves. In Morse D, Steiner RM, and Fernandez J (eds): Guide to prosthetic cardiac valves. New York, Springer-Verlag, 1985. pp. 53-77.

41.   Steponkus PL, Wolfe J, and Dowgert MF. Stresses induced by contraction and expansion during a freeze-thaw cycle: a membrane perspective.   In Morris GJ and Clarke A (eds): Effects of Low Temperatures on Biological Membranes. New York, academic Press, 1981. pp. 307-322.

42.   Thompson R, Yacoub M, Ahmed M, Somerville W, and Towers M. The use of 'fresh' unstented homograft valves for replacement of the aortic valve. *J Thorac Cardiovasc Surg.* 79: 896-903. (1980).

43. Van Der Kamp AWM, Visser WJ, Van Dongen JM, Nauta J, and GaUaard H. Preservation of aortic heart valves with maintenance of cell viability. *Journal of Surgical Research* 30: 47-56 (1981).

44. Weerasinghe A, Maria-Benedicta E, and Taylor KM. First Redo heart valve Replacement. *Circulation*. 99: 655-658. (1999).

45. Zavazava N, Simon A, Sievers HH, Bernhard A, and Muller-Ruchholtz W. Porcine valves are reendothelialized by human recipient endothelium *in vivo*. *J Thorac Cardiovasc Surg*. 109: 702-706 (1995).

CHAPTER 2

OSMOTIC PARAMETERS OF PORCINE HEART VALVE DERIVED ENDOTHELIAL CELLS AND FIBROBLASTS

2.1 Introduction

What happens when a cell is introduced into a hypertonic solution of impermeant solutes, such as salt? The higher solute concentration outside the cell forces water to leave the cell, down the osmotic gradient. Water will continue to leave the cell until the intracellular salt concentration equals the extracellular salt concentration. At this point, the cell has reached the equilibrium volume fraction. The rate at which water permeates the cell membrane, hydraulic conductivity (L_p), affects the change in cell volume over time and can be described by

$$\frac{dV}{dt} = -L_pART(\pi^e - \pi^i)$$

[1]

where V is the water volume, A is the surface area of the cells, π is the osmolality of the extracellular (e) and intracellular (i) solution, R is the universal gas constant, and T is absolute temperature. The effect of temperature on this parameter is characterized by its activation energy (E_a). If a cell is exposed to a highly hypertonic solution that causes all 'free' water to leave the cell, the cell reaches its osmotically inactive fraction (V_b). The osmotically inactive fraction (V_b) refers to the fraction of cell volume not participating in osmotic interactions, including proteins and lipid membranes and bound water. The Boyle-van't Hoff relationship (8) describes the cell volume as a function of osmotic pressure and can be used to calculate V_b.

25

$$V = \frac{\pi}{\pi_{iso}}(V_{iso} - V_b) + V_b \qquad [2]$$

where V is volume at osmotic pressure π, π_{iso} is the isotonic osmotic pressure, V_{iso} is the isotonic cell volume, and V_b is osmotically inactive fraction.

If however, a cell is introduced into a hypertonic solution with a cryoprotectant, the movement of solutes is complicated. Initial exposure results in dehydration of the cell and decreased cell volume as an osmotic gradient is formed. An additional gradient is present involving the cryoprotectant. To equilibrate, the cryoprotectant enters the cell. The rate at which the cryoprotectant permeates the cell membrane is represented by the solute permeability (P_s). This is described by

$$\frac{dS}{dt} = P_s(\Delta C_s) + (1 - \sigma)\frac{dV}{dt} \qquad [3a]$$

$$\frac{dV}{dt} = -LpART(\pi_n^e - \pi_n^i) + \sigma(\pi_s^e - \pi_s^i) \qquad [3b]$$

where S is solute concentration, P_s is solute permeability, ΔC_s is the difference between extracellular and intracellular solute concentration, σ (sigma) is the reflection coefficient, n is the nonpermeating solute, and s is the permeating solute. The reflection coefficient describes the interaction of the solute with water in the membrane. We have chosen to set the reflection coefficient to equal 1. This implies that the cryoprotectant and water have no interactions in the membrane, therefore L_p has no affect on P_s and vice versa. The influx of cryoprotectant into the cell causes water to rehydrate the cell. As a result, the cell returns to its isotonic volume.

26

Since L_p and P_s are temperature-dependent and can be described by the Arrhenius activation energy, E_a.

$$P = P_{ref} \exp(-\frac{E_a}{R}(\frac{1}{T_{ref}} - \frac{1}{T}))$$ [4]

where P is the permeability, and P_{ref} is permeability at the reference temperature. The activation energy is found by solving for equation 4 for E_a with experimental measurements of permeability. Permeability values are calibrated from the kinetics of volume change. Typically there are two ways to do this, as outlined by Acker *et al.* (1). Cellular osmotic responses have been measured optically or by electrical measurement techniques. Measuring cells optically allow for direct measurements, detailed kinetics and experiments at high osmolalities, while electrical techniques have the advantages of being rapid, reproducible, and allow the study of multiple cell populations of a variety of sizes and shapes.

To date there have been no experiments conducted to determine the osmotic parameters of endothelial cells and fibroblasts derived from the heart valve leaflets (porcine or human). Endothelial and fibroblast viability have been examined with regard to cryopreservation techniques including procurement processes (4,8,7), cryopreservation solutions (5), and storage conditions (2,3,5,6). These studies are necessary, but a more comprehensive understanding is needed on a cellular level.

This study was designed to define osmotic parameters for porcine heart valve derived endothelial and fibroblast cells. Both cell types were exposed to solutions of impermeant solutes and the cell volume tracked as a function

27

of time using an electrical particle size analyzer. Cell volumes were also tracked as cells were exposed to, and diluted from 1M and 2M concentrations of cryoprotectants. These experiments were conducted at different temperatures and provide the cellular volume kinetics necessary to define the values of cellular and osmotic parameters.

2.2. Materials and Methods

Tissue Isolation

Hearts from a local abbitoir were obtained shortly after market pigs were slaughtered. Porcine hearts underwent 15-20 minutes warm ischaemic time before being bagged in isotonic PBS (Dubelco's Phosphate Buffered Saline, Gibco BRL) at 4°C, pH 7.1, and transported in ice water. Tissues were exposed to 1 hour to 1.5 hours cold ischaemic time. Hearts were dissected in PBS at 4°C to maintain hypothermic conditions and to prevent dehydration of tissues. For each heart, the pericardial sac was removed. Left and right auricles were removed to expose the tricuspid and mitral valves and to allow access to the aortic valve annulus. The ascending aortic root and pulmonic artery were trimmed to leave at least 2 cm of vessel above the annulus. Scissors were used to separate the vessels from each other and the two valve conduits were removed leaving 1 cm of tissue below the annulus. The three leaflets were then excised from each valve, washed, and maintained in PBS at 4°C.

Cell Culture

Sets of 3 leaflets from a single valve were enzymatically treated with 2 ml 0.05% Trypsin – EDTA (Gibco BRL) for 5 minutes at 37°C. Each leaflet was then mechanically treated by light scraping with a rubber policeman to remove the endothelial cells. An equal volume of M199 culture medium (Gibco BRL) supplemented with 20% (v/v) fetal calf serum (FCS), 10 ml Penicillin/Streptomycin (Gibco BRL; 5000 units/ml Penicillin, 5000 ug/ml Streptomycin), and 2.5 ml Gentamicin (Gibco BRL; 10mg/ml) to neutralize the Trypsin.

Leaflets were then minced with scissors and enzymatically treated with 5 ml collagenase II (70µg/ml; Boerhinger-Mannheim, Germany) per set in 15 ml centrifuge tubes (Fisher Brand). Samples were incubated at 37°C in a water bath for 30 minutes. Tubes were centrifuged (Model TJ-6 Centrifuge, Beckman, USA) at 2000 rpm for 10 minutes. The collagenase supernatant was discarded and the tissue pellet resuspended in 5 ml supplemented M199 tissue culture medium as above. The cell suspension was also cultured in 12 well culture plate (Corning, USA) at 37°C in 95% air + 5% CO_2.

Endothelial and fibroblast culture media were changed the next day and every 2 or 3 days afterwards. Once cultures reached 80% confluency, they were passaged with Trypsin and mechanical treatment as before. The subsequent cell suspensions were transferred to 25 cm^2 polystyrene tissue culture flasks (Corning, USA) and volume adjusted to 10 ml using supplemented M199 culture media. These were cultured until confluent.

29

Kinetics of Cell Volume Change

a) Impermeant Solute

After reaching confluency cell cultures were trypsinized. Cell suspension was equilibrated to the experimental temperature of either 22°C, 10°C or 4°C. Experimental solutions of impermeant solute were prepared by diluting 10X Dubelco's Phosphate Buffered Saline (Gibco BRL) to 1x, 2x, 3x, 4x, and 5x isotonic (~300, ~600, ~900, ~1200, and ~1500 mOsm, respectively) and adjusted to pH 7.1 with NaOH or HCl as necessary. Osmolarity was measured (μOsmette osmometer, Precision Instruments) in triplicate for each solution and the mean average calculated. The experimental solutions were cooled to the experimental temperature and 250μl of the cell suspension was injected into 10 ml of the experimental solution. PBS solutions were maintained at the experimental temperature with a custom made water bath. A Coulter Particle Size Analyzer (Coulter Electronics Inc., Germany) measured cell size and the data collected by a personal computer connected via Cell Size Analyzer (GCCC, Spruce Grove, AB, Canada). The change in cell volume over duration of time was calibrated and normalized by measuring latex beads of known diameter. Three different cell suspension were tested in triplicate for each condition giving n = 9.

b) Solute Permeability

Solutions of the permeant solutes 1M and 2M DMSO, glycerol, and PG were prepared by adding the appropriate mass of the CPA to isotonic PBS.

Cell suspensions were prepared in the same fashion as before. In determining the solute permeability of CPAs during addition the various CPA solutions were used rather than hypertonic solutions in the previous experiment.

To determine solute permeability during removal of CPAs, cell suspensions were prepared in the fashion as before were then aliquoted into 7 volumes of 700μl in microcentrifuge tubes. Cells were pelleted by microcentrifugation (table-top microcentrifuge, Fisher, USA) at 7000 rpm for 10 minutes. Pellets were resuspended in 1.5 ml of the various experimental solutions (1M and 2M DMSO, Glycerol, and PG) and allowed to equilibrate with the solute at the experimental temperature. Experiments were conducted as described previously, using 1x PBS as the experimental solution used to measure cell kinetics on return to isotonic conditions.

2.3. Results

Isotonic Volume

The isotonic volumes for endothelial cells and fibroblasts were determined from volume distributions under isotonic conditions. These measurements were calibrated using spherical latex beads (15μm diameter, Coulter). Isotonic volumes were averaged over all experimental temperatures since there is no temperature dependence. The isotonic volumes of endothelial cells and fibroblasts were $2513\pm154\mu m^3$ and $2866\pm195\mu m^3$, respectively.

Osmotically Inactive Fraction

For each cell sample tested in impermeant solute, V_b was calculated from the data and equation 2. A mean and standard error was determined for each cell type at each temperature and osmolality (**Table 2.1**). The osmotically inactive fractions were pooled for each temperature and each concentration of impermeant. Since there was no concentration or temperature difference in the osmotically inactive fraction, all samples in impermeant solutes were pooled to give one value to describe each cell type. Endothelial cells (0.399±0.009) demonstrated an osmotically inactive fraction slightly larger than that of fibroblasts (0.368±0.006).

Hydraulic Conductivity

Values for L_p were determined from cell volume kinetics in hypertonic conditions (PBS and addition of cryoprotectants). Mean and standard errors for the values were calculated at each temperature for each solution (**Table 2.2**). Values at each temperature were pooled since there was no concentration dependence.

Cryoprotectant Permeability During Addition

Figures 2.4 to **2.9** are representative of the kinetics of volume change from exposure to cryoprotectant solutions. The 2M PG, 1M Glycerol and 2M glycerol experimental sets however were discarded. The 2M PG data indicated a possible interaction of the cryoprotectant with the cells of the calibration beads so reliable data could not be obtained (**Figure 2.7**). Experiments with glycerol were discarded based on the low permeability of

32

glycerol in the cells. The slow permeation of glycerol to endothelial cells (**Figure 2.8**) and fibroblasts (**Figure 2.9**) does not allow an accurate determination of P_s for glycerol.

As before, from each exposure of cells to cryoprotectants at each temperature a value was determined for P_s. The mean and standard error was determined for each condition (**Table 2.3**). Since concentration dependence was not a factor, the data for 1M and 2M DMSO were pooled to obtain values for each temperature.

Cryoprotectant Permeability During Removal

Figures 2.10, 2.11 and **2.12** are representative data of cell kinetics during the removal of 1M DMSO, 2M DMSO and 1M PG, respectively. Values of P_s (**Table 2.4**) were determined in the same fashion as those for the addition of cryoprotectants.

Activation Energies

Activation energies were calculated for L_p, and cryoprotectant P_s during addition and removal by fitting the experimental data to the Arrhenius equation (**Figures 2.13, 2.14,** and **2.15**). Activation energies for hydraulic conductivity and solute permeability (DMSO and PG) are listed in **Table 2.5**.

2.4. Discussion

While endothelial cells and fibroblasts have different morphologies *in situ* and in culture, cell volumes are the same. The osmotically inactive fraction (V_b) of porcine heart valve endothelial cells and fibroblasts differed

33

little as well. What is then important is the cell's characteristic response to its environment based upon its L_p and P_s, and their respective E_a.

Comparison of hydraulic conductivities for any cell type can be misleading. Because of the strong temperature dependence, L_p can only be compared at specific temperatures. In this study, endothelial cells and fibroblasts have the same L_p at 22°C. The activation energy of L_p however, is higher for endothelial cells (11.6±0.2 kCal/mol) than that for fibroblasts (9.2±0.2 kCal/mol). Because of differences in the activation energy, endothelial cells and fibroblasts will behave differently under identical conditions.

DMSO and PG permeabilities for endothelial cells and fibroblasts are different at the temperatures tested. Once again, comparing P_s at one temperature can be misleading. As **Table 2.3** and **Figure 2.13** show, at 22°C, DMSO and PG permeability of endothelial cells is higher for fibroblasts. However at 4°C, DMSO and PG permeability of fibroblasts is higher for endothelial cells. The important factor in making comparisons is the activation energy. For DMSO, the activation energy for Ps is greater for endothelial cells, but greater for fibroblasts with PG.

Generally the solute permeability during removal is assumed to be the same as that of the P_s during addition. These experiments showed different values for P_s during removal. However these values are based upon the Boyle-van't Hoff plot, which assumes a linear extrapolation under hypotonic conditions. It has been shown previously that cell expansion does not follow

34

this linear pattern (McGann – unpublished data). Cells undergoing a dilution of this sort could be limited by the cell membrane tension and expansion past this limitation most probably leads to lysis.

These parameters for endothelial cells and fibroblasts determine the cellular response. An understanding of these fundamental characteristics is essential in formulating any successful cryopreservation protocol. This study has shown the major differences between endothelial and fibroblast cells to be in L_p and P_s, and their relative activation energies. Based on the cellular responses in these experiments, we can expect that endothelial cells and fibroblasts will respond different when cryopreserved.

2.5. References

1.   Acker JP, Pasch J, Heschel I, Rau G, and McGann LE. Comparison of optical measurement and electrical measurement techniques for the study of osmotic responses of cell suspensions. *Cryo-Letters*. 20: 315-324. (1999).

2.   Adam M, Fei HJ, Lange P, and Wolfinbarger U. The effect of liquid nitrogen submersion on cryopreserved human heart valves. *Cryobiology*. 27: 605-614 (1990).

3.   Brockbank KG, Carpenter JF, and Dawson PE. Effects of storage temperature on viable bioprosthetic heart valves. *Cryobiology*. 29: 537-542. (1992).

4. Brockbank KG and Dawson PE. Influence of whole heart postprocurement cold ischemia time upon cryopreserved heart valve viability. *Transplantation Proceedings* 25: 3188-3189 (1993).

5. Feng XJ, Walter PJ, and Herman AG. Effects of storage temperature and fetal calf serum on the endothelium of porcine aortic valves. *J Thorac Cardiovasc Surg* 111: 218-230 (1996).

6. Kashima I, Yozu R, Shin H, Yamada T, Hata J, and Kawada S. Effect of storage temperature on cell viability in cryopreserved canine aortic, pulmonic, mitral and tricuspid valve homografts. *Japanese J Thorac Cardiovasc Surg.* 47: 153-157. (1999).

7. McNally RT and Brockbank KGM. Issues surrounding the preservation of viable allograft heart valves. *Journal of Medical Engineering & Technology.* 16: 34-38. (1992).

8. Moustapha A, Ross DB, Bittira B, Van-Velzen D, McAllister V, Lannon C, and Lee T. Aortic valve grafts in the rat: evidence for rejection. *J Thorac Cardiovasc Surg.* 114: 891-902 (1997).

9. O'Brien MF, Stafford 0, Gardner Metal. The viable cryopreserved allograft aortic valve. *J Cardiac Surg.* 2 [Suppl]: 153-167 (1987).

10. Shaddy RE, Naftel DC, Kirklin JK, Boyle G, McGiffin DC, Towbin JA, Ring S, and Pearce B. Outcome of cardiac transplantation in children: survival in a contemporary multi-institutional experience. *Circulation* 94 (9 Suppl 2): 69-73 (1996).

11. Shaddy RE, Thompsoin DD, Osborne KA, Hawkins JA, and Fuller TC. Persistence of humana leukocyte antigen (HLA) antibodies after one year in children receiviing cryopreserved valve allografts. *Am J Cardiol.* 80: 358-359 (1997).

12. Suh H, Lee JE, Park J--C, Han D-W, Yoon C-S, Park YH, and Cho BK. Viability and enzymatiьc activity of cryopreserved porcine heart valve. *Yonsei Med J.* 40 (2): ṭ184-190. (1999).

13. Woods EJ, Zieger MAьJ, Lakey JRT, Liu J, and Critser JK. Osmotic characteristics of isoolated human and canine pancreatic islets. *Cryobiology.* 35: 106-1 13. (1997).

Figure 2.1. Cell volume kinetics of endothelial cells exposed to 5x isotonic PBS at 22°C. Blue circle = mean relative volume cell over time intervals of 3sec. Black circle = number of cells averaged for each data point. Black line = fitted curve to data using least-square error method.
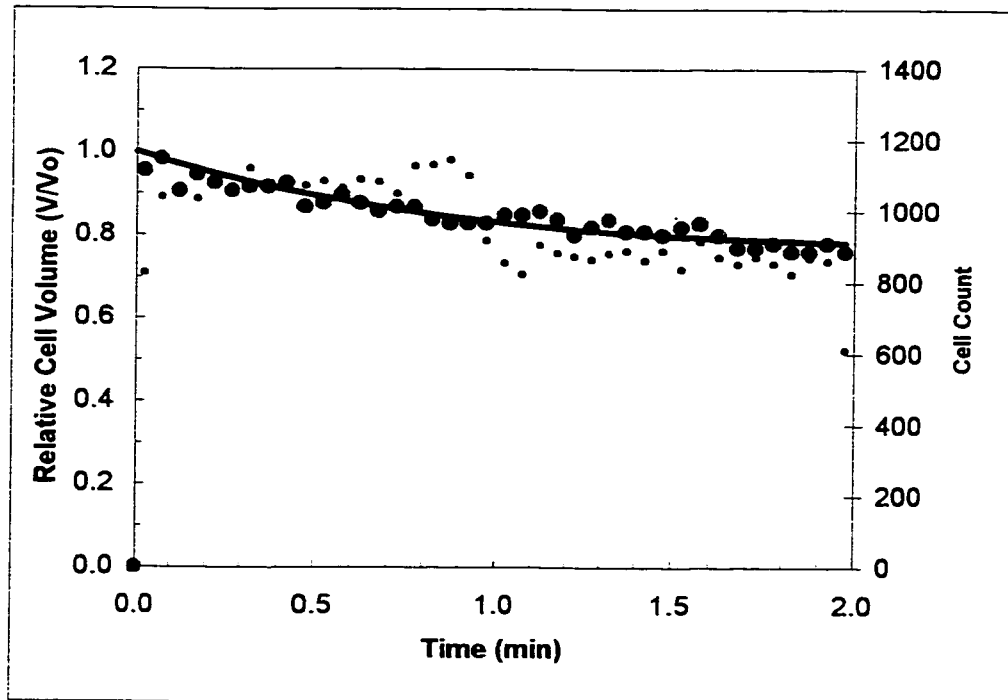
Figure 2.2. Cell volume kinetics of fibroblast cells exposed to 2x isotonic PBS at 4°C. Blue circle = mean relative cell volume over time intervals of 3sec. Black circle = number of cells averaged for each data point. Black line = fitted curve to data using least-square error method.

38

Table 2.1 Endothelial and Fibroblast Cell Suspensions: Osmotically Inactive Fraction (Vb). (mean ± standard error)

Endothelial V_b (V/V$_o$)

	4°C	10°C	22°C	Aggregate
2x PBS	0.515 ± 0.014 [n=6]	0.380 ± 0.025 [n=6]	0.372 ± 0.032 [n=9]	0.415 ± 0.021 [n=21]
3x PBS	0.498 ± 0.009 [n=6]	0.365 ± 0.015 [n=6]	0.360 ± 0.012 [n=9]	0.401 ± 0.015 [n=21]
4x PBS	0.488 ± 0.007 [n=6]	0.347 ± 0.019 [n=6]	0.355 ± 0.008 [n=9]	0.392 ± 0.016 [n=21]
5x PBS	0.490 ± 0.010 [n=6]	0.340 ± 0.019 [n=6]	0.343 ± 0.009 [n=8]	0.386 ± 0.017 [n=20]
Aggregate	0.498 ± 0.005 [n=24]	0.358 ± 0.010 [n=24]	0.358 ± 0.009 [n=35]	0.399 ± 0.009 [n=83]

Fibroblast V_b (V/V$_o$)

	4°C	10°C	22°C	Aggregate
2x PBS	0.414 ± 0.030 [n=10]	0.362 ± 0.015 [n=8]	0.364 ± 0.036 [n=8]	0.383 ± 0.017 [n=26]
3x PBS	0.386 ± 0.004 [n=10]	0.415 ± 0.006 [n=9]	0.365 ± 0.027 [n=9]	0.389 ± 0.010 [n=28]
4x PBS	0.377 ± 0.020 [n=8]	0.347 ± 0.018 [n=9]	0.351 ± 0.020 [n=9]	0.358 ± 0.011 [n=26]
5x PBS	0.370 ± 0.005 [n=8]	0.326 ± 0.019 [n=9]	0.328 ± 0.019 [n=9]	0.340 ± 0.010 [n=26]
Aggregate	0.388 ± 0.010 [n=36]	0.363 ± 0.009 [n=35]	0.352 ± 0.013 [n=35]	0.368 ± 0.006 [n=106]

Table 2.2 Endothelial and Fibroblast Cell Suspensions: Hydraulic Conductivity (L_p) During Exposure to Hypertonic Solutions and Cryoprotectants (1M DMSO, 2M DMSO, and 1M PG). (mean + standard error)

	Endothelial L_p (um/min/atm)			Fibroblast L_p (um/min/atm)		
	4°C	10°C	22°C	4°C	10°C	22°C
2x PBS	0.078 ± 0.002 [n=6]	0.171 ± 0.015 [n=6]	0.432 ± 0.014 [n=9]	0.117 ± 0.010 [n=10]	0.265 ± 0.017 [n=8]	0.417 + 0.014 [n=8]
3x PBS	0.082 ± 0.003 [n=6]	0.200 ± 0.012 [n=6]	0.431 ± 0.010 [n=9]	0.114 ± 0.009 [n=10]	0.239 ± 0.016 [n=9]	0.385 ± 0.015 [n=9]
4x PBS	0.078 ± 0.004 [n=6]	0.187 ± 0.012 [n=6]	0.413 ± 0.010 [n=9]	0.112 ± 0.008 [n=8]	0.266 ± 0.005 [n=9]	0.393 ± 0.011 [n=9]
5x PBS	0.184 ± 0.105 [n=6]	0.215 ± 0.004 [n=6]	0.419 ± 0.015 [n=8]	0.110 ± 0.005 [n=8]	0.262 ± 0.005 [n=9]	0.400 ± 0.013 [n=9]
1M DMSO	0.120 ± 0.002 [n=8]	0.158 ± 0.004 [n=6]	0.455 ± 0.048 [n=9]	0.069 ± 0.004 [n=9]	0.136 ± 0.009 [n=9]	0.323 ± 0.011 [n=9]
2M DMSO	0.137 ± 0.005 [n=9]	0.188 ± 0.005 [n=6]	0.342 ± 0.053 [n=8]	0.100 ± 0.004 [n=8]	0.226 ± 0.023 [n=9]	0.393 ± 0.013 [n=9]
1M PG	0.134 ± 0.005 [n=8]	0.174 ± 0.007 [n=9]	0.501 ± 0.041 [n=9]	0.173 ± 0.026 [n=9]	0.466 ± 0.042 [n=9]	0.646 ± 0.025 [n=9]
Aggregate	0.119 ± 0.013 [n=49]	0.184 ± 0.004 [n=45]	0.429 ± 0.013 [n=61]	0.114 ± 0.006 [n=62]	0.266 ± 0.014 [n=62]	0.422 ± 0.013 [n=62]

40
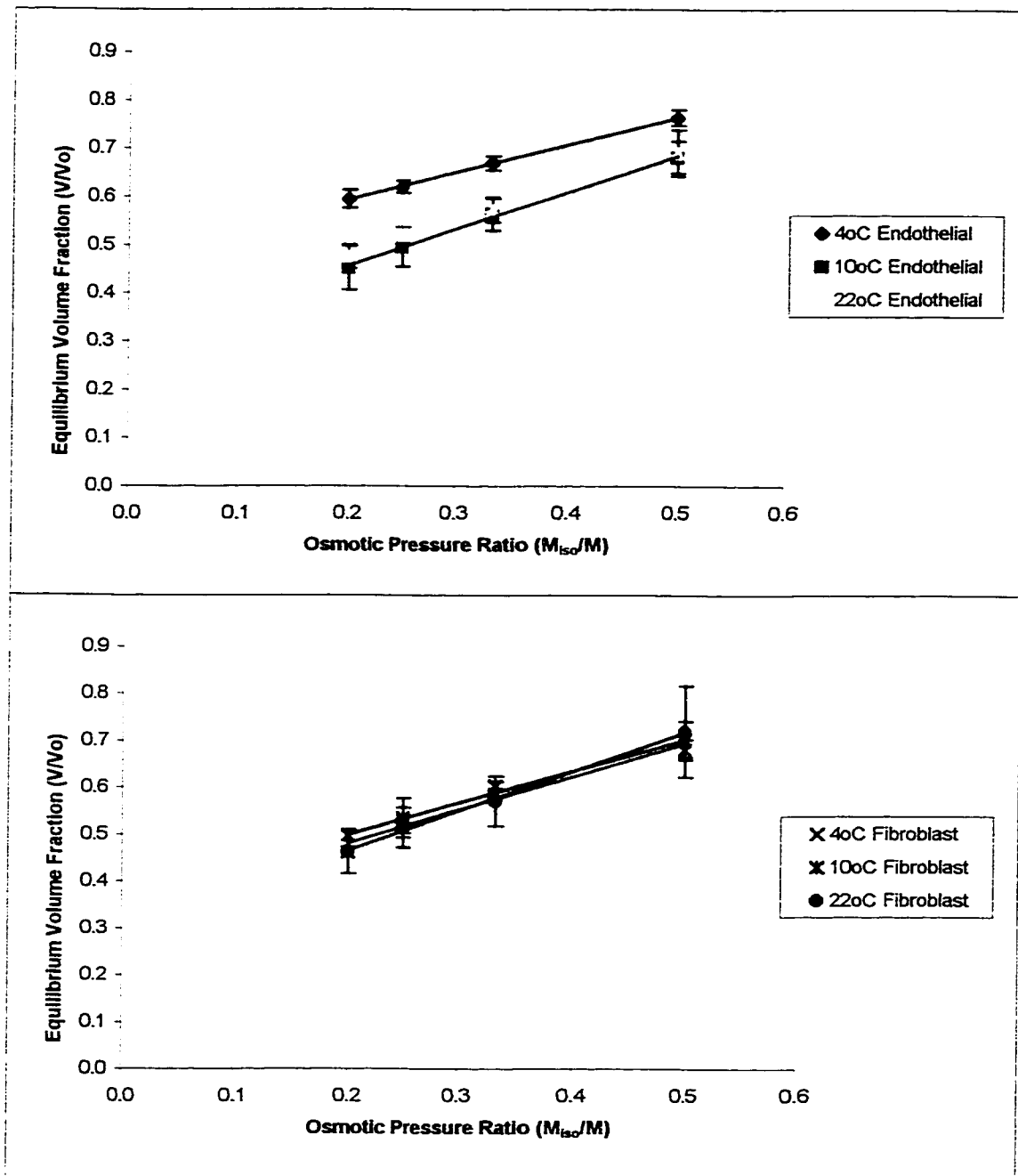
Figure 2.3. Boyle van't Hoff plot of endothelial and fibroblast equilibrium volume fractions at 4°C, 10°C, and 22°C. Endothelial (top) and fibroblast (bottom) V_b can be determined by extrapolation to the y-intercept. Error bars = standard error.
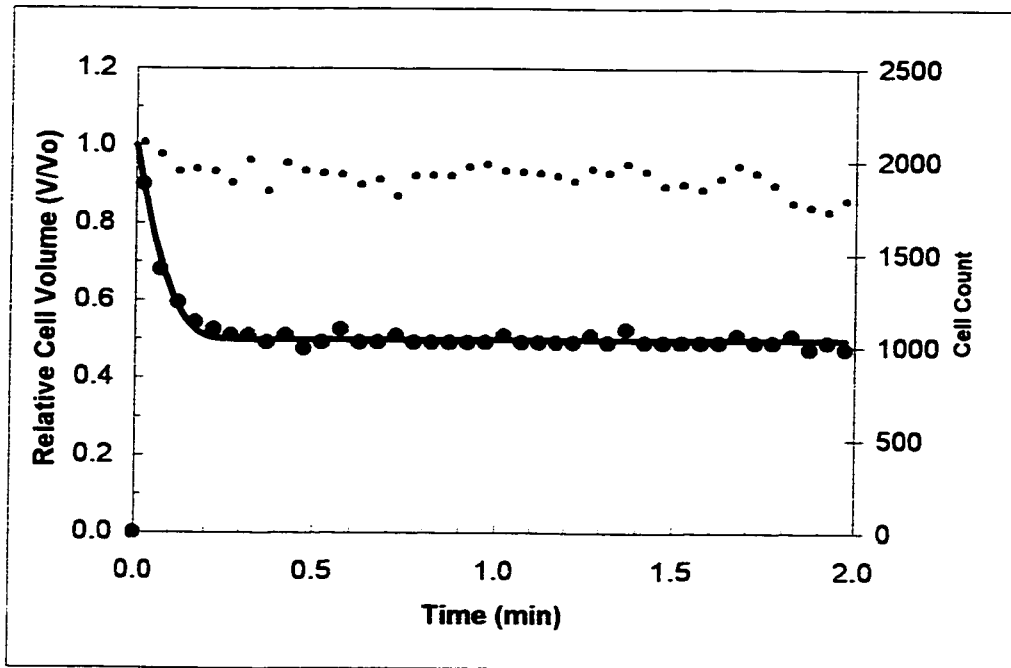
Figure 2.4. Cell volume kinetics of endothelial cells exposed to 1M DMSO at 4°C. Blue circle = mean relative volume cell over time intervals of 3sec. Black circle = number of cells averaged for each data point. Black line = fitted curve to data using least-square error method.
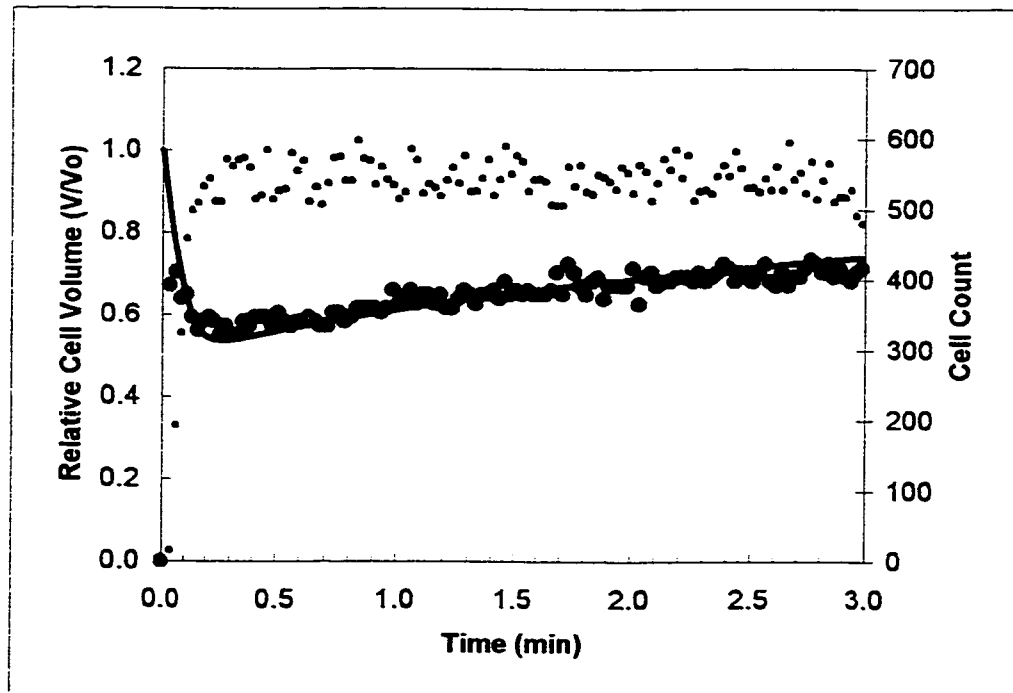
Figure 2.5. Cell volume kinetics of endothelial cells exposed to 2M DMSO at 4°C. Blue circle = mean relative volume cell over time intervals of 1.5sec. Black circle = number of cells averaged for each data point. Black line = fitted curve to data using least-square error method.

Figure 2.6. Cell volume kinetics of fibroblast cells exposed to 1M PG at 22°C. Blue circle = mean relative volume cell over time intervals of 1.5sec. Black circle = number of cells averaged for each data point. Black line = fitted curve to data using least-square error method.
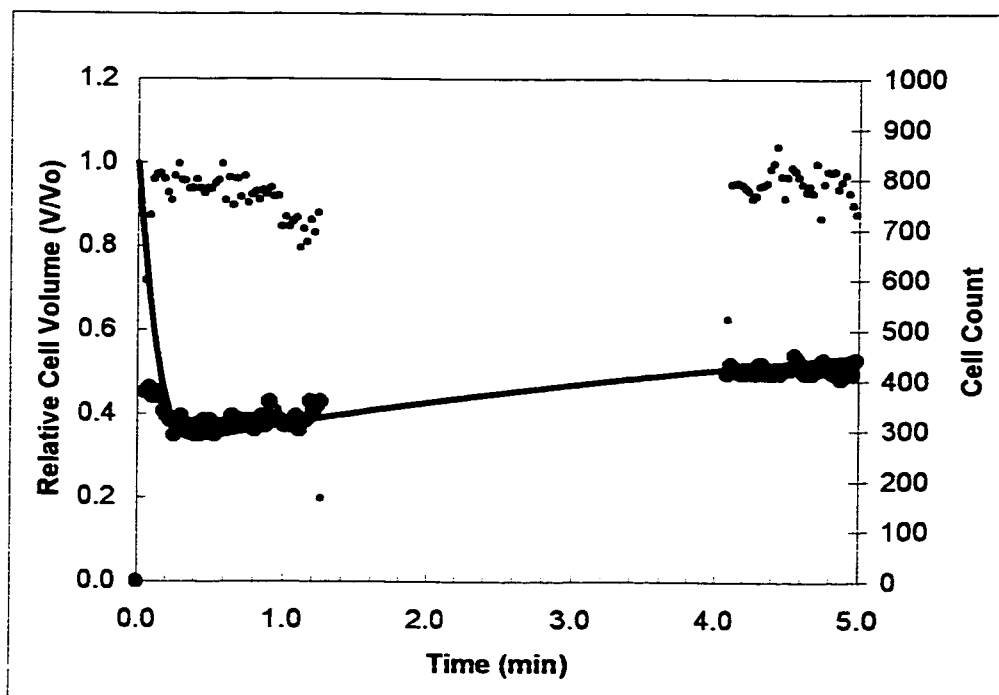
Figure 2.7. Cell volume kinetics of fibroblast cells exposed to 2M PG at 4°C. Blue circle = mean relative volume cell over time intervals of 1.5sec. Black circle = number of cells averaged for each data point. Black line = fitted curve to data using least-square error method.
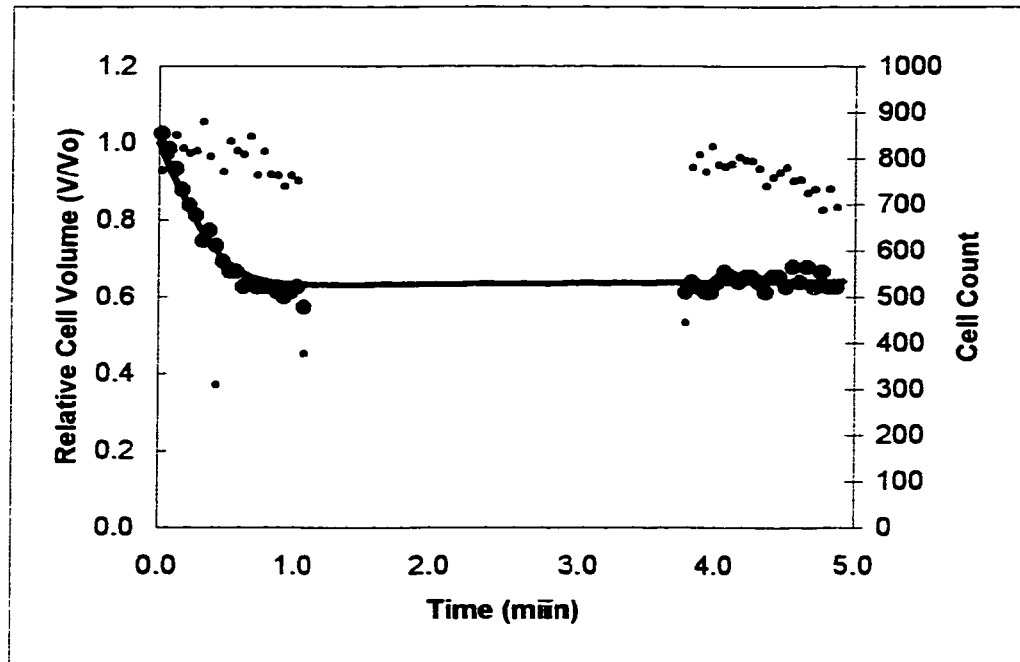
Figure 2.8. Cell volume kinetics of endothelial cells exposed to 1M glycerol at 4°C. Blue circle = mean relative volume cell over time intervals of 3sec. Black circle = number of cells averaged for each data point. Black line = fitted curve to data using least-square error method.

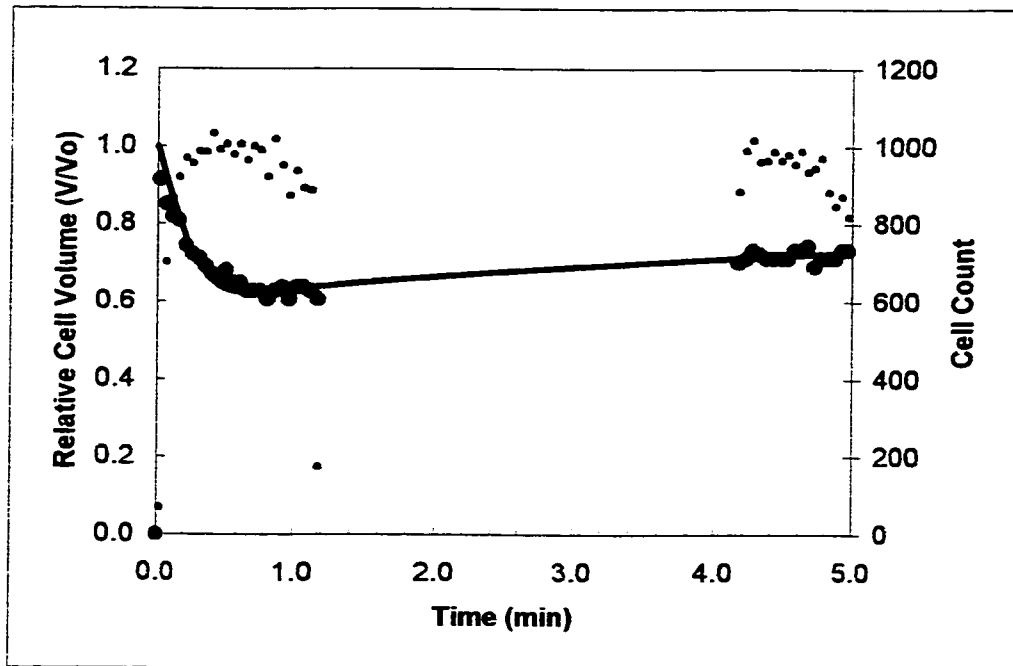**Figure 2.9.** Cell volume kinetics of endothelial cells exposed to 2M glycerol at 22°C. Blue circle = mean relative volume cell over time intervals of 1.5sec. Black circle = number of cells averaged for each data point. Black line = fitted curve to data using least-square error method.

Table 2.3 Endothelial and Fibroblast Cell Suspensions: Solute Permeability (P_s) During Addition of Cryoprotectants (1M DMSO, 2M DMSO, and 1M PG). (mean ± standard error)

	Endothelial P_s (um/min)			Fibroblast P_s (um/min)		
	4°C	10°C	22°C	4°C	10°C	22°C
1M DMSO	0.303 ± 0.012 [n=8]	3.476 ± 0.173 [n=6]	24.292 ± 1.730 [n=9]	0.715 ± 0.081 [n=9]	2.172 ± 0.177 [n=9]	8.502 ± 1.079 [n=9]
2M DMSO	0.333 ± 0.044 [n=9]	3.098 ± 0.174 [n=6]	20.695 ± 3.305 [n=8]	0.450 ± 0.028 [n=8]	0.836 ± 0.074 [n=9]	7.461 ± 0.738 [n=9]
Aggregate	0.319 ± 0.024 [n=17]	3.287 ± 0.130 [n=12]	22.599 ± 1.801 [n=17]	0.590 ± 0.055 [n=17]	1.504 ± 0.187 [n=18]	7.982 ± 0.647 [n=18]
1M PG	0.361 ± 0.038 [n=8]	3.781 ± 0.446 [n=9]	16.242 ± 1.639 [n=9]	0.534 ± 0.130 [n=9]	0.839 ± 0.236 [n=9]	7.814 ± 0.946 [n=9]
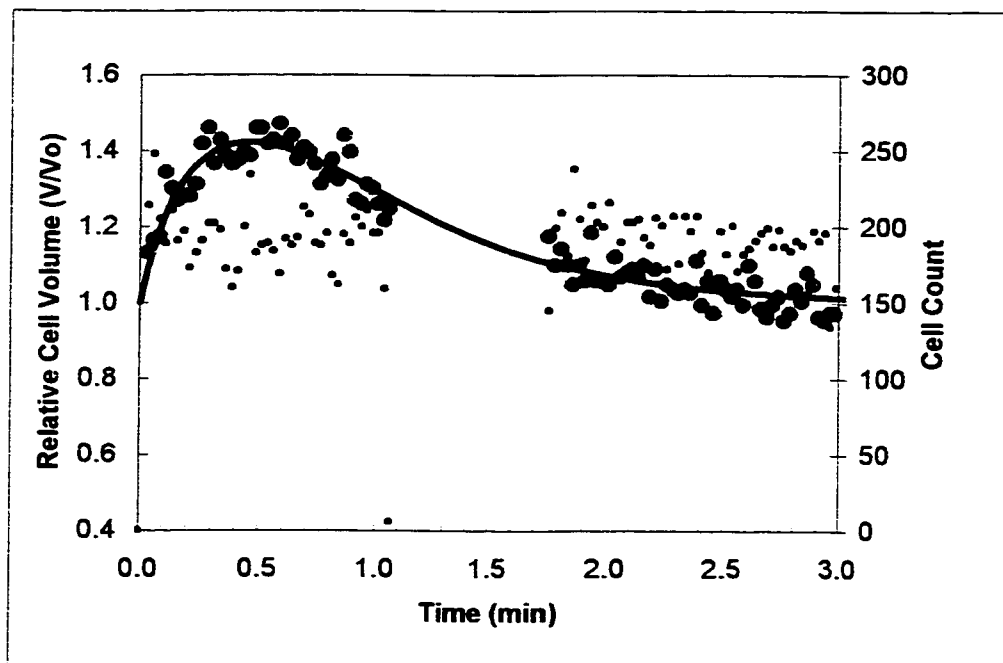
Figure 2.10. Cell volume kinetics of endothelial cells equilibrated to 1M DMSO then returned to isotonic conditions at 4°C. Blue circle = mean relative volume cell volume over time intervals of 3sec. Black circle = number of cells averaged for each data point. Black line = fitted curve to data using least-square error method.
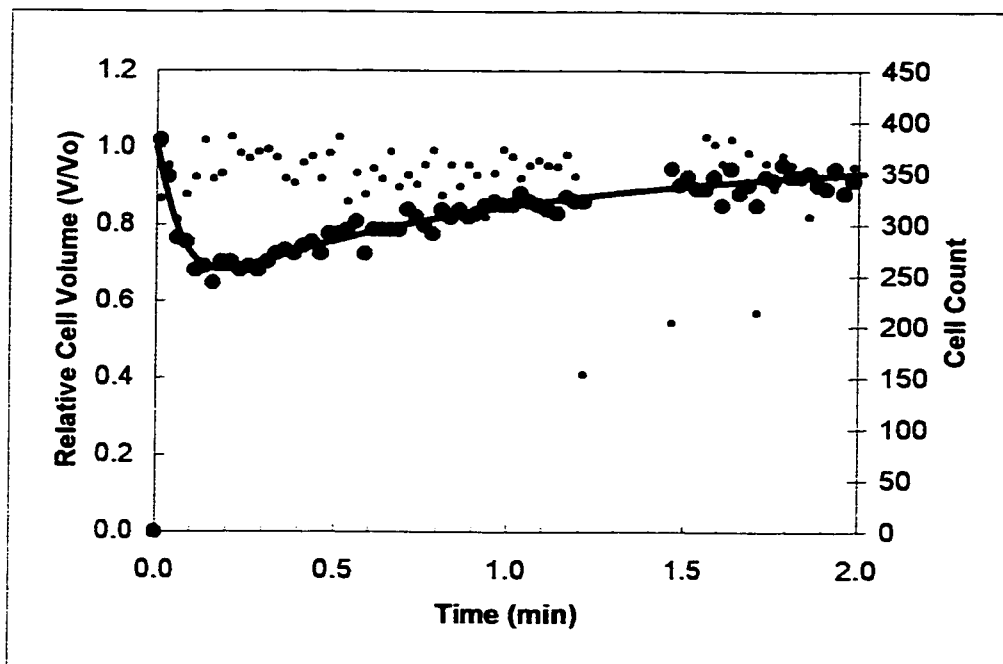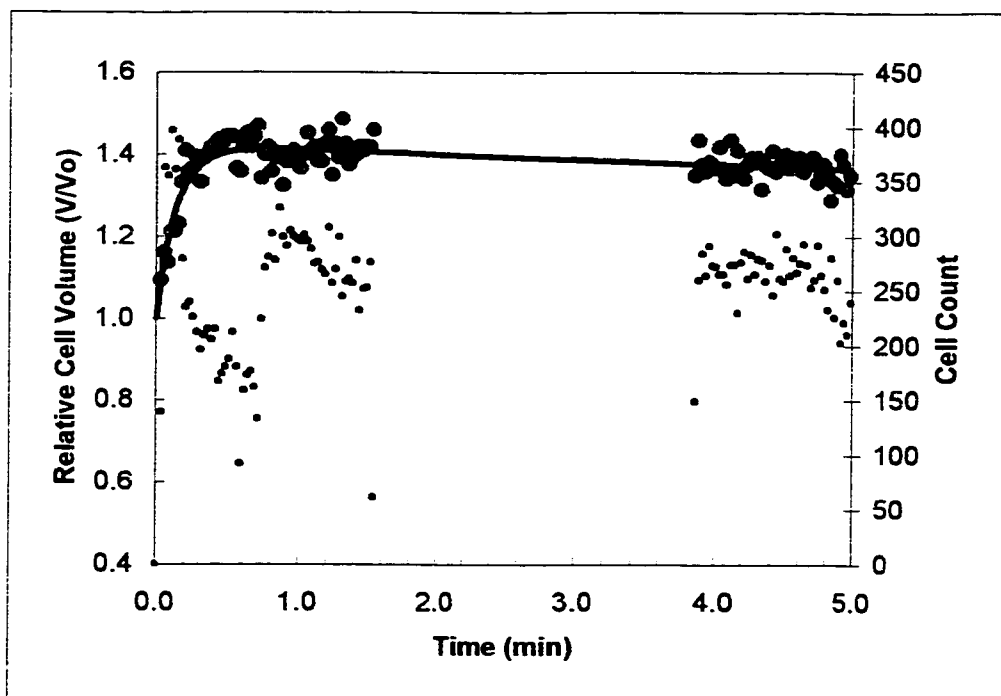

Figure 2.11. Cell volume kinetics of fibroblast cells equilibrated to 2M DMSO then returned to isotonic conditions at 10°C. Blue circle = mean relative volume cell volume over time intervals of 1.5sec. Black circle = number of cells averaged for each data point. Black line = fitted curve to data using least-square error method.

46
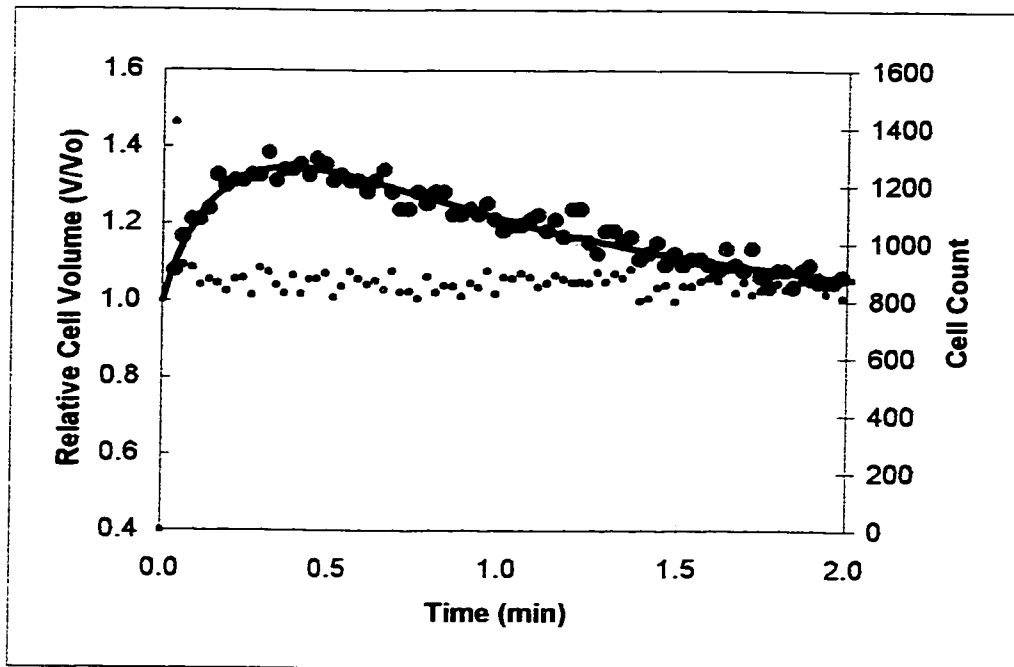
Figure 2.12. Cell volume kinetics of endothelial cells equilibrated to 1M PG then returned to isotonic conditions at 22°C. Blue circle = mean relative volume cell volume over time intervals of 1.5sec. Black circle = number of cells averaged for each data point. Black line = fitted curve to data using least-square error method.
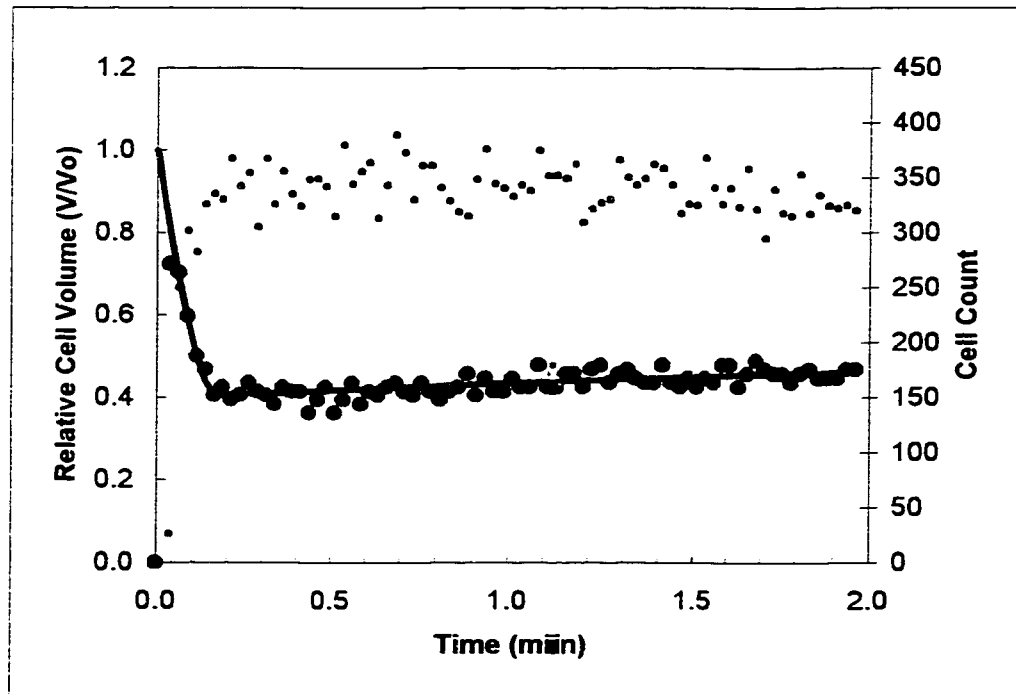
Table 2.4 Endothelial and Fibroblast Cell Suspensions: Solute Permeability (P_s) During Removal of Cryoprotectants (1M DMSO, 2M DMSO, and 1M PG). (mean ± standard error)

	Endothelial P_s (um/min)			Fibroblast P_s (um/min)		
	4°C	10°C	22°C	4°C	10°C	22°C
1M DMSO	0.922 ± 0.126 [n=8]	1.794 ± 0.037 [n=8]	7.304 ± 0.628 [n=9]	1.552 ± 0.030 [n=9]	2.451 ± 0.099 [n=9]	8.161 ± 1.196 [n=9]
2M DMSO	1.708 ± 0.223 [n=9]	2.824 ± 0.167 [n=9]	11.638 ± 2.320 [n=8]	3.424 ± 0.117 [n=8]	5.021 ± 0.495 [n=8]	15.654 ± 0.789 [n=9]
Aggregate	1.338 ± 0.162 [n=17]	2.279 ± 0.150 [n=17]	9.343 ± 1.227 [n=17]	2.433 ± 0.240 [n=17]	5.021 ± 0.495 [n=17]	15.654 ± 0.789 [n=18]
1M PG	0.880 ± 0.055 [n=9]	2.097 ± 0.095 [n=9]	13.375 ± 2.307 [n=7]	1.466 ± 0.067 [n=8]	2.561 ± 0.109 [n=9]	5.829 ± 0.307 [n=9]
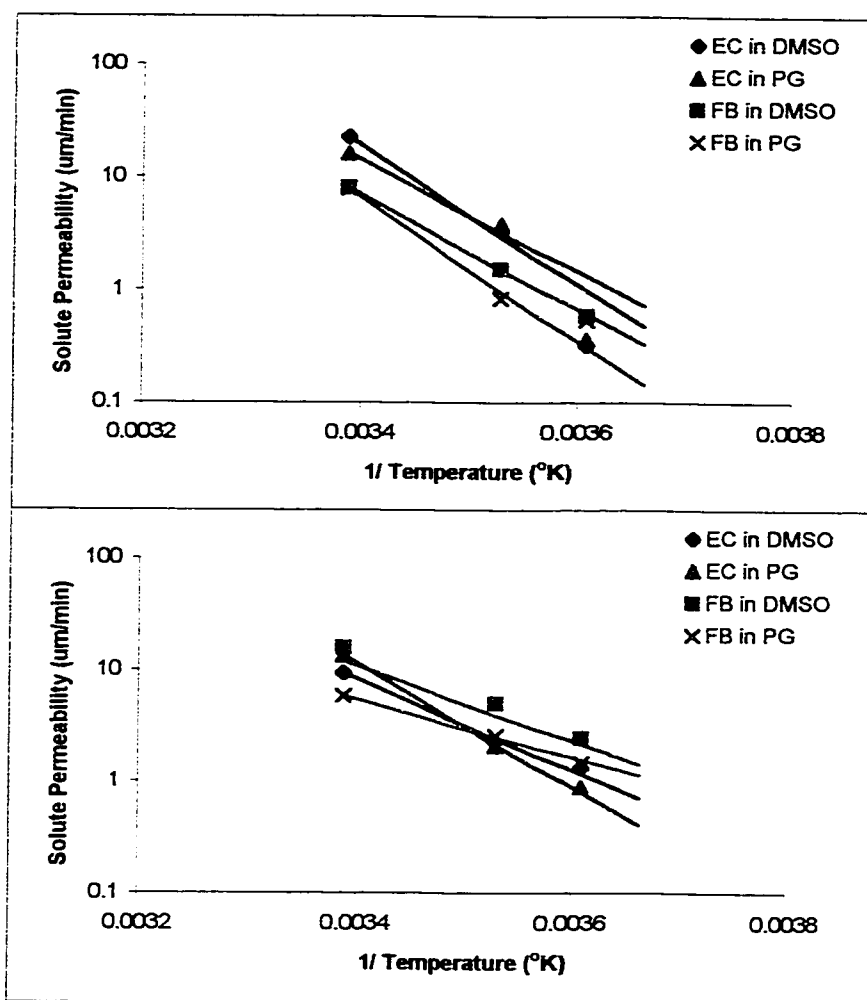
Figure 2.13. Solute permeability of endothelial cells (EC) and fibroblasts (FB) during addition (top) and removal (bottom) of dimethyl sulfoxide and propylene glycol.

Table 2.5 Osmotic Parameters of Endothelial Cells and Fibroblasts. (mean ± standard error)

	V_o (um³)	V_b (V/Vo)	L_p* (um/min/atm)	E_a of L_p (kCal/mol)	$P_{s(DMSO)}$** (um/min)	E_a of $P_{s(DMSO)}$ (kCal/mol)	$P_{s(PG)}$** (um/min)	E_a of $P_{s(PG)}$ (kCal/mol)
Endothelial	2513 ± 154 [n=17]	0.399 ± 0.009 [n=83]	0.087 ± 0.010	11.6 ± 0.2	0.473 ± 0.017	28.2 ± 0.4	0.724 ± 0.024	22.7 ± 0.6
Fibroblast	2866 ± 195 [n=18]	0.386 ± 0.006 [n=106]	0.122 ± 0.011	9.2 ± 0.2	0.329 ± 0.021	23.2 ± 0.5	0.143 ± 0.030	29.1 ± 0.8

*Extrapolated to 0°C from data at 4°C, 10°C, and 22°C.

**Extrapolated to 0°C from data at 4°C, 10°C, and 22°C; Based on addition of cryoprotectants.

CHAPTER 3

GRADED FREEZING OF INTACT HEART VALVE LEAFLETS AND VIABILITY ASSAY BY CONFOCAL MICROSCOPY

3.1 Introduction

Assessments of Viability

Ultimately, the goal of cryopreservation is to achieve a viable tissue or cell after thawing. However, the terms 'viable' or 'viability' can be quite ambiguous. As defined by Pegg (25), "viable cells, tissues and organs are those that are alive or capable of living." What is it that we mean by "living"? In basic biology classes, all living things are characterized as having 3 distinct qualities – growth, reproduction, and irritability. Does this fit within the context of cryopreservation? At -196°C, a cell shows no growth, no replication, and no response to stimulus. Is it dead or alive? Pegg proposed that viability be defined as the ability of a sample to exhibit a specific function(s) as expressed as a proportion of the function(s) exhibited by an identical sample prior to treatment (25). What then is an appropriate function to assess viability?

Viability assays or outcomes can be categorized into 5 major groupings (25). These are: (a) cell membrane integrity, (b) cellular metabolic activity, (c) mechanical properties of the tissue, (d) cellular mitotic activity, and (e) complete *in vivo* function.

Viability assays involving complete *in vivo* function for heart valves were reviewed extensively in Chapter 1, and remain the paradigm to testing tissues. It is the paradigm because complete *in vivo* function requires all

51

other activities and properties to be synchronized. However, to perform *in vivo* assays of tissues cryopreserved by novel protocols in humans is unethical. Hence animals models are required. Such a model has been developed and used by Moustapha *et al.* (20) to test rejection in rats. It seems reasonable that any tissue cryopreserved by new methods or procedures is tested in animal models prior to clinical trials in humans. However, to warrant sacrificing animals in experimental procedures for *in vivo* assessments, evidence of viability is then necessary by the other four methods. It is necessary to note that these studies with cryopreservation protocols are variable. Most procedures use 10% DMSO but, cooling and warming rates varied.

Although heart valve viability has been tested in numerous cases using the mitotic activity of the cells, basal mitotic activity is low since cells of the heart valve leaflet function to maintain the collagen-elastin matrix. Generally, assessments have measured either DNA (12) or protein synthesis (2,15,18).

Al-Janabu *et al.* (2) utilised the common technique of radio-labeled amino acids and scintillation counts to measure uptake and incorporation into proteins in fresh aortic and pulmonary valve allografts. They had concluded that protein synthesis diminishes with the age of fresh heart valves.

Lupinetti *et al.* (15) went further to examine the synthesis of procollagen in fresh and cryopreserved aortic valves. This study evaluated synthesis of procollagen, a precursor to collagen, when fresh and cryopreserved rat aortic valve grafts were implanted heterotopically into the

52

abdominal aorta. Grafts were excised after 2 to 21 days and stained immunocytochemically for procollagen. The production of procollagen exhibited was equal or exceeded procollagen production of native valves regardless of preservation. It was concluded that the fibroblasts of these valves were viable.

Mechanical properties have also been used as a measure of heart valve outcome after cryopreservation. Historically heart valve leaflets were evaluated upon the basis of its elastic properties (22,24), but contractile properties have also been used to characterize the outcome (30).

The effect of antibiotic–nutrient preservation on the elasticity of human aortic valves was tested by Ng and Wright (22). Leaflets from valves were fastened to a pressure chamber by steel rings and when pressure on one surface was increased, the extension of the leaflet cusp was measured. This gave pressure-volume curves which exhibited a decrease in elasticity with length of time valves were stored in antibiotic-nutrient media.

In another study, contractile properties were used to evaluate the effect of cryopreservation. Although contractility is not normally a function of heart valve leaflets, Wassenaar et al. felt it may provide an additional model to verify viability (30). In this study, fresh leaflets responded to potassium (K^+; 100 mmol/L) with an isometric contraction of 1.6 ± 0.14 mN. However, cryopreserved valvular leaflets expressed a contraction only 24% that of fresh leaflets. By this measure of outcome, cryopreservation was detrimental to the heart valve.

Another alternative for determining viability involves measuring metabolic activity. Metabolic activity for heart valves has generally been done in two fashions, either by metabolite uptake (3,11) or by enzymatic activity (14,27,28).

Metabolite uptake, like protein synthesis, requires radiolabels and autoradiography techniques. Armiger (3) utilized these techniques to determine the uptake of tritiated glucosamine for each layer of the canine valve leaflet (ventricularis, spongiosa, and fibrosa). The spongiosa, for example, showed 10.0 ± 4.5 grain counts/unit area in freshly collected samples, while cryopreserved samples had 0.7 ± 0.7 grain counts/unity area. Cryopreserved specimens showed significantly diminished uptake levels of tritiated glucosamine at all 3 layers.

An extensive evaluation was performed by Suh *et al.* (27) on the enzymatic activity of cryopreserved porcine heart valves. The activities of 19 different enzymes were analyzed after 24 hours warm ischaemic time, subsequent 24 hours cold ischaemic time and then cryopreservation. Warm ischaemic time of 24 hours reduced fibroblast enzymatic activity to $57.0\pm10.2\%$ ($p<0.05$) and subsequent cold ischaemic treatment reduced viability significantly ($p<0.05$). However, cryopreservation following these treatments showed no effect on enzyme activity.

Armiger (3) had determined viability decreases with cryopreservation, yet Suh *et al.* (27) concluded otherwise using enzyme activity as an assay. Is there a more consistent viability assay?

Perhaps the most basic viability assay is that of physical integrity. Within a tissue, such as a heart valves leaflets, this has two components – the collagen/elastin matrix and the cellular components of the tissue. Cryopreservation of heart valves have been evaluated macroscopically (29) and by electron microscopy (either scanning or transmission) (1,5,6,7,10,13). Cellular viability has also been examined by dye exclusion techniques (23,31) which evaluate cell membrane integrity.

Electron microscopy has been used to visualize both endothelial cells (1,5,7,8,19,35), collagen bundles in the matrix (26,13), and fibroblasts (6). Endothelial cells occur as elongated and polygonal forms on the leaflet surface (13) and following cryopreservation show loss of plasma membrane integrity and presence of karyolysis (7) through transmission electron microscopy.

Scanning electron microscopy of valve leaflets generally showed a lack of endothelial cells, although patchy areas of endothelial cells were present (1). Although, electron microscopy typically showed a loss of endothelium, Mohan et al. (19) have also shown the presence of a confluent endothelial monolayer following cryopreservation.

In discussing water permeability, solute permeability, volume expansion or contraction, and intracellular versus extracellular environments, the critical factor is the cell membrane. Without an intact membrane, the cell ceases to function regardless of DNA or protein synthesis, enzyme activity, or

mechanical property of the tissue. Therefore, a better alternative for assessing cell viability would be to evaluate cell membrane integrity.

Membrane integrity for heart valves has been examined using a dual stain of FDA/PI (fluorescein diacetate/propidium iodide) and flow cytometry (23). Fibroblasts were enzymatically isolated from fresh or cryopreserved heart valves and stained with FDA/PI before being scanned by flow cytometry. Cells that were stained positive for FDA and negative for PI were viable. Only cells having an intact cell membrane could exclude PI. Niwaya *et al.* (23) found that fibroblasts viability was >70% in a cryopreserved allograft. However, this value is most likely inflated as damaged cells can be lost during cryopreservation and isolation. This can be partially overcome if cell membrane integrity could be examined *in situ*.

Graded Freezing and Assessment

These experiments evaluated cell membrane integrity of heart valve leaflets cryopreserved by graded freezing. Graded freezing resolves progressive damage to the cells caused by either "solution effects" or intracellular ice formation. Graded freezing has been used previously to examine cellular damage to granulocytes (4,32), fibroblasts (18), and lymphocytes (18). Briefly, samples are cooled at 1°C/min to –5°C, ice nucleation initiated and held at –5°C for 5 min to allow the release of latent heat of fusion. Samples continue to be cooled at 1°C/min and at 5°C intervals from –5 to –40°C, samples are removed and either thawed immediately or immersed in liquid nitrogen. Cells were assayed for cell membrane integrity

with FDA. Typical recoveries from graded freezing of cells in suspension are illustrated in **Figure 3.1**.

Thawed samples typically showed high recovery at high sub-zero temperatures, which diminished with decreased temperatures. Plunged samples showed low recoveries at high sub-zero temperatures. The recovery increased then fell to give a range of temperatures that yielded highest recovery. At lower sub-zero temperatures, damage from rapid cooling in plunged samples were minimal and gave recoveries like those in thawed samples at those temperatures. The addition of cryoprotectants shifted these curves to the right and upwards. Recoveries with cryoprotectants generally increased recovery at lower sub-zero temperatures. However, these results were only typical for cells in suspensions but, cells in tissues will be more complex.

3.2 Materials and Methods

Graded Freezing

Porcine heart valve leaflets were obtained in the same methods as previously described in Chapter 2.

The 3 leaflets from either aortic or pulmonic valve were assigned randomly to either the "control", "thaw" or "plunge" group. The control group was maintained in 500µl PBS (Gibco BRL) at 4°C throughout the experiment until confocal microscopy analysis was performed. Both the thaw and plunge groups were placed in a flat-bottomed glass vial (¼" internal diameter, 1 ¾" in height) in 500 µl of the experimental solution (PBS, 1M DSO, 2M DMSO, or

1M PG) and allowed to equilibrate at 4°C for 1 hour. Samples were then cooled at a rate of 1°C/min to -5°C in a controlled-rate ethanol bath (Multi-Cool Bath, FTS Systems Inc., USA), then were nucleated by applying cooled tweezers to the exterior of the vials. Samples were held at -5°C for 5min before continuing to cool at 1°C/min to -40°C. At each experimental temperature (4, -5 (after holding), -10, -15, -20, -25, -30 and -40°C), leaflets from the same valve were chosen - one was thawed in a 37°C water bath and stored at 4°C while the other sample was immediately plunged into liquid nitrogen, then thawed in the same fashion. [The rapid cooling and warming rates were experimentally determined to be 158°C/min and 234°C/min by directly measuring and averaging 3 samples plunged in liquid nitrogen from 0°C, then warmed in a 37°C water bath. Measurements were made using a copper/constantan thermocouple (Omega, USA) and digital thermocouple thermometer (Digi-Sense, USA).] Following thawing of frozen samples, leaflets were removed and washed in PBS at 4°C. Removal of cryoprotectants was done by placing the leaflets in microfuge tubes (Fisher Brand) with 1.5 ml PBS and stored at 4°C in ice water for at least 1 hour. Each condition was repeated in triplicate for n=3.

Cell Membrane Integrity Assay

While samples were in PBS at 4°C following the graded freeze to remove the cryoprotectants, they were concurrently stained with SYTO/EB. SYTO/EB stain is a dual fluorescent stain able to assess cell membrane integrity (32). SYTO 13 (Molecular Probes, Eugene, OR) permeates the cell

membrane, complexes with DNA and fluoresces green when excited by laser or ultraviolet light. EB (Sigma Chemical Company, Mississuaga, ON), on the other hand, is only able to enter cells which have damaged cell membranes and also complexes with DNA (9) Upon excitation by laser or ultraviolet light, EB fluoresces red. Cells stained red by EB masks the green fluorescence in that cell. The dual stain together differentiates between intact and damage cells. This damage has been shown to correlate to cell viability of cells (33).

The SYTO/EB stain was prepared by adding 150 µl of 25 µM EB stock solution and 150 µl of 12.5µM SYTO 13 stock solution to 15 ml PBS. Final concentrations were 2.5 µM EB and 1.25 µM SYTO. This solution was used to stain the samples and to remove cryoprotectants from the samples over the minimum duration of 1 hour.

Confocal Microscopy and Analysis

Each sample after being stained was set on a glass slide and covered with a glass coverslip to minimize dehydration of the sample. By using a single-photon laser confocal microscope (MD Multiprobe 2001, Molecular Dynamics, USA), the dual fluorescence of the SYTO/EB stain was imaged and captured by computer (Silicon Graphics Indigo, USA) at increasing depths into the sample. Images were taken at depths of 0µm, 30µm, 60µm and 90µm into the samples. The opacity of the samples limited the depth of imaging. The images at 0µm represented endothelial cells on the surface of the leaflet while images at 30µm, 60µm and 90µm represented fibroblast cells in the leaflet matrix (**Figure 3.2**).

For each image, the number of 'viable' and 'nonviable' cells were counted. Green cells were considered viable, while red and yellow cells were considered nonviable. Yellow cells were the result of cells stained with SYTO and insufficient EB to mask the SYTO stain completely. Percent recovery was calculated as the number of viable cells per total cell count in each image. A relative recovery was determined for the thawed and plunged samples by dividing the percent recovery of the experimental sample by the percent recovery of the internal control sample. The mean and standard error of relative recoveries for triplicate samples were determined and plotted against the temperature of initial rapid cooling (**Figure 3.3**). Trendlines were determined for conditions of freezing solution and image depth in the leaflet.

3.3 Results

Graded Freezing

Trendlines for leaflets frozen in PBS, 1M DMSO, 2M DMSO, and 1M PG are presented in **Figures 3.4, 3.5, 3.6**, and **3.7**, respectively. Depths of 0μm, 30μm, 60μm, and 90μm are shown for thawed and plunged samples separately. Complete graphical analysis is presented in **Appendix I**.

In all test solutions, plunged samples showed lower cell recovery than thawed samples. However, thawed samples did not exhibit 100% recovery at all temperatures. This substantiates Mazur's two-factor hypothesis of cell injury during freezing (16). Cell membranes become damaged during both low cooling rates (1°C/min) and high cooling rates (immersion in liquid nitrogen).

Thawed and plunged samples frozen in each solution exhibited decreasing cell recovery with increasing depths into the tissue. Trendlines showed greatest recovery from 0um to 30um to 60um to 90um. An exception was exhibited by freezing in 1M DMSO, which showed lowest recovery at 0um. Since cells at the 0um depth represent the endothelial cells, fibroblasts had better recovery under this freezing condition. However, the general decrease in recovery with increase in depth of the tissue suggested that a there is another factor leading to cell damage in tissues.

Samples frozen in PBS were controls for graded freezes with cryoprotectants. Comparing the trendlines for PBS samples (**Figure 3.4**) to cryoprotectant samples (**Figures 3.5, 3.6,** and **3.7**) showed an increase in viability. In PBS samples, viability of thawed samples decreases as the temperature of rapid cooling decreases. In these samples, the trendlines exhibited 0% recovery between -30 and -40°C. Trendlines for plunged samples ranged in viability of 10-20%. Cryoprotectants increased the relative recovery of thawed and plunged samples. Thawed samples lower temperatures (-30°C to -40°C) were increased to 40-80% recovery at -40°C, while leaflets plunged in cryoprotectants increased recovery to 20-60%. This demonstrates the cryoprotective properties of DMSO and PG.

In some cases, the recoveries of the internal control samples were lower than its experimental samples and this inflated the relative recovery of leaflets from that valve. Consequently, some trendlines extend beyond 100% relative recovery. In the extreme case, the trendline of relative recovery for

samples thawed from 1M PG was greater than 100% at all temperatures. These occurred only for depths of 0μm, and suggested handling to be the source of damage.

Cytotoxicity

Leaflets that were exposed to cryoprotectant solutions at 4°C, were also analyzed by confocal microscopy to determine the effect of cryoprotectants on cells in the tissue. Viabilities were compared to internal controls to obtain relative recoveries (**Figure 3.8**). Data showed 1M DMSO to be least toxic to both endothelial cells and fibroblasts. 2M DMSO demonstrated greater toxicity than 1M PG in endothelial cells but, 2M DMSO and 1M PG exhibited comparable recoveries for fibroblasts. Although cryoprotectants increased recovery during freezing, they were detrimental to cell membrane integrity when cells were exposed at 4°C.

3.4 Discussion

One major characteristic of all conditions tested was the decreased viability of fibroblasts with increasing depths into the leaflet. During freezing of a tissue, extracellular ice formation begins forming from outside the tissue. As it progresses, ice begins to form at the surface of the tissue. If ice forms around the tissue and progresses in towards the centre, solutes are excluded from the ice and increases the solute concentration. Cells are then exposed to high solute concentrations at the inner depths of the leaflets. This was exhibited for thawed and plunged samples in PBS, 1M and 2M DMSO, and

1M DMSO PG. We have termed this phenomenon "solute centralization" and this phenomenon would be difficult to overcome in larger tissues.

To rule out the possibility that this was a result of inadequate equilibration of cryoprotectants, theoretical permeation with DMSO was determined (**Figure 3.9**). Based on the diffusion coefficient of DMSO for articular cartilage (21), a diffusion time of 2.5 to 3.0 min for a heart valve leaflets of 450µm in thickness. Articular cartilage is composed of cartilage (21), although the organization of fibres is slightly different. The diffusion coefficient described by Muldrew *et al.* (21) for DMSO would differ little for PG since the diffusion coefficient is related to the molecular weight. DMSO and PG have molecular weights of 78.13 and 76.09 g/mol, respectively. Theoretically, the diffusion of PG into the leaflet would also be 2.5 to 3.0 min. Cryoprotectant toxicity can also be ruled out as a cause of solute centralization since the phenomenon was exhibited in the absence of cryoprotectants (**Figure 3.4**).

The other major conclusion arising from these experiments was the demonstration of selective preservation. In samples frozen with PBS, 2M DMSO and 1M PG, endothelial cells (0µm trendlines) had greater viability compared to fibroblasts (**Figure 3.5**). Only 1M DMSO showed higher recovery for fibroblasts over endothelial cells (thawed and plunged samples). This was also shown by determining the mean and standard error of relative recoveries of samples frozen in PBS, 1M and 2M DMSO, and 1M PG at depths of 0µm, 30µm, 60µm and 90µm across all temperatures (**Figure 3.10**).

1M DMSO samples showed higher recovery with fibroblasts than with endothelial cells. The ability to select for cell type preservation during freezing can be quite advantageous. This is similar to cryosurgery.

This investigation has resulted in two major conclusions that must be considered prior to cryopreservation. Firstly, cellular membrane damage results from low and high cooling rates as proposed by Mazur *et al.* (16) but, also from concentration of solutes within a tissue due to exclusion by ice formation (i.e. solute centralization). In cryopreserving heart valves, the damage to cells within the tissue can be decreased by decreasing cryoprotectant concentration. Secondly, conditions of freezing allow for the selection of cell types. Freezing a tissue can selectively ablate one cell type while preserving another. If the endothelial cells of heart valve leaflets are sites of recognition for host to graft rejection, a cryopreservation process which selectively eliminates endothelial cells while maintaining fibroblasts can possibly improve patient prognosis.

3.5. References

1.   Adam M, Fei Hu J, Lange P, and Wolfinbarger U. The effect of liquid nitrogen submersion on cryopreserved human heart valves. *Cryobiology.* 27: 605-614 (1990).

2.   Al-Janabi N, Gibson K, Rose J, and Ross DN. Protein synthesis in fresh aortic and pulmonary value allografts as an additional test for viability. *Cardiovascular Research* 7: 247-250 (1973).

3. Armiger LC. Viability studies of human valves prepared for use as allografts. *Ann Thorac Surg* 60: 5118-5121. (1995).

4. Arnaud F, Yang H, and McGann LE. Freezing injury of granulocytes during slow cooling: Role of the granulocytes. Cryobiology. 33: 391-403. (1996).

5. Courtman DW, Pereira CA, Omar S, Langdon SE, Lee JM, and Wilson GJ. Biomechanical and ultrastructural comparison of cryopreservation and a novel cellular extraction of porcine aortic valve leaflets. *Journal of Biomedical Materials Research* 29: 1507-1516. (1995).

6. Crescenzo DG, Hilbert SL, Barrick MK, Corcoran PC, St. Louis JD, Messier RH, Ferrans VJ, Wallace RB, and Hopkins RA. Donor heart valves: Electron microscopic and morphometric assessment of cellular injury induced by warm ischemia. *J Thorac Cardivasc Surg* 103: 253-258. (1992).

7. Crescezno DG, Hilbert SL, Messier RH, Domkowski PW, Barrick MK, Lange PL, Ferrans VJ, Wallace RB, and Hopkins RA. Human cryopreserved homografts: Electron microscopic analysis of cellular injury. *Ann Thorac Surg* 55: 25-31. (1993).

8. Deck JD. Endothelial cell orientation on aortic valve leaflets. *Cardiovascular Research.* 20: 760-767. (1986).

9. Edidin M. A rapid, quantitative fluorescence assay for cell damage by cytotoxic antibodies. *J. Immunol.* 104:1303-1306. (1970).

10. Fischlein T, Schutz A, Haushofer M, Frey R, Uhlig A, Detter C, and Reichart B. Immunologic reaction and viability of cryopreserved homografts. *Ann Thorac Surg.* 60: S122-S126. (1995).

11. Gall KL, Smith SE, Wilmette CA, and O'Brien Mark. Allograft heart valve viability and valve processing variables. *Ann Thorac Surg.* 65: 1032-1038. (1998).

12. Henney AM, Parker DJ, and Davies MJ. Estimation of protein and DNA synthesis in allograft organ cultures as a measure of cell viability. *Cardiovascular Research.* 14: 154-160. (1980).

13. Hurle JM, Colvee E, and Fernandez-Teran MA. The surface anatomy of the human aortic valve as revealed by scanning electron microscopy. *Anat Embryol.* 172: 61-67. (1985).

14. Lu J-L, Chiu Y-T, Sung J-W, Hwang B, Chong C-K, Chen S-P, Mao SJ, Yang PZ, and Chang Y. XTT-Colorimetric assay as a marker of viability in cryoprocessed cardiac valve. *J Mol Cell Cardiol* 29: 1189-1194. (1997).

15. Lupinetti FM, Kneebone JM, Rekhter MD, Brockbank KG, and Gordon D. Procollagen production in fresh and cryopreserved aortic valve grafts. *J Thorac Cardiovasc Surg* 113: 102-107. (1997).

16. Mazur P, Liebo SP, and Chu EHY. Two-factor hypothesis of freezing injury. *Exptl Cell Res.* 71: 345-355. (1971).

17. McGann LE, Yang H, and Walterson M. Manifestations of cell damage after freezing and thawing. *Cryobiology.* 25: 178-185. (1988).

18.   McGregor CGA, Bradley JF, McGee JO, and Wheatley DJ. Tissue culture, protein and collagen synthesis in antibiotic sterilized canine heart valves. *Cardiovascular Research* 10: 389-393. (1976).

19.   Mohan R. Letters to the Editor: Cryopreserved heart valve allografts can have a normal endothelium. *J Thorac Cardiovasc Surg* 108: 985-986. (1997).

20.   Moustapha A, Ross DB, Bittira B, Van-Velzen D, McAllister V, Lannon C, and Lee T. Aortic valve grafts in the rat: evidence for rejection. *J Thorac Cardiovasc Surg* 114: 891-902. (1997).

21.   Muldrew K, Sykes B, Schachar N, and McGann LE.   Permeation kinetics of dimethyl sulfoxide in articular cartilage.   *Cryo-Letters*. 17: 331-340. (1996).

22.   Ng YL and Wright EC.   Effect of preservation on the elasticity of human aortic valve homografts.   *Thorax*. 30: 266-270. (1975).

23.   Niwaya K, Sakaguchi H, Kawachi K, and Kitamura S. Effect of warm ischemia and cryopreservation on cell viability of human allograft valves. *Ann Thorac Surg* 60: 5114-5117. (1995).

24.   Parker R, Randev R, Wain WH, and Ross DN.   Storage of heart valve allografts in glycerol with subsequent antibiotic sterilization.   *Thorax*. 33: 638-645. (1978).

25.   Pegg DE. Viability assays for preserved cells, tissues, and organs. *Cryobiology*. 26: 212-231. (1989).

26. Shon YH and Wolfinbarger L Jr. Proteoglycan content in fresh and cryopreserved porcine aortic tissue. *Cryobiology* 31: 121-132. (1994).

27. Suh H, Lee JE, Park J-C, Han D-W, Yoon C-S, Park YH, and Cho BK. Viability and enzymatic activity of cryopreserved porcine heart valve. *Yonsei Med J.* 40 (2): 184-190. (1999).

28. Villalba R, Concha M, and Gomez-Villagran JL. Tetrazolium reductase activity in human heart valves. *Ann Thorac Surg.* 66: 1860-1872. (1998).

29. Wassenaar C, Wijsmuller EG, Van Herwerden LA, Aghai Z, Van Tricht CM, and Bos E. Cracks in cryopreserved aortic allografts and rapid thawing. *Ann Thorac Surg* 60: S165-S167. (1995).

30. Wassenaar C, Bax WA, Van Suylen R-J, Vuzevski VD, and Bos E. Effects of cryopreservation on contractile properties of porcine isolated aortic valve leaflets and aortic wall. *J Thorac Cardiovasc Surg* 113: 165-172. (1997).

31. Wilcek P, Szydlowska I, Lotsyz D, and Religa Z. The use of flow cytometry for the investigation of viability of heart valve-derived fibroblasts. *Folia Histochemica et Cytobiologica.* 34 (Suppl 1): 41-42. (1996).

32. Yang H, Arnaud F, and McGann LE. Cryoinjury in human granulocytes and cytoplasts. Cryobiology. 29: 500-510. (1992).

33. Yang, H., Jia, X.M., Ebertz, S. and McGann, L.E. Cell Junctions are targets for freezing injury. *Cryobiology.* 33: 672-673. (1996).

34. Yang H, Acker J, Chen A, and McGann L. In situ assessment of cell viability. *Cell Transplantation* 7: 443-451. (1998).

35. Yankah AC, Wottge H-U, Muller- Hermelink HK, Feller AC, Lange P, Wessel U, Dreyer H, Bernhard A, and Muller-Ruchholtz. Transplantation of aortic and pulmonary allografts, enhanced viability of endothelial cells by cryopreservation, importance of histocompatibility. *J Cardiac Surg.* 1 (3 Suppl): 209-220 (1987).
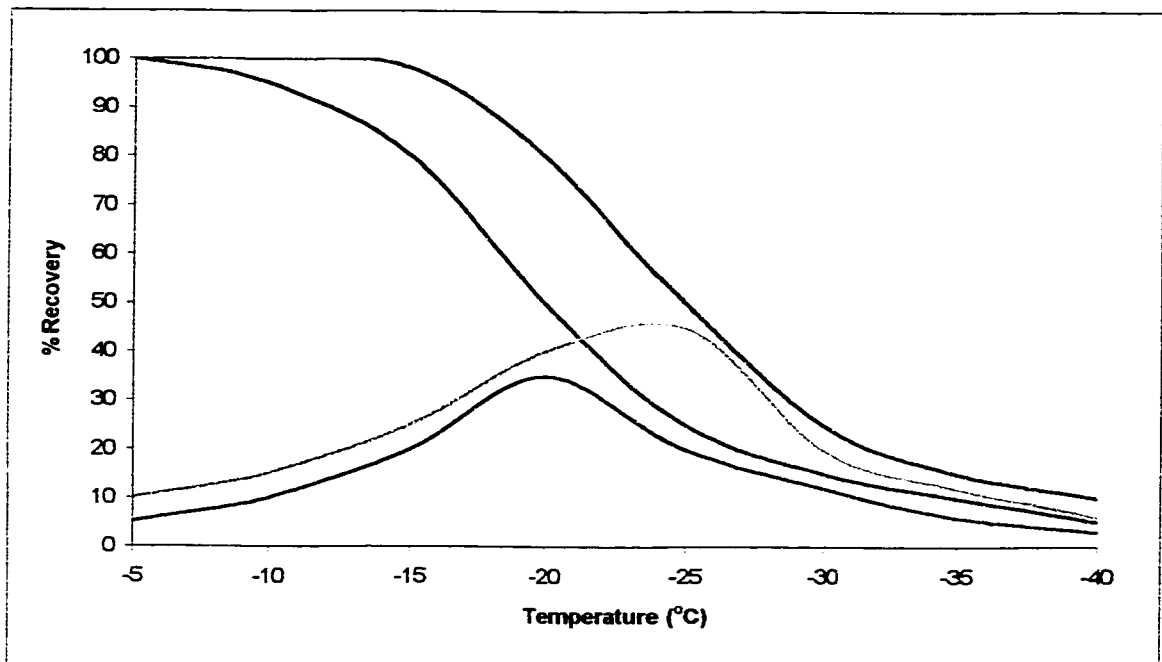
Figure 3.1. Percent recovery of cell suspensions after graded freezing. Green = thawed samples in PBS; Blue = plunged samples in PBS. Red = thawed samples in CPA; Orange = plunged samples in CPA.
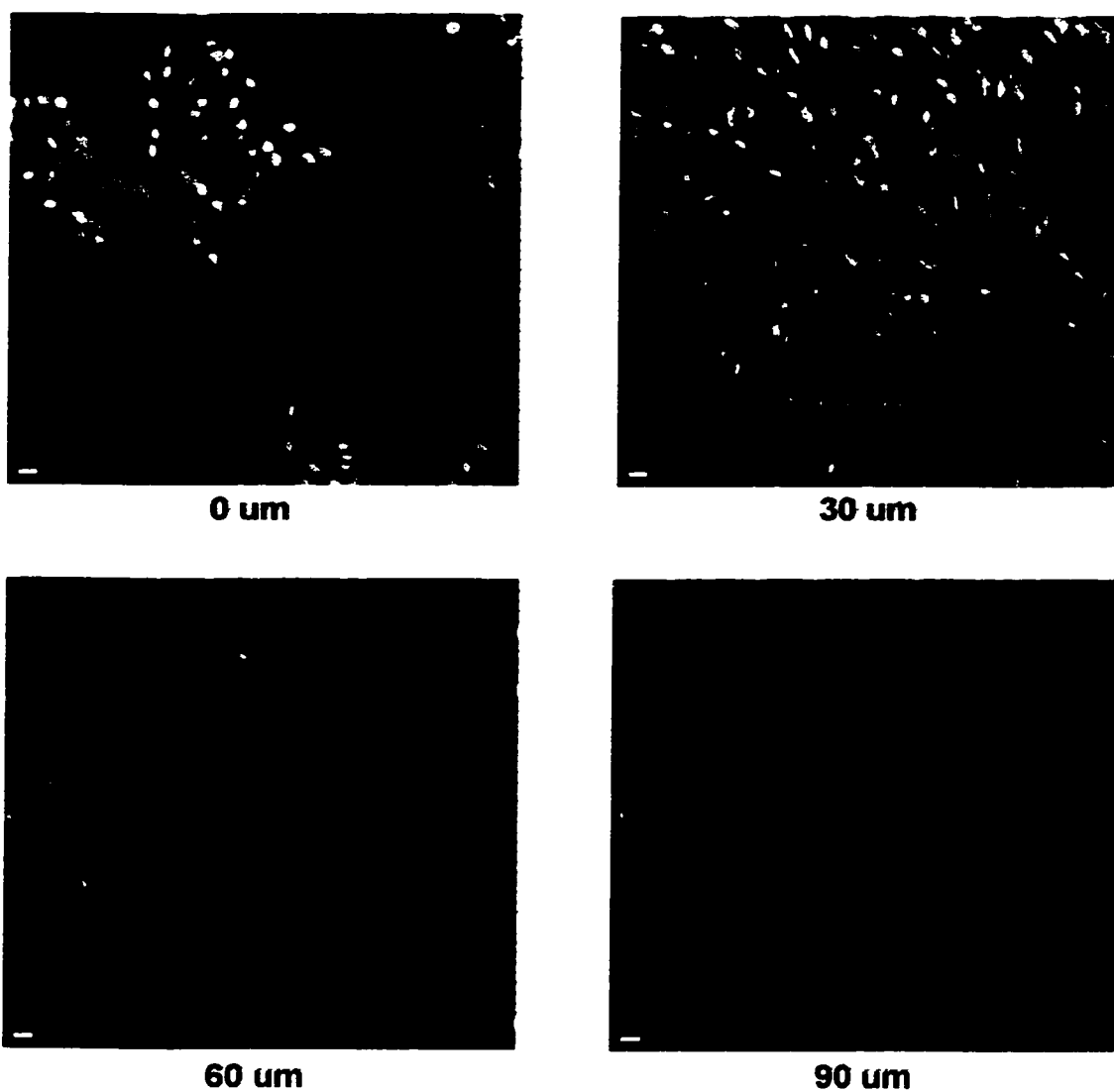
0 um

30 um

60 um

90 um

Figure 3.2 Confocal images of leaflet at depths of 0um, 30um, 60um, and 90um. Leaflet was frozen in isotonic PBS after cooling at 1°C/min to -20°C, then plunged in liquid nitrogen. 100x magnification.
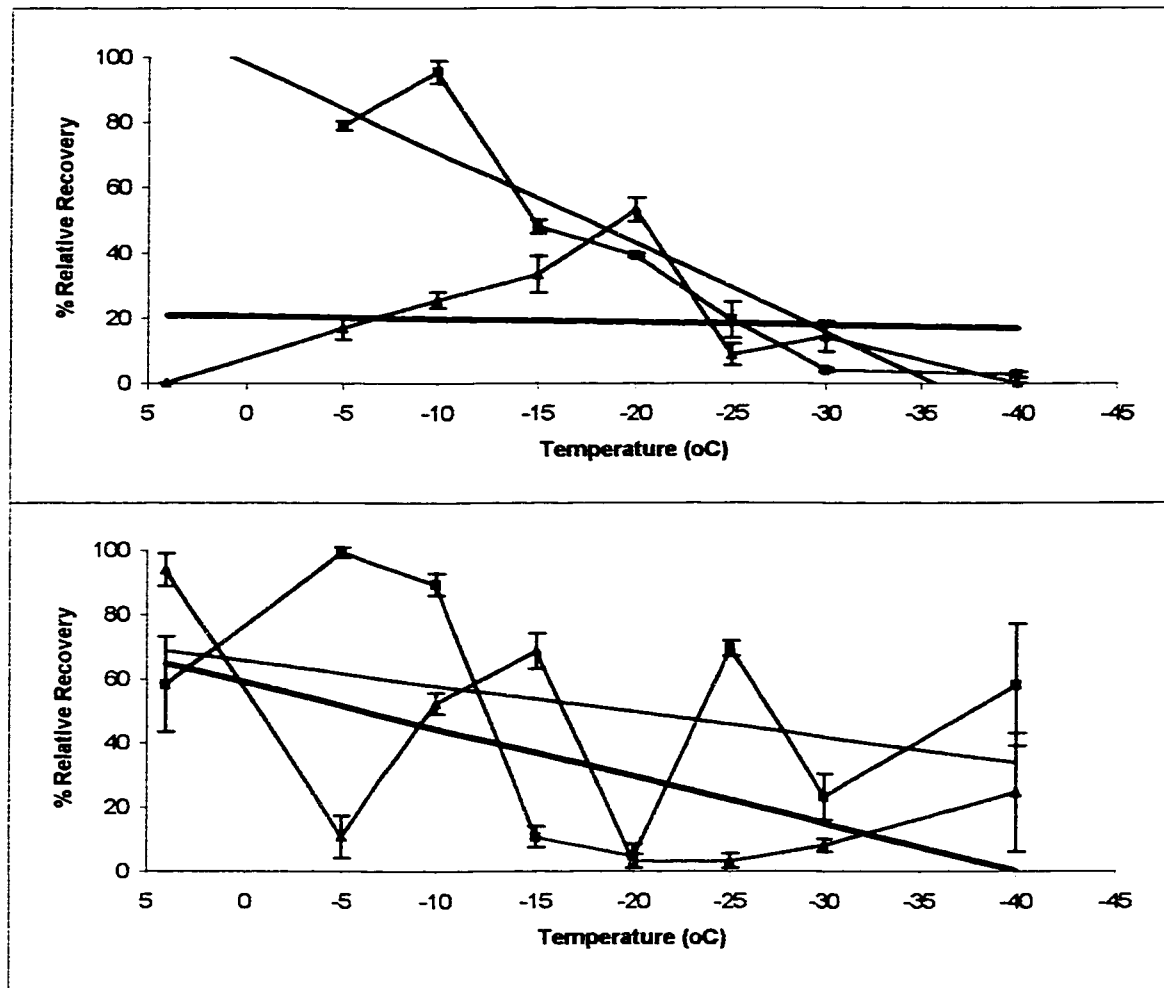
Figure 3.3. Use of trendlines to represent graded freezing data. (Top) Graded
freeze of leaflets in PBS; viability at 30 um depths into leaflet. (Bottom) Graded freeze
of leaflets in 2M DMSO; viability at 60um depths into leaflet. Blue = thawed samples,
Green = plunged samples. Thin black line = trendline for thawed samples;
Thick black line = trendline for plunged samples. Data points represent
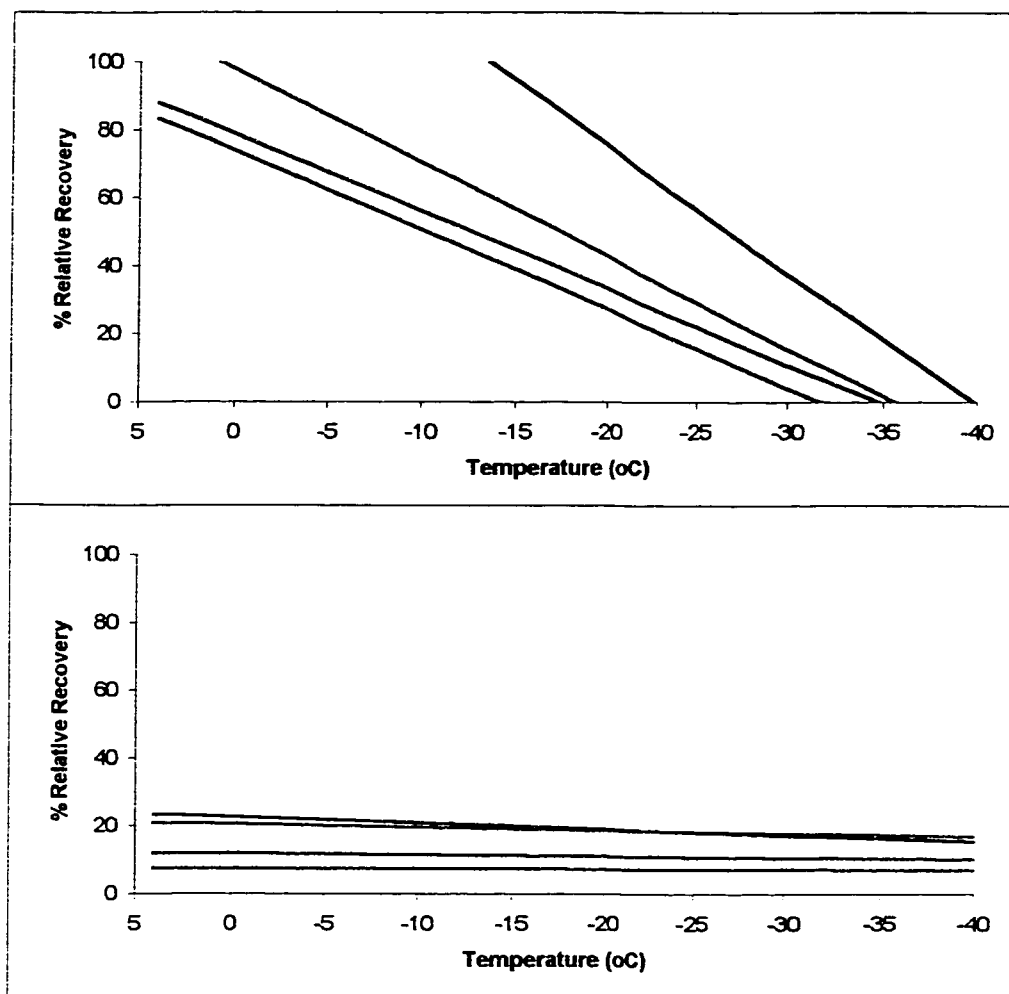mean + standard error for each condition (n = 3).

Figure 3.4. Trendlines of relative recoveries of graded freezing of leaflets in 1x PBS. (Top) thawed samples; (Bottom) plunged samples

Black = 0um   Blue = 30um   Green = 60um   Red = 90um

Figure 3.5. Trendlines of relative recoveries of graded freezing of leaflets in 1M DMSO. (Top) thawed samples; (Bottom) plunged samples

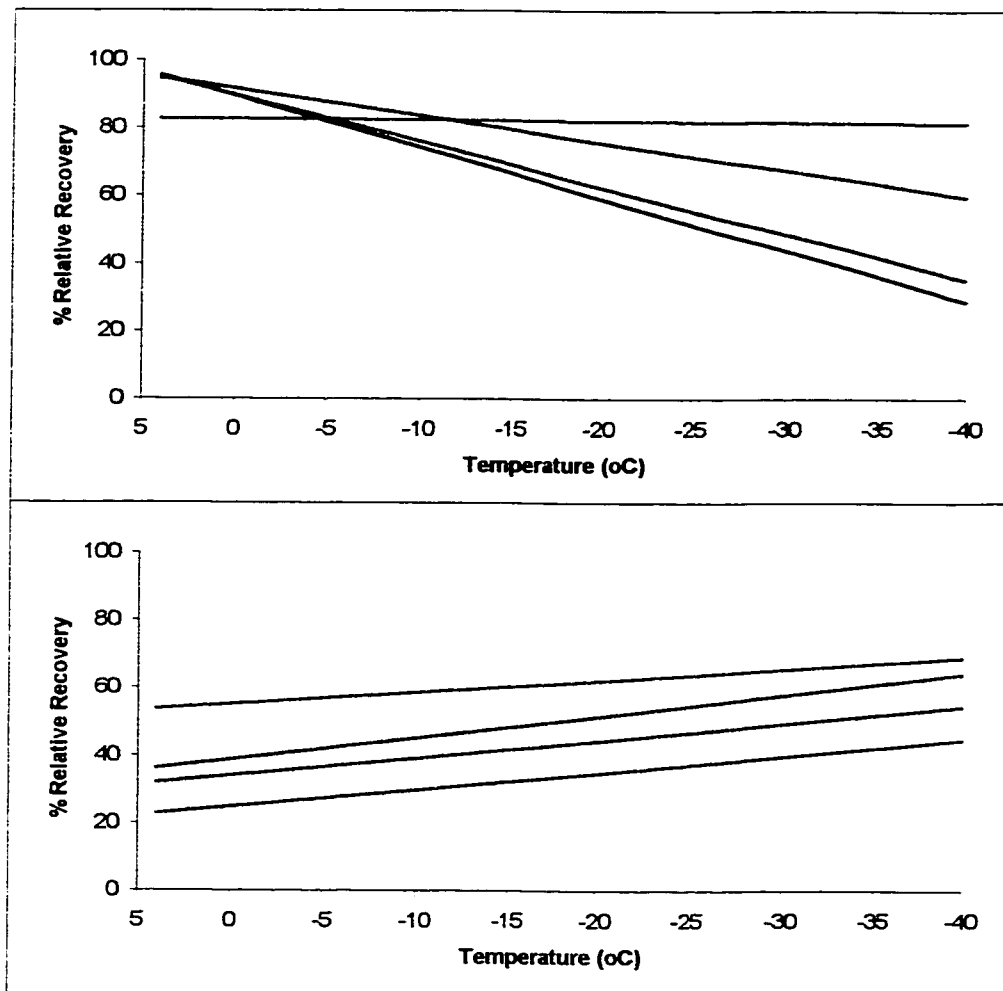Black = 0um   Blue = 30um   Green = 60um   Red = 90um

Figure 3.6. Trendlines of relative recoveries of graded freezing of leaflets in 2M DMSO. (Top) thawed samples; (Bottom) plunged samples

Black = Oum   Blue = 30um   Green = 60um   Red = 90um

Figure 3.7. Trendlines of relative recoveries of graded freezing of leaflets in1M PG. (Top) thawed samples; (Bottom) plunged samples

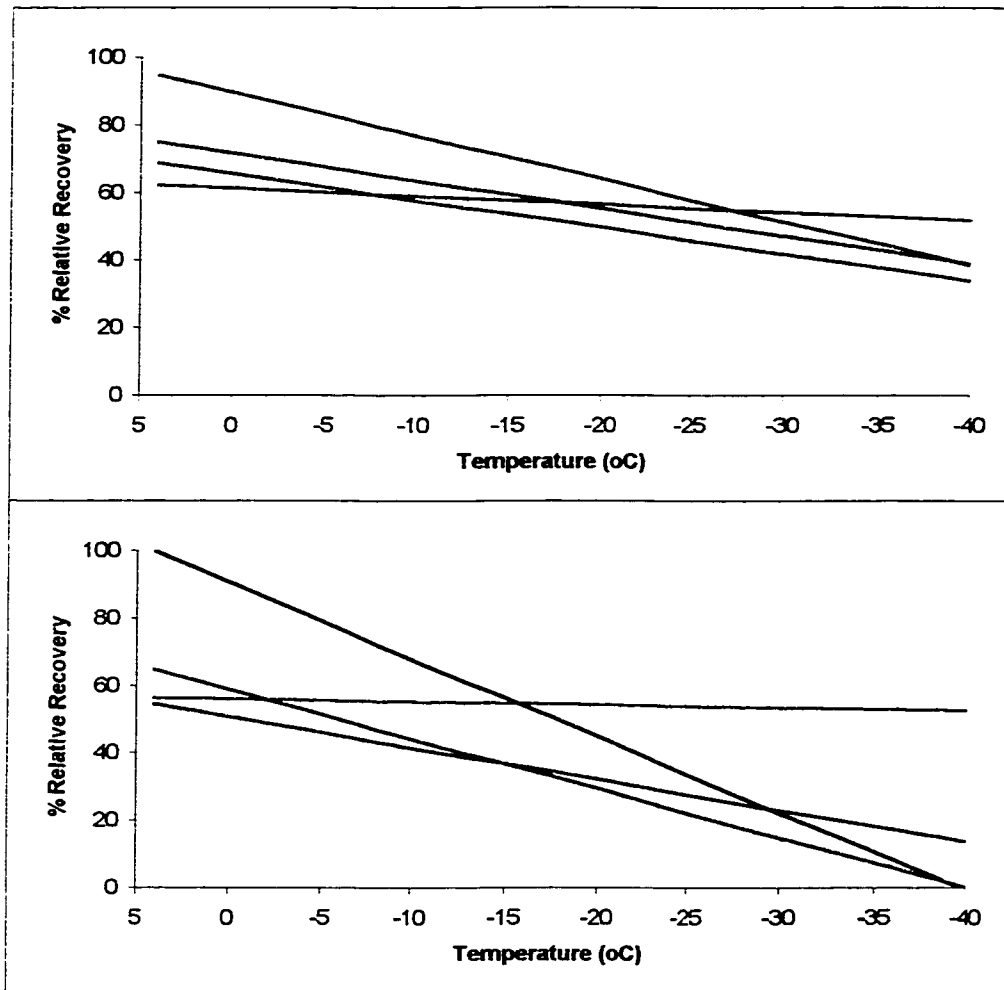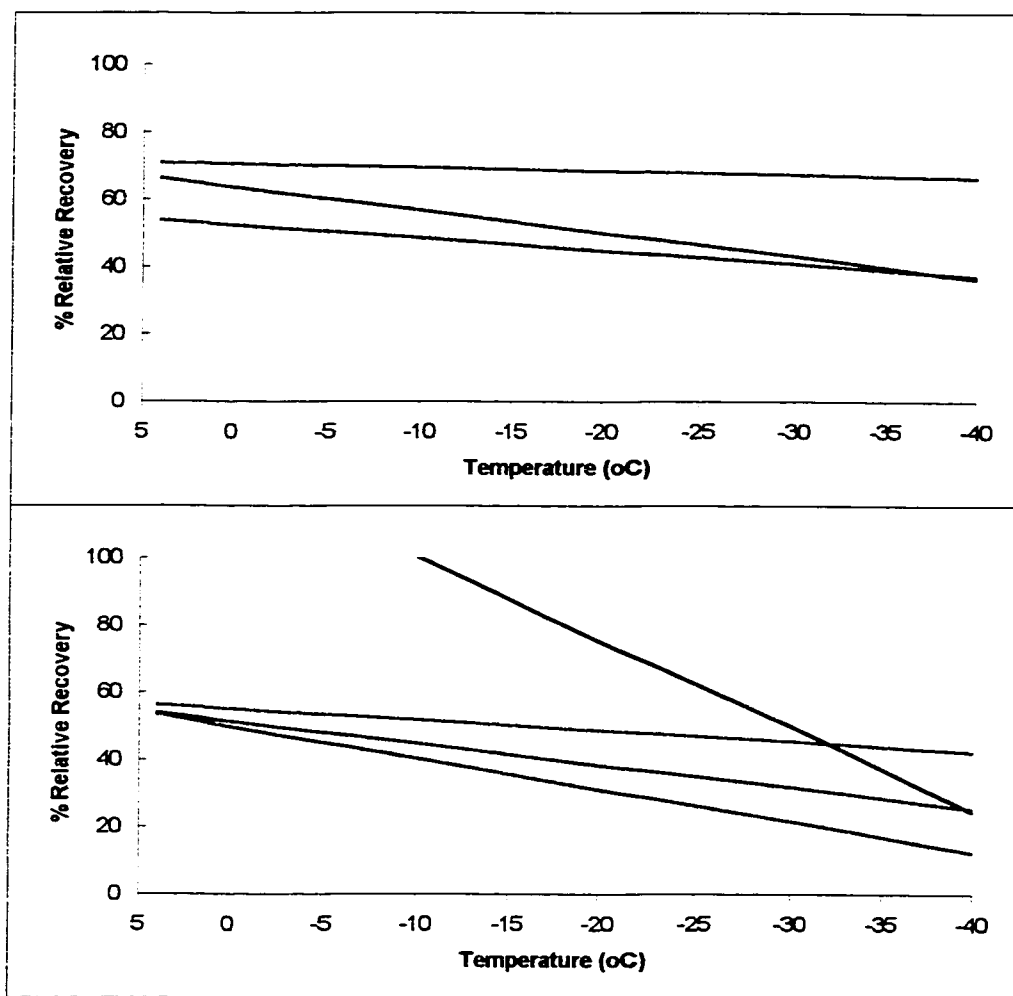Black = 0um   Blue = 30um   Green = 60um   Red = 90um
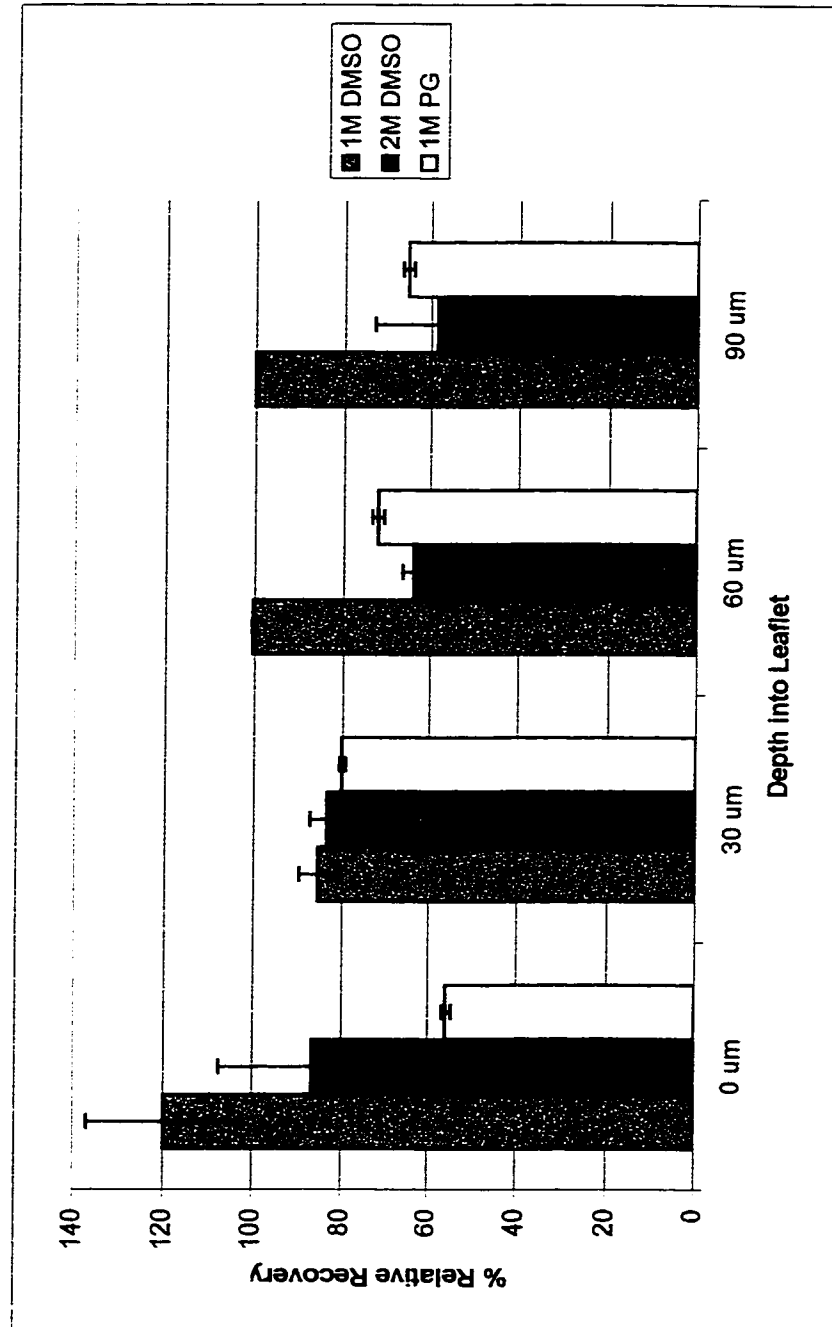
76

Figure 3.8. Toxicity of cryoprotectants to endothelial cells (0um) and fibroblasts (30, 60, and 90 um). Mean ± standard error of samples (n = 3).

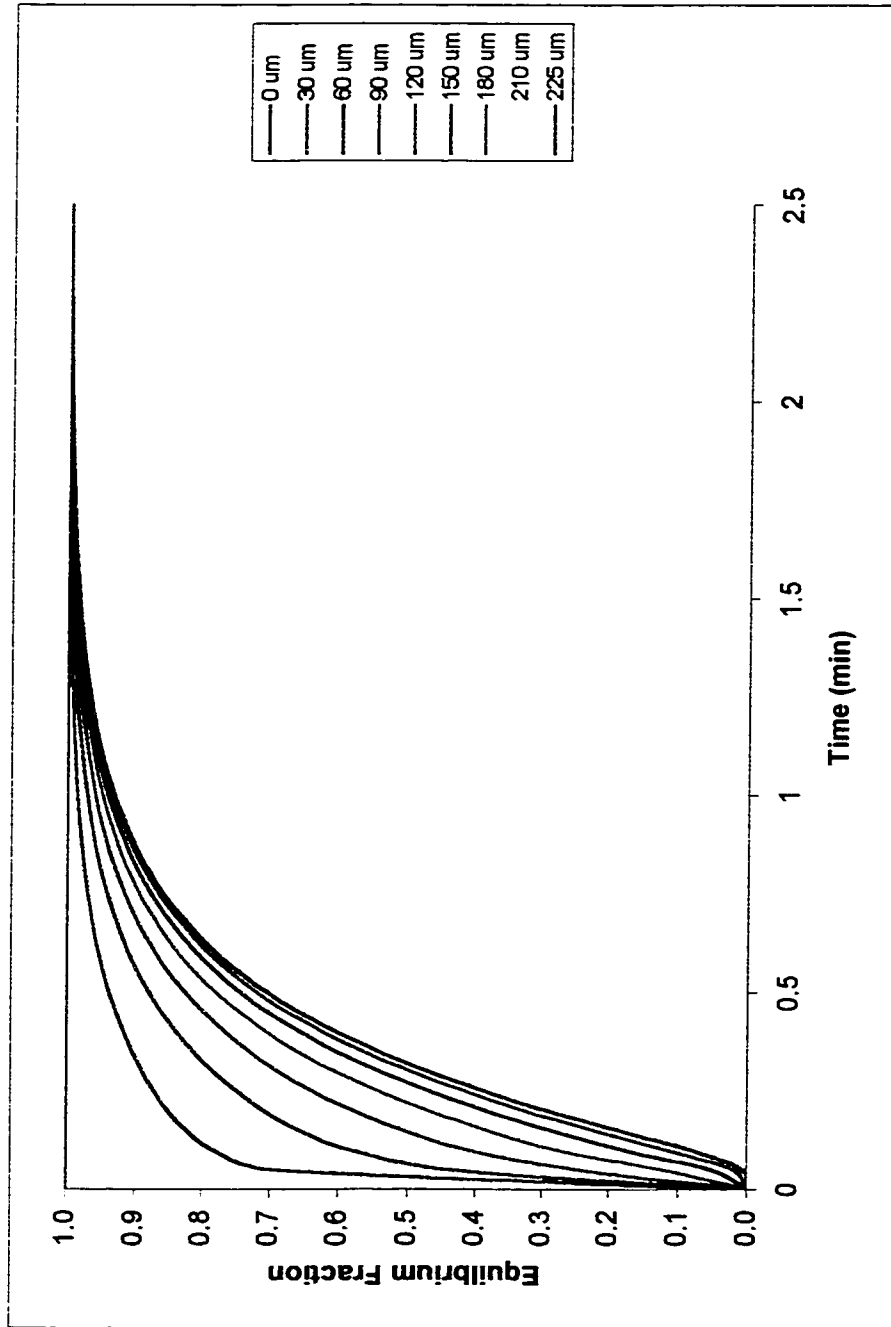**Figure 3.9.** Theoretical permeation of DMSO into an intact porcine heart valve leaflet at increasing depths. Based upon a thickness in tissue of 450um and a diffusion coefficient of $1.00E-5$ cm^2/sec.
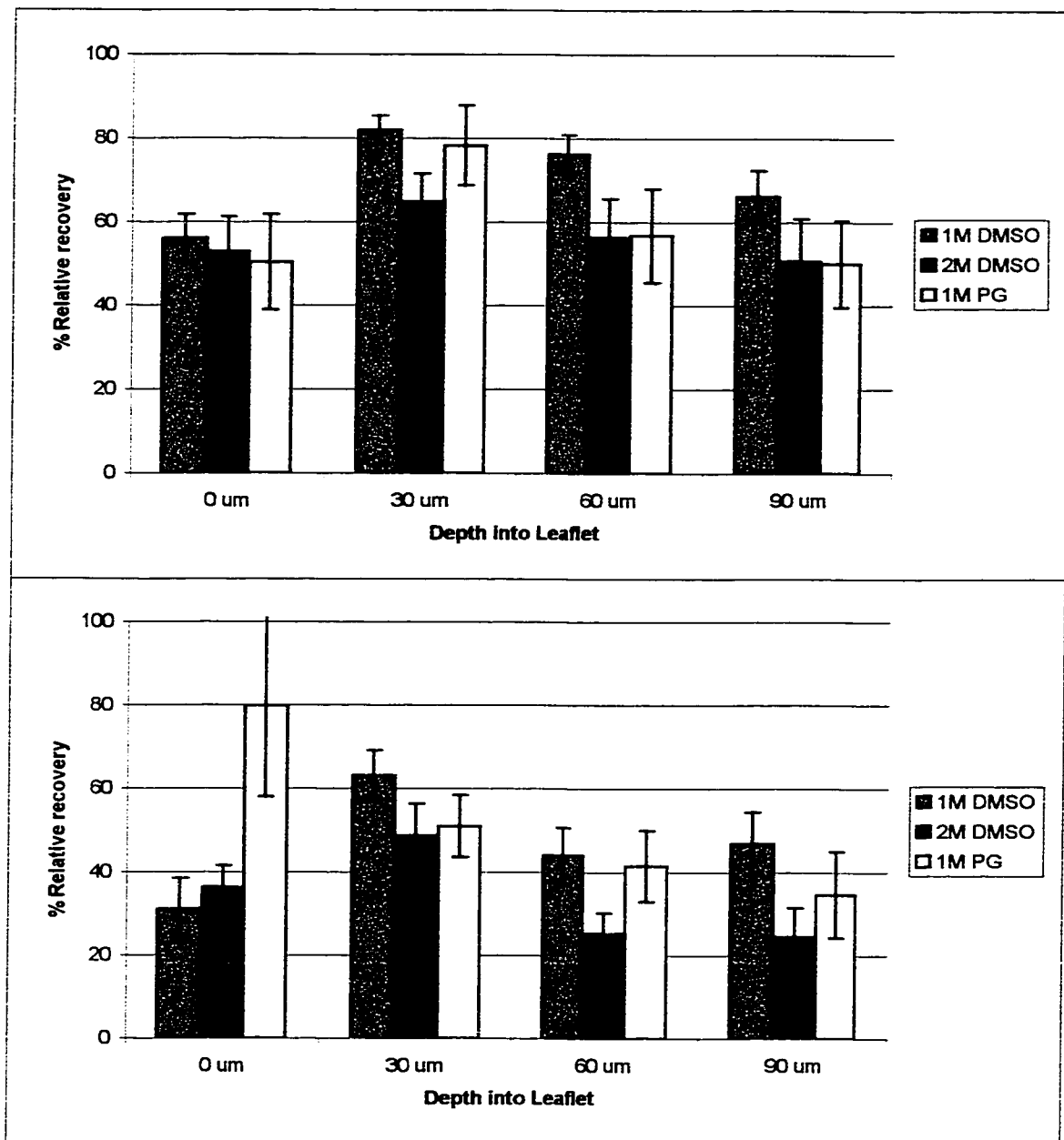
78

Figure 3.10. Selective viability of endothelial cells (0um) versus fibroblasts (30, 60, and 90 um). Mean ± SE for samples frozen in each cryoprotectant at each depth. (Top) thawed samples; (Bottom) plunged samples.

CHAPTER 4

COMPUTER SIMULATIONS OF CELLULAR RESPONSE USING THE CRYOSIM3 PROGRAM

4.1. Introduction

In many cases, experiments in cryobiology are conducted using known initial conditions and the results can only describe the end conditions. The mechanism of how those results occurred is usually speculative. One way to test these speculations is to model the response by computer. Computer simulations have been used to model fluid dynamics, aerodynamics, space flight, car collisions, business and economics, electrical circuits, and astrodynamics, to name a few.

Computer simulations have the advantages of being fast, precise and cost effective. Simulations have the ability to perform a virtual experiment in minutes while actual experiments would require weeks or months. The high precision of computer calculations offers reproducible data. However, the precision of the output data is dependent upon the accuracy of the model and precision of parameters entered into the simulation. The ability to simulate an experiment is also highly cost efficient. Experiment costs can be upwards of thousands of dollars while computer simulations are inexpensive in comparison. Simulation programs also allow the opportunity to perform experiments that would either be time consuming or difficult with given resources. On the other hand, computer simulations are purely theoretical and may not be representative of all possible variables involved. However, it

80

is clear that the advantages offered by computer simulation programs far outweigh the disadvantages. Overall, computer simulations are a good way to test our understanding.

The use of simulations in cryobiology is not a novel technique. Rubinsky and Pegg (5) have previously used a mathematical simulation to examine the freezing process of organs. Mathematical modeling of the thermodynamics involved was correlated to experimental data. Similarly, Poledna and Berger (4) have used computer simulations to visualize ice formation and the frozen region surrounding a cryoprobe in liver tissue. The simulation data for the simulated solution and experimental measurements show differences smaller than the experimental error. This validates the practical importance of computer simulations. However, these types of simulations have examined physical mechanisms but were unable to provide microscopic evaluations of cellular response.

An evolution in computer simulations occurred when Pazhayannur and Bischof (1) began looking more specifically at cellular conditions with their simulation program. The simulation model used in this study attempted to determine the hydraulic conductivity and its activation energy for rat liver cells. The values were then used to determine water transport in liver tissue. Reasonable agreement between the simulation and experimental data was obtained. The value of simulations is evident, yet these simulations lack critical information necessary for improving cryopreservation techniques.

The CryoSim3 program was developed by Dr. L.E. McGann, Ph.D. (University of Alberta, Edmonton, Canada) and provides additional information from the simulation. The Windows®-based program has a user interface (**Figure 4.1**) which allows parameters to be changed. Cell parameters include isotonic volume, osmotically inactive fraction, isotonic salt concentration, and either variable or constant cell surface area. Typically, a variable surface area is more appropriate for biological cells in suspensions as supported by Steponkus *et al.* (6).

Osmotic parameters defined in the simulation program are hydraulic conductivity, its activation energy; type of cryoprotectant, the permeability of the cryoprotectant, its activation energy; the reflection coefficient; and the reference temperature for hydraulic conductivity and solute permeability. The current version of the simulation program allows the incorporation of one of four cryoprotectants (DMSO, ethylene glycol, glycerol, and PG).

Initial conditions of the extracellular and intracellular environment with respect to impermeant and permeant solutes. The cryopreservation procedure can be specified as rate segments. With a defined starting temperature, steps of the protocol can be entered as a cooling or warming rate to specific temperatures or as a holding phase for a defined length of time. The program is, however, limited to a starting temperature equal to or above 0°C.

Modeling cellular response requires an understanding of phase diagrams and freezing-point depression (2,3). The CryoSim3 program

82

determines cellular response using the initial parameters and properties of the solutes involved. These include sodium chloride (NaCl), potassium chloride (KCl), DMSO, glycerol, ethylene glycol, and PG. Freezing-point depression data was curve-fit to a quadratic function.

$$T_{fp} = Am + Bm^2 \qquad [1]$$

where T_{fp} is the freezing-point depression in degrees C, m is molality, and A and B constants for the solute. The values of A and B are found in **Appendix II**. This describes a dynamic relationship of solute molality and freezing-point depression, which is used in determining the output data from the simulation.

Like the input data, the output data of the program is easily manageable. The output data can be pasted into a spreadsheet and graphical analysis performed. The CryoSim3 program provides information about conditions in the cell and its environment. The program provides 1000 data points at equal intervals time during the simulation. Both time and temperature are recorded at each interval. Also included in the output are the absolute and relative cell volumes. The degree of supercooling and intracellular and extracellular concentrations of impermeant and permeant solutes is also calculated from the simulation.

The aim of this study is to use computer simulations to determine the conditions and environments of the endothelial cells and fibroblasts during different steps of the cryopreservation protocol. A number of different aspects of the protocol are examined, including the specific effects the osmotic parameters, equilibration of cryoprotectants, varying cooling rates, graded

freezings, varying warming rates, and removal of cryoprotectants. The data from these simulated experiments will provide insight into cellular response to cryopreservation.

4.2. Computer Simulations

Validating the CryoSim3 Program

To ensure the computer simulation program was functioning properly, osmotic simulations were performed with and without cryoprotectants. Results of these simulations were used as input data in a separate curve-fitting program to derive the osmotic parameters, which were then used compared to the parameters used in the simulation.

Simulations were performed modeling endothelial cell response to hypertonic conditions (2x, 3x, 4x, and 5x PBS) (**Figure 4.2**) using an osmotically inactive fraction of 0.399, hydraulic conductivity of 0.429 $\mu m/min/atm$. The data from the simulation of endothelial cells exposed to 2x PBS at 22°C was plotted as relative volume versus time (**Figure 4.3**). By curve-fitting the data, values for V_b and L_p were determined to be 0.399 and 0.435 $\mu m/min/atm$. Determined values in comparison with simulation values for V_b and L_p, showed errors of 0.0% and 1.4%, respectively, indicating that the simulation program models water movement within acceptable errors.

Similarly, a simulation of fibroblasts exposed to 1M DMSO at 22°C was performed using a hydraulic conductivity of 0.430 $\mu m/min/atm$ and solute permeability of 7.98 $\mu m/min$. Determined L_p and P_s values were 0.460 $\mu m/min/atm$ and 7.99 $\mu m/min$, respectively (**Figure 4.5**). This gives errors of

7.0% for L_p and 0.1% for P_s. The error for this simulation demonstrated that the simulation program satisfactorily models cryoprotectant and water movement.

The Effect of Osmotic Parameters on Cell Volume Kinetics.

To understand the role of each osmotic parameter, simulations were performed to demonstrate the effect of changes in osmotic parameters on cellular volume kinetics. This understanding helps when comparing osmotic parameters of different cell types.

A "baseline" cell response was simulated for a cell exposed to 3X isotonic PBS (**Table 4.1**). Subsequent simulations were performed with changes to a single parameter for each simulation. Parameters examined were isotonic volume, osmotically inactive fraction, hydraulic conductivity, its activation energy, and presence of 1M DMSO.

Figure 4.6 represents simulations of a cell having parameters outlined in **Table 4.1**. The baseline kinetic simulated using the parameters in **Table 4.1** were changed in four parameters. V_o was changed to 4000 μm^3. This resulted in a curve that reached the equilibrium volume fraction slower. A larger isotonic volume requires more water to be removed from the cell. Since the hydraulic conductivity remains unchanged, it requires more time for water to exit the cell. A decrease in osmotically inactive fraction from 0.4 to 0.2 had 2 implications: firstly, there was a decrease in equilibrium volume fraction, secondly, the time required to reach equilibrium increased. Both effects result from the larger volume of free water. Increasing L_p to 0.4

μm/min/atm led to an increase in slope during cell shrinkage. The cell reached equilibrium volume fraction faster with an increase in L_p. Reduction of the activation energy from 10 to 5 kCal/mol reflects a change in water permeability. The baseline kinetic with an L_p of 0.2 μm/min/atm at $T_{ref}=0°C$ will change more with an E_a of 10 kCal/mol at 22°C; L_p will be smaller and hydraulic conductivity lower.

Figure 4.7 examined the role of each parameter in the presence of a cryoprotectant (1M DMSO). Changing V_o to 4000 μm^3 in the presence of DMSO is similar to exposure to hypertonic PBS. The curve is shifted to the right. More time is required for water to leave the cell then return. Decreasing V_b to 0.2 moves the curve down as before as more active water is in the cell and is able to exit the cell. Changing L_p to 0.4 μm/min/atm lead to an increase in slope during cell shrinkage. In addition, the minimum volume was decreased. The increased water permeability means faster water movement and further cell shrinkage occurs compared to the baseline curve. An increase in L_p activation energy to 20 kCal/mol magnifies this situation as the increased E_a reflects the increase in L_p. Decreasing P_s has a similar effect. A smaller P_s results in more cell shrinkage compared to the baseline curve. As there is less cryoprotectant moving into the cell, water leaves the cell to compensate for the increasing extracellular solute concentration and osmotic gradient. Like the Lp activation energy, Ps activation energy reflects change in permeability due to temperature. The lower E_a means a lower P_s, as previously described.

These simulations illustrate the effect of each parameter individually. However, it is critical to recognize that cell types differ in each of these parameters. This fact makes it difficult to compare the response of cells as differences in osmotic parameters have additive and antagonistic effects and can also vary in magnitude. Cellular response is a complex interaction of a number of parameters.

Simulations of Cryoprotectant Equilibration of Endothelial Cells and Fibroblasts.

Endothelial cells and fibroblasts were exposed to 1M DMSO, 2DMSO, and 1M PG over the duration of 1 hour at 4°C by computer simulation. Parameters used were determined previously (**Table 2.5**). **Figures 4.8** and **4.9** illustrate the time for endothelial cells and fibroblasts, respectively, to equilibrate to 1M DMSO, 2M DMSO, and 1M PG.

Equilibration times were determined from the simulation data. Equilibration can be measured in two ways. Firstly, by return to isotonic volume and secondly by intracellular cryoprotectant concentration. In this study, equilibration was defined using two different criteria: return to 99% of the isotonic volume and intracellular cryoprotectant concentration at 99% of the extracellular concentration. Time of equilibration for each cell type and cryoprotectant is shown in **Table 4.2**. For all cryoprotectants, endothelial cells equilibrated more rapidly than fibroblasts, based on both volume and concentration criteria. Endothelial cells equilibrated most rapidly with 1M DMSO, then 1M PG and finally 2M DMSO. Fibroblasts, on the other hand,

equilibrated most rapidly in 1M DMSO, then 2M DMSO, and finally 1M PG. Equilibration of intracellular cryoprotectant concentration occurred before cell volumes returned to the isotonic volume.

Generally, equilibration required less than 1 hour. The critical factor is cryoprotectant concentration, which protects the cell from "solution effects" (McGann). Since the toxic effects of the cryoprotectants have been shown to occur previously in Chapter 3, shortening the time for equilibration during cryopreservation reduces the toxicity experienced by the cells.

Simulations of Varying Cooling Rates

Endothelial cells and fibroblasts were cooled and frozen at varying cooling rates (1, 10, 25, 50, 75 (fibroblasts only), 100, and 158°C/min). Parameter used were previously determined (**Table 2.5**). cells were cooled from the starting temperature of 0°C. Both cell types were cooled in isotonic PBS and 1M DMSO. Cells in 1M DMSO were assumed to be equilibrated and hence hand an intracellular and extracellular cryoprotectant concentration of 1M.

During cooling, the degree of supercooling in cells influences the likelihood of intracellular ice formation during the rapid freezing phase of cryopreservation. Comparing the cooling rate of 50°C/min for endothelial cells and fibroblasts (with or without cryoprotectants) (**Figure 4.10**), maximum supercooling for fibroblasts occurs between -15°C and -20°C, while at 50°C/min endothelial cells continued to supercool at -40°C.

The addition of a cryoprotectant to the cryopreservation solution leads to decreased supercooling for both cell types. The initial supercooling when cells are cooled at 1°C/min was practically eliminated in the presence of 1M DMSO. Permeating cryoprotectants are considered to protect against "solution effects" but this study shows 1M DMSO to partially protect against intracellular ice formation as well by reducing the degree of supercooling.

Simulations of Graded Freezing

Simulations of the conditions from graded freezing experiments were performed for both endothelial cells and fibroblasts in isotonic PBS, 1M DMSO, 2M DMSO, and 1M PG. Parameters used were previously determined (**Table 2.5**). Cells in cryoprotectants were equilibrated and had identical intracellular and extracellular cryoprotectant concentrations.

The graded freezing protocol called for cells to be cooled from 0°C to -5°C at a rate of 1°C/min. The cells were then held for 5 minutes to allow for release of latent heat of fusion. Each simulation was identical to this point in the protocol. Simulations then rapidly cooled (158°C/min; determined previously in Chapter 3) cells at -5, -10, -15, -20, -25, -30, and -40°C after being cooled to the experimental temperature at 1°C/min.

Graphical analysis plotted the degree of supercooling at -40°C against the temperature which rapid cooling was initiated. **Figure 4.11** represents results for endothelial cells in PBS, 1M DMSO, 2M DMSO, and 1M PG. **Figure 4.12** represents results for fibroblasts in PBS, 1M DMSO, 2M DMSO and 1M PG.

Endothelial cells and fibroblasts show a decrease in supercooling when the cells are cooled slowly (1°C/min) to lower temperatures prior to rapid cooling. Supercooling in all solutions was near 0°C at -40°C indicating that slow cooling to -40°C decreased the likelihood of IIF. With the addition of cryoprotectants, endothelial cells and fibroblasts showed increased supercooling compared to graded freezing in PBS alone. Endothelial cells and fibroblasts showed greatest supercooling with 2M DMSO, 1M DMSO, then 1M PG.

Supercooling in fibroblasts was less than endothelial cells with all experimental solutions. This was due to the increased solute permeability for fibroblasts with DMSO and PG. The higher P_s leads to greater concentrations of cryoprotectants intracellularly thus displacing more water and decreasing the supercooling of water. The higher degree of supercooling in endothelial cells suggests a greater likelihood of intracellular ice formation. From comparisons of experimental graded freezing data presented in Chapter 3 and simulation data, greater supercooling of endothelial cells in PBS, 2M DMSO, and 1M PG correlates to low endothelial cell recovery. The lower recovery in 1M DMSO must be a result of this and another form of cellular injury.

Simulations of Cryoprotectant Removal from Endothelial Cells and Fibroblasts.

Simulations were performed with endothelial cells and fibroblasts held at 4°C for the duration of 1 hour in isotonic PBS. Two sets of values for solute

permeability and its activation energy were used for each cell type. The first set, were values determined from returning cells equilibrated in cryoprotectants to isotonic conditions ('removal'). The second set used were values determined from experimental exposure to cryoprotectants ('addition'). Parameters used are listed in **Table 4.3**.

Figure 4.13 shows cell volume kinetics from the simulated removal of cryoprotectants. Using the first set of values, endothelial cell volume increased greater than that of fibroblasts using the same cryoprotectant. This increased volume also reflects a longer time to return to isotonic volume. For both cell types, volume increase is greatest with 2M DMSO, then 1M PG and finally 1M DMSO. The large volume expansions can be remedied by performing step-wise dilutions. However, the CryoSim3 program was unable to perform that procedure.

Using the second set of values, kinetics generally showed larger cell volume increases compared to volumes using the first set of values. Removal of cryoprotectants for endothelial cells resulted in faster return to isotonic volume and lower volume increases. This was due to higher P_s values for DMSO and PG at 4°C for endothelial cells.

To determine which set of values was more accurate, simulated kinetics for the removal of 1M DMSO from fibroblasts were compared to experimental volume kinetics (**Figure 4.14**). The experimental data fitted closer with volume kinetics based on values of the first set. Although the

91

kinetics was not exact, the use of the 'removal' values for Ps and Ea were better at modeling cellular response to cryoprotectant removal.

Based on these volume kinetics, times for removal can be determined from simulations. Like equilibration removal of cryoprotectants was judged either on return to 101% isotonic volume or 1% of initial intracellular cryoprotectant concentration. **Table 4.4** show removal times. Fibroblasts returned to isotonic volume and reduced cryoprotectant concentration faster than endothelial cells with each cryoprotectant tested. Like equilibration, removal of cryoprotectants intracellularly occurs before the cells return to isotonic volume. Again, cryoprotectant concentration is the critical factor to consider.

4.3. Conclusions

Computer simulations were able to provide a number of important insights into the response of endothelial cells and fibroblasts to cryopreservation.

Typical cryopreservation protocols use at least 1 hour for equilibration and cryoprotectant removal. These simulations have shown that equilibration and removal of cryoprotectants can be done in less than 1 hour.

The simulations have also examined the degree of supercooling at varying cooling with and without cryoprotectants. The differences in cell and osmotic parameters have shown that fibroblasts undergo less supercooling than endothelial cells. Endothelial cells as a result have a greater likelihood of forming intracellular ice.

By understanding the osmotic response of cells during cryopreservation, a procedure can be designed to improve conditions to which cells are exposed.

4.4. References

1. Pazhayannur PV and Bischof JC. Measurement and simulation of water transport during freezing in mammalian liver tissue. *J Biotech Eng.* . 119: 269-77. (1997).

2. Pegg DE. Equations for obtaining melting points and eutectic temperatures for the ternary system dimethyl sulphoxide / sodium chloride / water. *Cryo-Letters.* 7: 387-394. (1986).

3. Pegg DE and Arnaud FG. Equations for obtaining melting points in the quaternary system propane-1,2-diol / glycerol / sodium chloride / water. *Cryo-Letters.* 9: 404-417. (1988).

4. Poledna J and Berger W. A mathematical model of temperature distribution in frozen tissue. *Gen Physiol Biophys.* 15: 3-15. (1996).

5. Rubinsky B and Pegg DE. A mathematical model for the freezing process in biological tissue. *Proc R Soc Lond B Biol Sci.* 234: 343-358. (1988).

6. Steponkus PL, Wolfe J, and Dowgert MF. Stresses induced by contraction and expansion during a freeze-thaw cycle: a membrane perspective. In Morris GJ and Clarke A (eds): Effects of Low Temperatures on Biological Membranes. New York, academic Press, 1981. pp. 307-322.

Figure 4.1. User interface of the CrySim3 computer simulation program. Fields allow for different conditions and parameters of cryopreservation.

Table 4.1. Baseline cell and osmotic parameters used to examine their effects on cell kinetics of an arbitrary cell.

Cell parameters	Osmotic Parameters	
V_{iso} = 3000 um3	T_{ref} = 0°C	
V_b = 0.400	L_p = 0.200	$E_a(L_p)$ = 10
C_{iso} = 0.3	P_s = 0.400	$E_a(P_s)$ = 20
Variable surface area	sigma = 1	

Initial Conditions	Rate Segments
Extracellular	Start temp. = 22°C
Imperment = 0.9 Osm/kg	
Permeant = 0 molal	Step 1: Hold for 5 min
Intracellular	
Imperment = 0.3 Osm/kg	
Permeant = 0 molal	

94
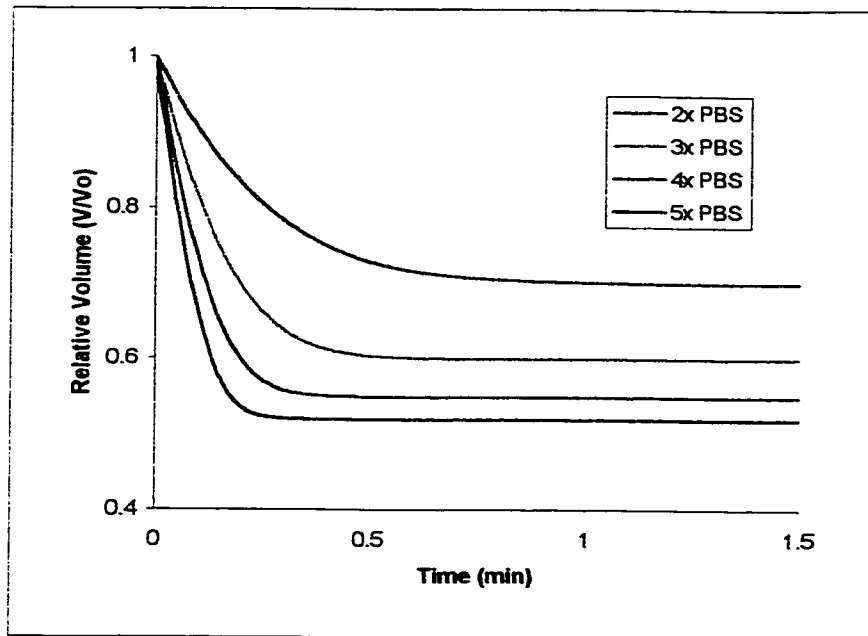
Figure 4.2. Simulated kinetics of endothelial cells exposed to hypertonic PBS solutions at 22°C. Simulation parameters based upon those in Chapter 2.
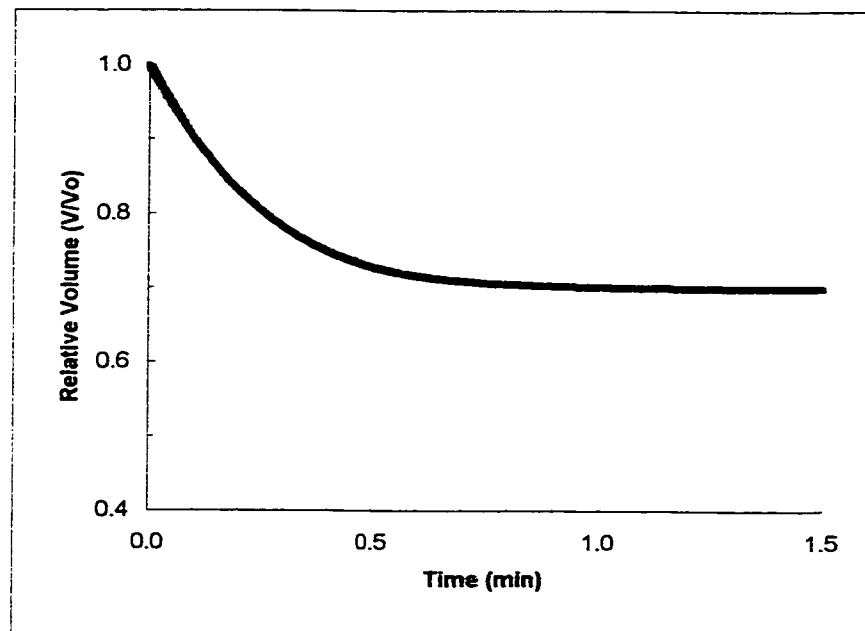

Figure 4.3. Determination of V_b and L_p from simulated kinetics of endothelial cells in 2x PBS solution at 22°C.
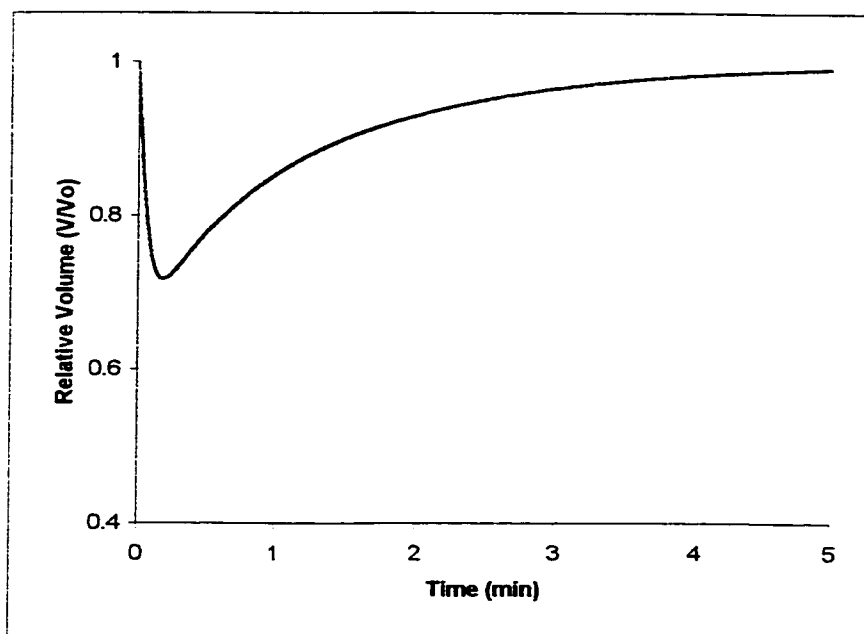Vb = 0.435, Lp = 0.399 um/min/atm

Figure 4.4. Simulated kinetic of fibroblasts exposed to 1M DMSO at 22°C. Simulation parameters based upon those in Chapter 2.
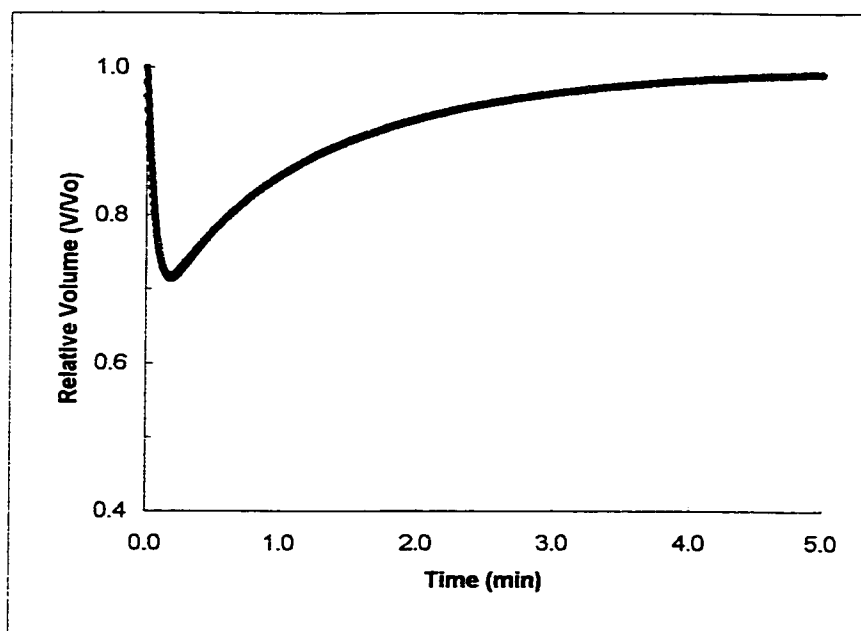

Figure 4.5. Determination of L_p and P_s from simulated kinetics of fibroblasts exposed to 1M DMSO at 22°C.
Lp = 0.460, Ps = 7.99 um/min

96

Table 4.3. Values of P_s and E_a used to simulate volume kinetics of cryoprotectant removal.

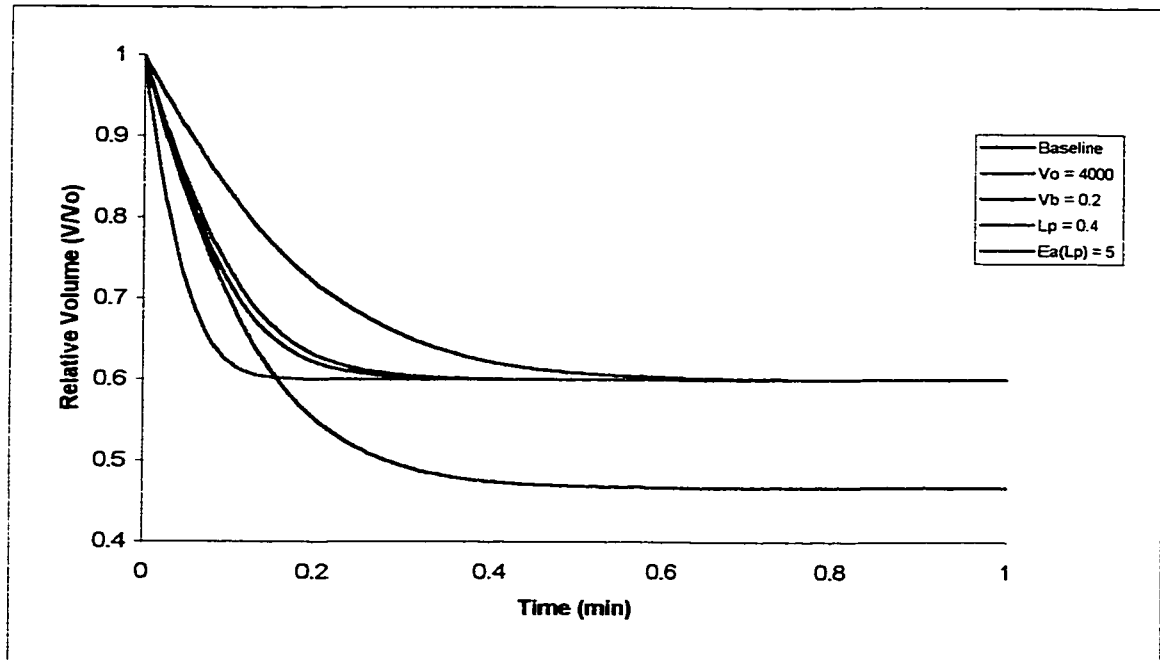|		Set 1: 'removal' experiments		Set 2: 'addition' experiments	
		P_s (um/min)*	E_a (kCal/mol)	P_s (um/min)*	E_a (kCal/mol)
Endothelial	DMSO	0.710	18.8	0.473	28.2
	PG	0.411	25.4	0.724	22.7
Fibroblast	DMSO	1.701	16.2	0.329	23.2
	PG	1.137	11.9	0.143	29.1

*Referenced to $0^{\circ}C$

97

Figure 4.6. Effect of changes to cell and osmotic parameters on cell kinetics of a cell having initial parameters in Table 4.1 and in 3x isotonic PBS.
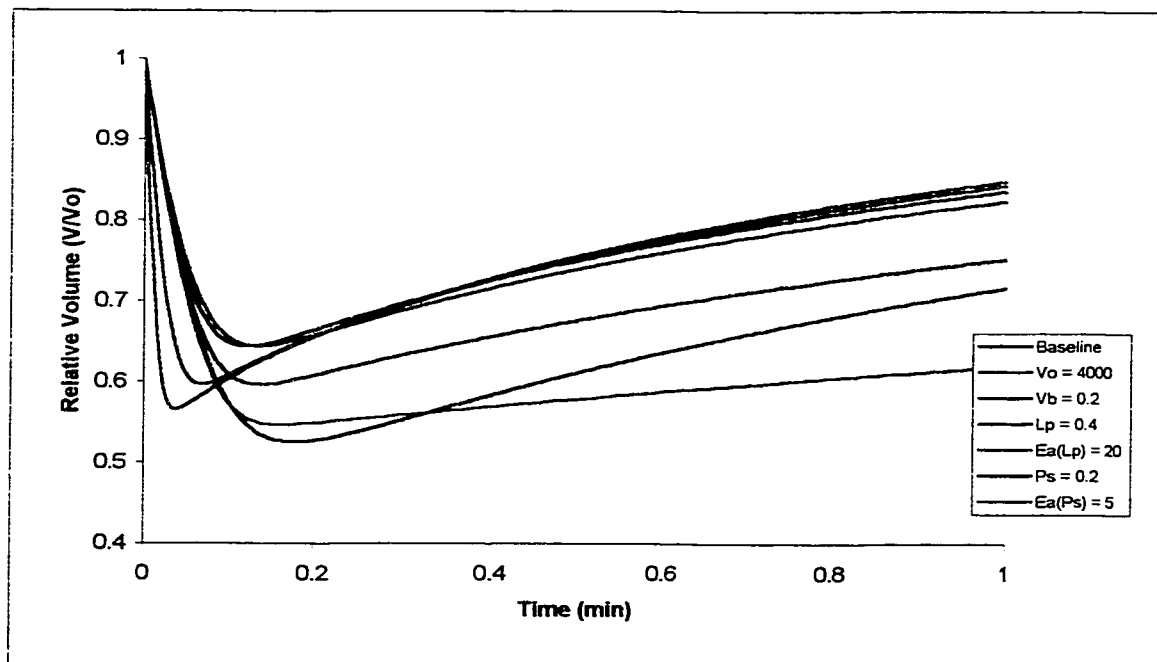

Figure 4.7. Effect of changes to cell and osmotic parameters on cell kinetics of a cell having initial parameters in Table 4.1 and in 1M DMSO.
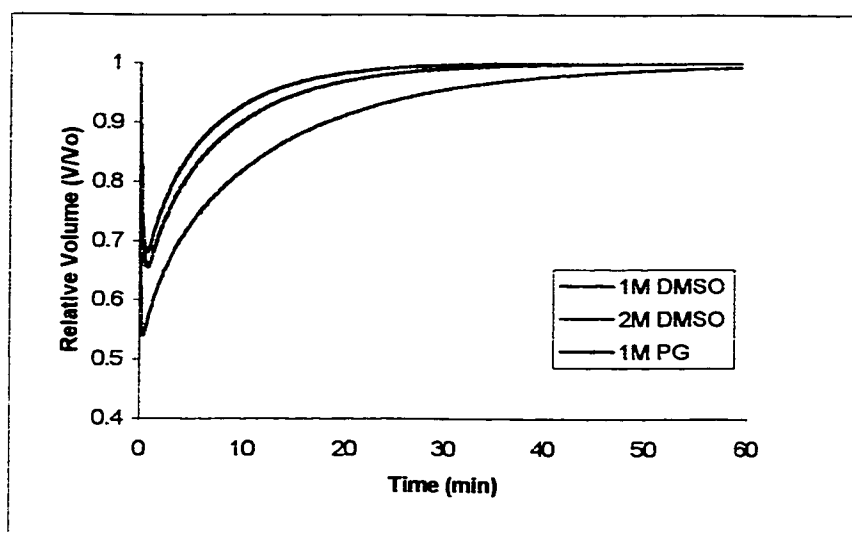
98

Figure 4.8. Equilibration during addition of cryoprotectants to endothelial cells at 4°C.
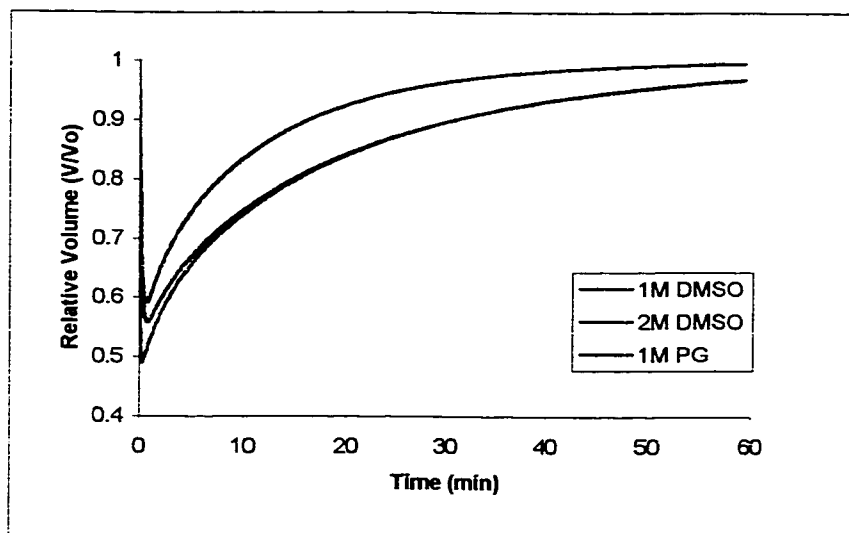

Figure 4.9. Equilibration during addition of cryoprotectants to fibroblasts at 4°C.

Table 4.2. Equilibration time (min) of endothelial cells and fibroblasts exposed to cryoprotectants at 4°C. Cells are equilibrated at 99% isotonic volume or at 99% intracellular cryoprotectant concentration.

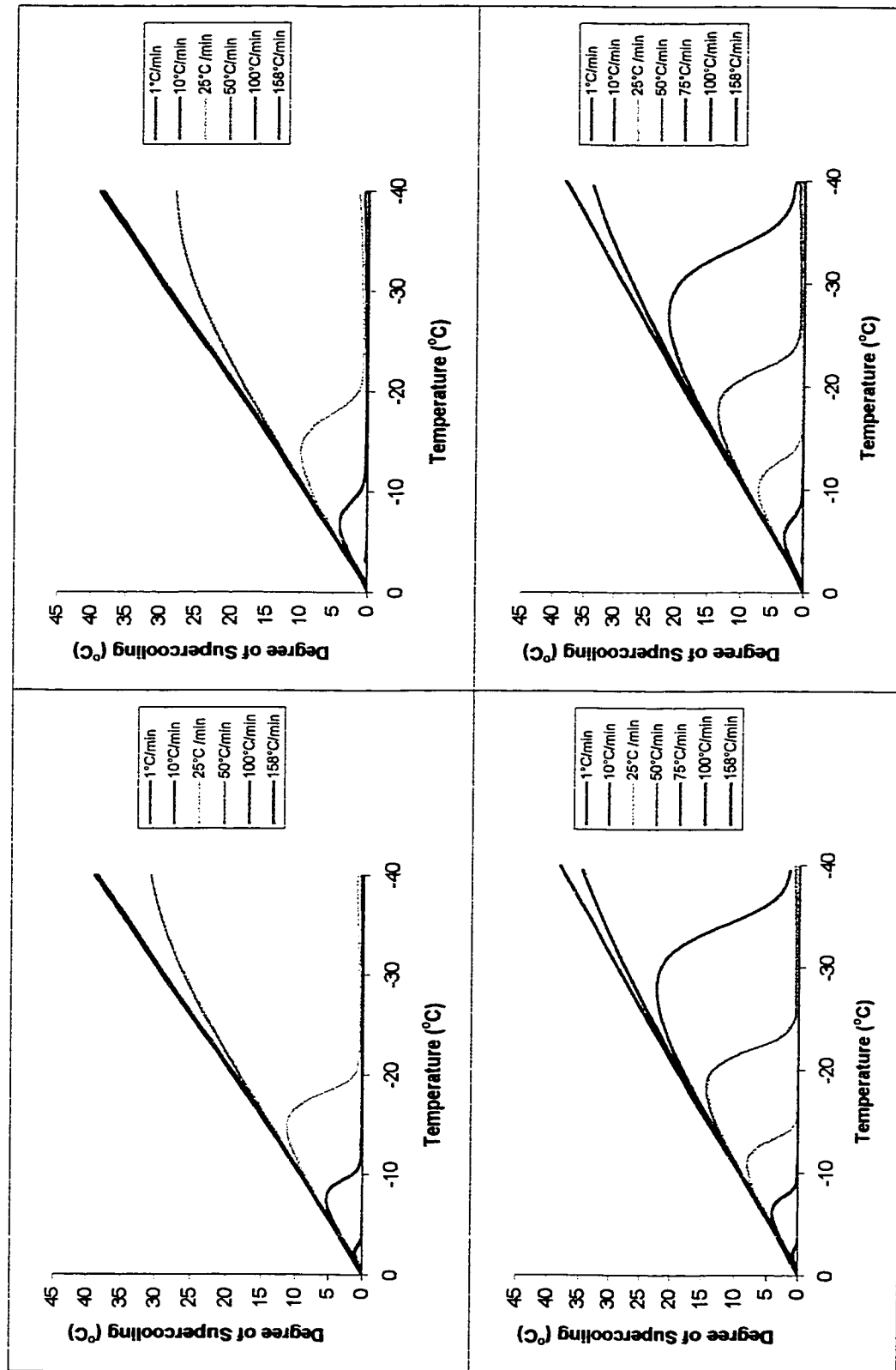|	Endothelial		Fibroblast	
	Volume	[CPA]	Volume	[CPA]
1M DMSO	30.4	19.6	48.7	33.1
2M DMSO	54.2	24.4	60+	42.1
1M PG	24.3	15.1	60+	60+

Figure 4.10. Degree of supercooling at varying cooling rates. Endothelial cells (top graphs) and fibroblasts (bottom graphs) with (right) and without (left) 1M DMSO in the cryoprotectant solution were determined from computer simulations.
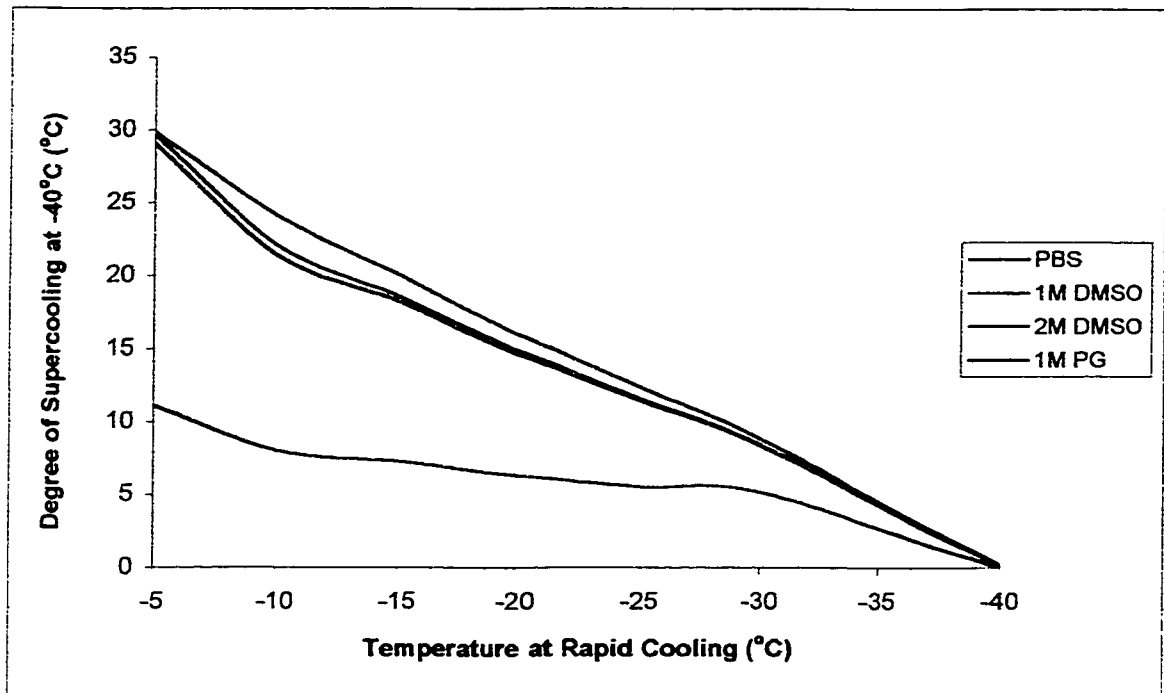
Figure 4.11. Degree of supercooling of endothelial cells at -40°C after simulated graded freezing in PBS, DMSO, and PG solutions.
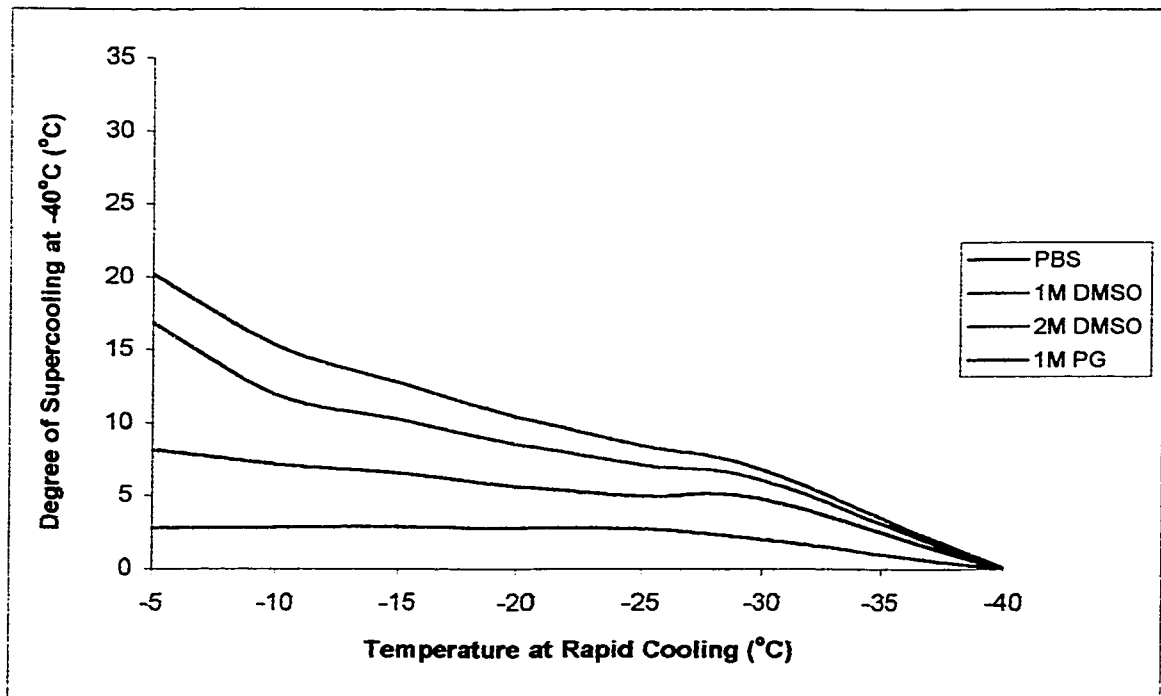

Figure 4.12. Degree of supercooling of fibroblasts at -40°C after simulated graded freezing in PBS, DMSO, and PG solutions.
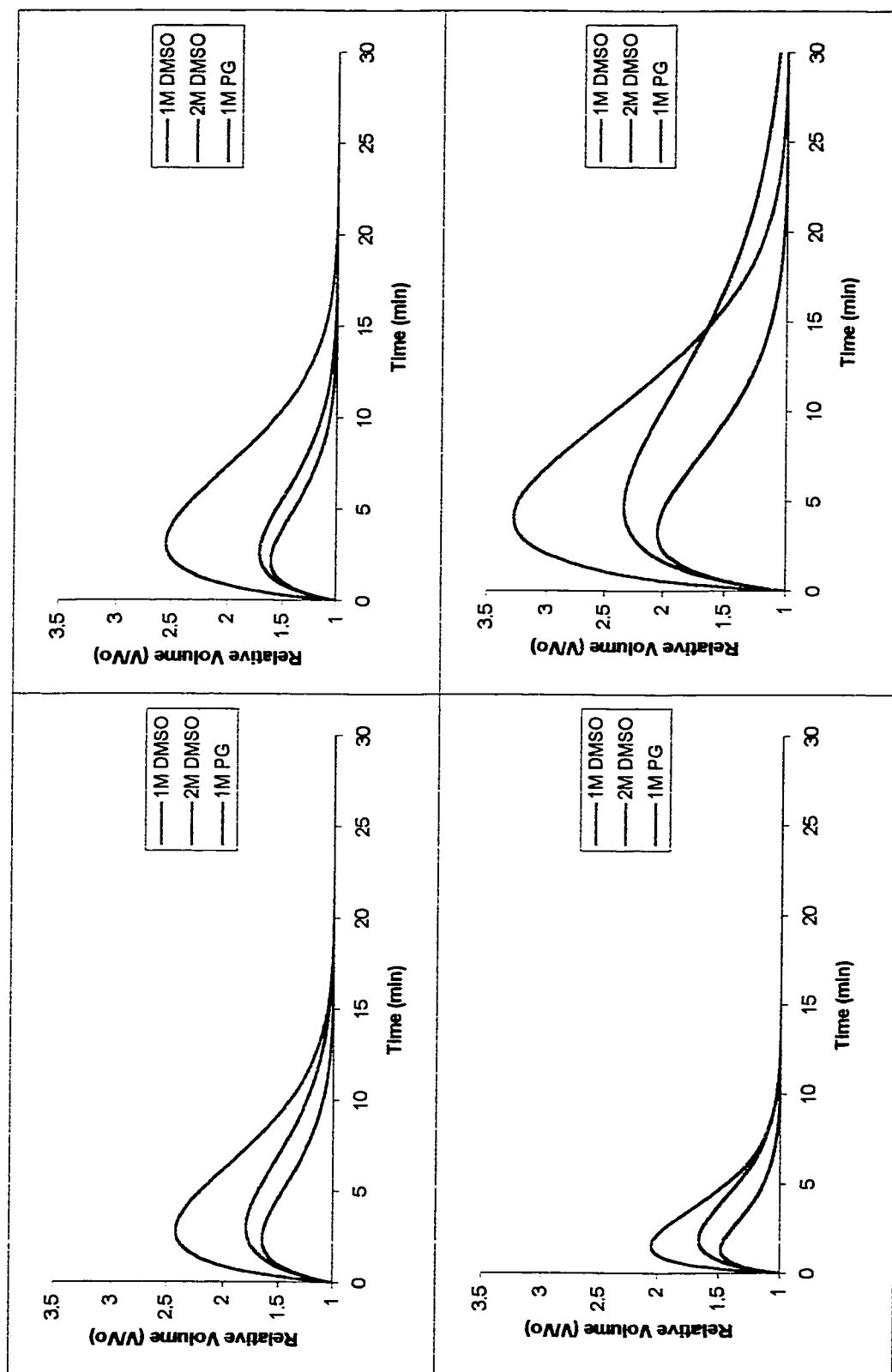
Figure 4.13. Relative volumes of endothelial cells (top graphs) and fibroblasts (bottom graphs) during removal of cryoprotectants at 4°C based on values of Ps and Ea from the removal of CPAs (left) or addition of CPAs (right) as determined in Chapter 2.
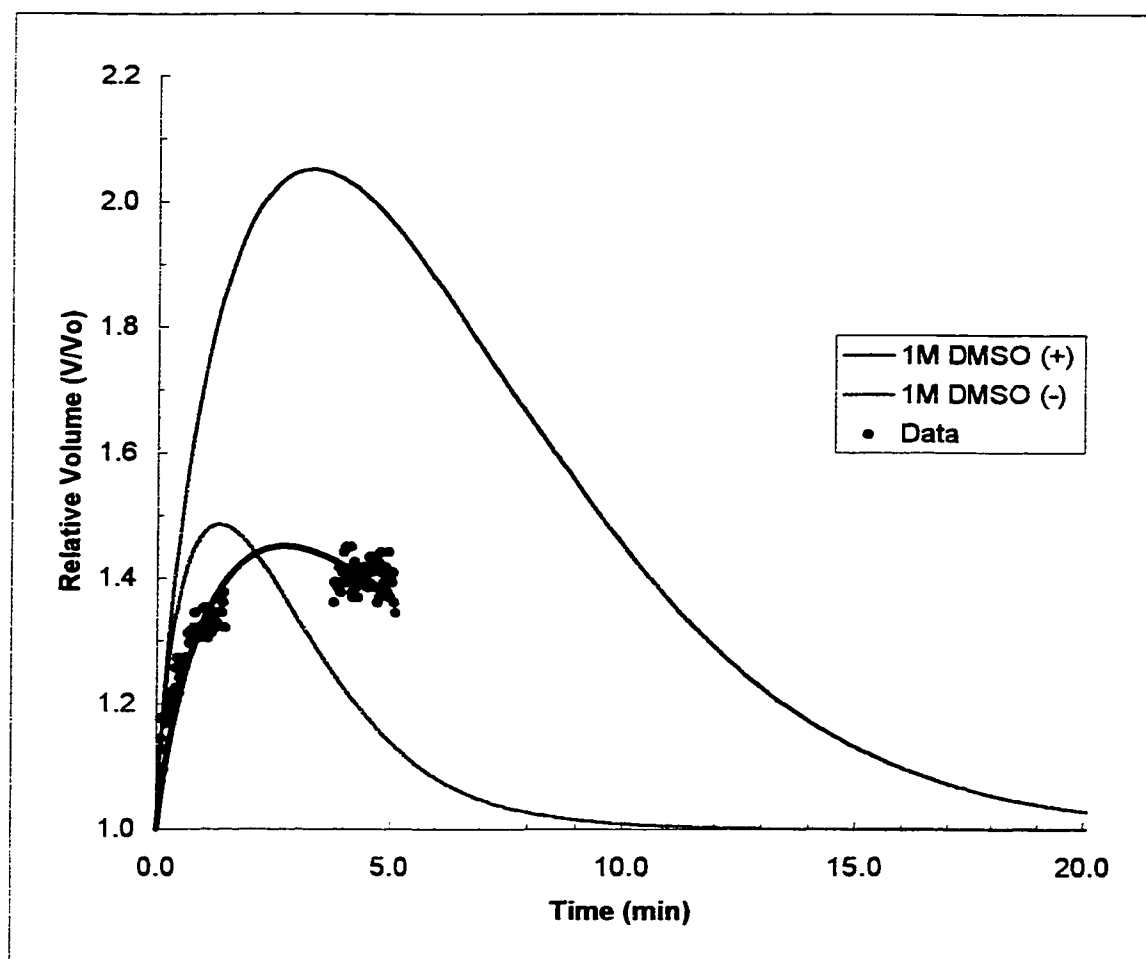
Figure 4.14. Comparison of simulated removal of 1M DMSO from fibroblast cells with experimental data. Removal of 1M DMSO was done at 4°C. (+) based on values from addition of CPAs in Chapter 2; (-) based on values from removal of CPAs in Chapter 2.

Table 4.4. Removal time (min) for endothelial and fibroblast cells after returning to isotonic conditions at 4°C post-thaw. Cryoprotectants are removed when cells are at 101% isotonic volume or at 1% intracellular cryoprotectant concentration. Times were based on values of P_s and E_a from the removal of CPAs data.

	Endothelial		Fibroblast	
	Volume	[CPA]	Volume	[CPA]
1M DMSO	15.2	8.4	9.1	3.8
2M DMSO	18.4	9.6	11.6	4.2
1M PG	18.1	12.5	11.7	6.7

CHAPTER 5

GENERAL CONCLUSIONS

5.1. Review of Thesis Objectives

The objective of this thesis was to investigate the osmotic parameters of endothelial cells and fibroblasts isolated from porcine heart valve leaflets during conditions of cryopreservation. The experimentally determined parameters were then used in computer simulations to model and predict cellular response in various other cryopreservation conditions. Correlating graded freezing simulations experimental data from graded freezing provided information about the limits of cellular viability in heart valves after cryopreservation. The limits can be used to set guidelines for optimal cryopreservation.

5.2. General Conclusions

Our current understanding of cryopreservation has been founded on principles developed by studies of cells in suspension. In examining cryopreservation of tissues, the complexity of interactions of cells with the environment has increased. Heart valve leaflets are relatively small tissues, but this investigation has established another form of cellular damage. Exclusion of solutes during extracellular ice formation in a tissue causes increased solute concentration localized to the centre of the tissue. This has been termed "solute centralization". As ice penetrates into the tissue from the exposed surfaces, solutes are excluded from the ice front. Consequently, solutes begin to concentrate at inner depths of the tissue. High solute

104

concentrations damage cells in suspension. Further increases in solute concentration would lead to greater degrees of damage to more cells in tissue systems. This phenomenon is magnified and more problematic for larger tissues and organs, as higher solute concentrations result from ice formation.

This thesis has also demonstrated the concept of selective preservation. Graded freezing experiments with 1M DMSO have shown that endothelial cells had reduced recovery compared to fibroblasts. For heart valves this can be beneficial since previous studies indicate that endothelial cells of heart valves initiate an immunological response. Eliminating endothelial cells with cryopreservation may improve the life span of heart valves after transplantation. However, improving the life span of heart valves also requires fibroblast viability. Yet, maximizing fibroblast recovery while reducing endothelial cell recovery requires an understanding of the cellular responses during cryopreservation.

This investigation has determined the parameters of cellular osmotic responses for endothelial cells and fibroblasts. For these two cell types, the hydraulic conductivity and solute permeability are the major differing factors to consider. The hydraulic conductivity for endothelial cells were determined to be lower than that of fibroblasts at 0°C and the difference in hydraulic conductivity would continue to increase as temperature decreased. This implies that during cryopreservation, the cell volume would be greater for endothelial cells than fibroblasts. With 1M DMSO, solute permeability at 0°C was greater for endothelial cells, but the activation energy indicates that the

solute permeability for endothelial cells will be lower at some temperature below 0°C. During cryopreservation, the decreased solute permeability with the decrease in temperature causes endothelial cells to respond slower to osmotic changes than fibroblasts. Once these parameters were established for endothelial cells and fibroblasts of heart valve leaflets, computer modeling allowed us to predict cellular response under various conditions during cryopreservation.

Modeling cellular response of endothelial cells and fibroblasts in this study indicate substantial differences under identical conditions. Naturally, these differences can be used to achieve the demonstrated selective preservation more effectively. Simulations using various cooling rates showed endothelial cells to undergo greater degrees of supercooling. This was true for cells in either PBS or 1M DMSO. The greater degree of supercooling was a result of the lower hydraulic conductivity and lower DMSO permeability at the sub-zero temperatures used during cryopreservation.

From the data and results in this study, we offer two recommendations to improve overall heart valve viability. Firstly, equilibrating the addition of 1M DMSO should be performed in 35 min to reduce the exposure time of cells to high solute concentrations. This reduces the toxic effects of DMSO on fibroblasts in order to retain high recovery of viability. We also recommend that the cryopreservation protocol be adapted such that heart valves are cooled at 25°C/min to -15°C then immediately immersed and stored in liquid nitrogen. This protocol takes advantage of the higher degree of supercooling

in endothelial cells with these conditions. The greater degree of supercooling increases the likelihood of intracellular ice formation and this is potentially damaging to the cell. This would be ideal if endothelial cells are damaged while fibroblasts are preserved since eliminating the endothelial cells will reduce rejection.

Of course, these adaptations to the current cryopreservation protocol for heart valves need to be validated in future research. Subsequent investigations should also attempt to extend the knowledge from these studies to human heart valves. Findings from this and other research will extend our understanding of tissue cryopreservation thus allowing us better procedures to potentially establish tissue and organ banks.

The findings of this thesis will hopefully advance and initiate further investigations of tissue preservation using a variety of techniques. For medical purposes, the cryopreservation of tissues and organs needs to be the focus. However, the successful replacement tissue or organ may not necessarily require preservation of all cells, as may be the case with heart valves. Perhaps we need to adapt our thinking of cryopreservation with regards to tissues and organs.
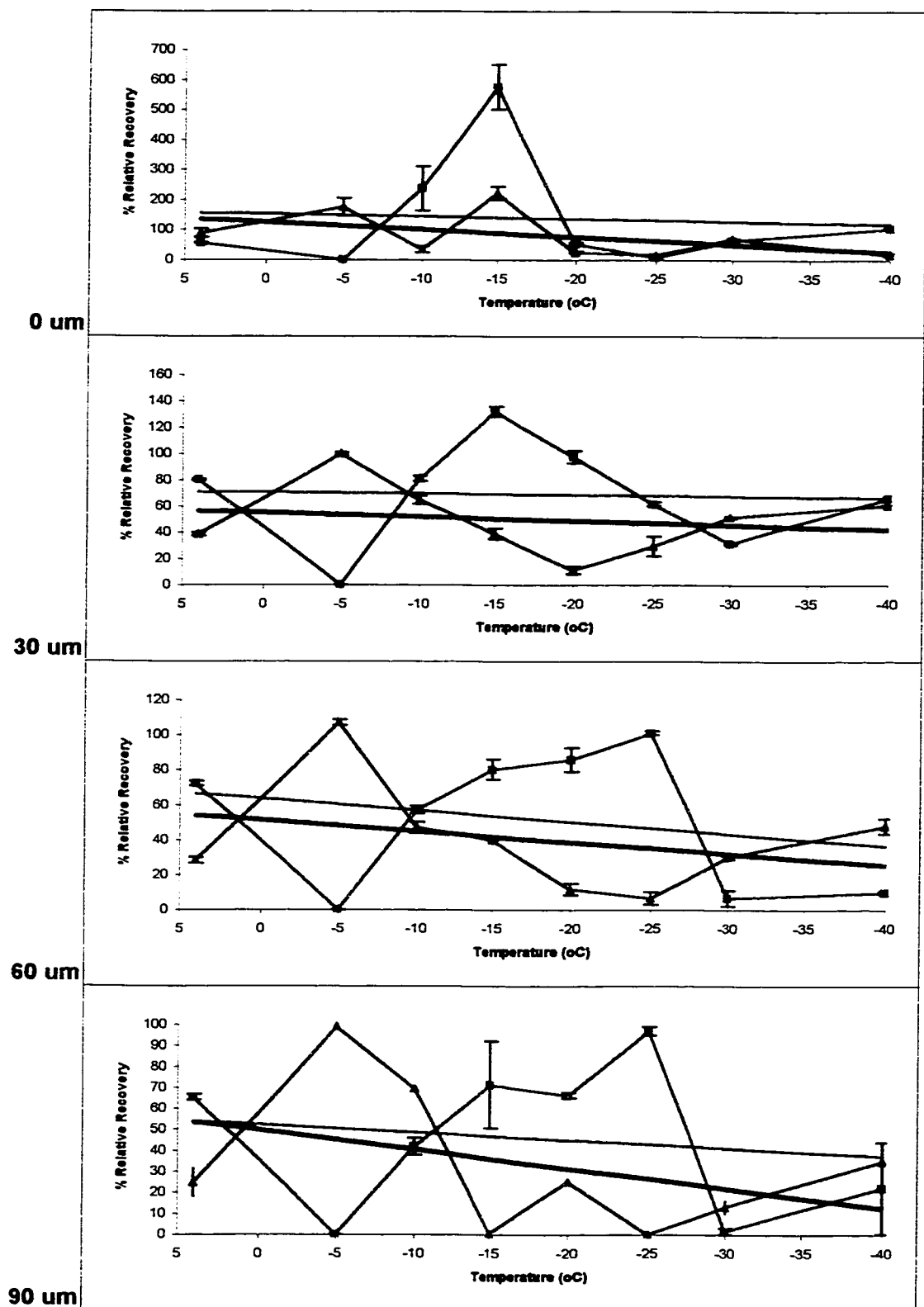
0 um

30 um

60 um

90 um
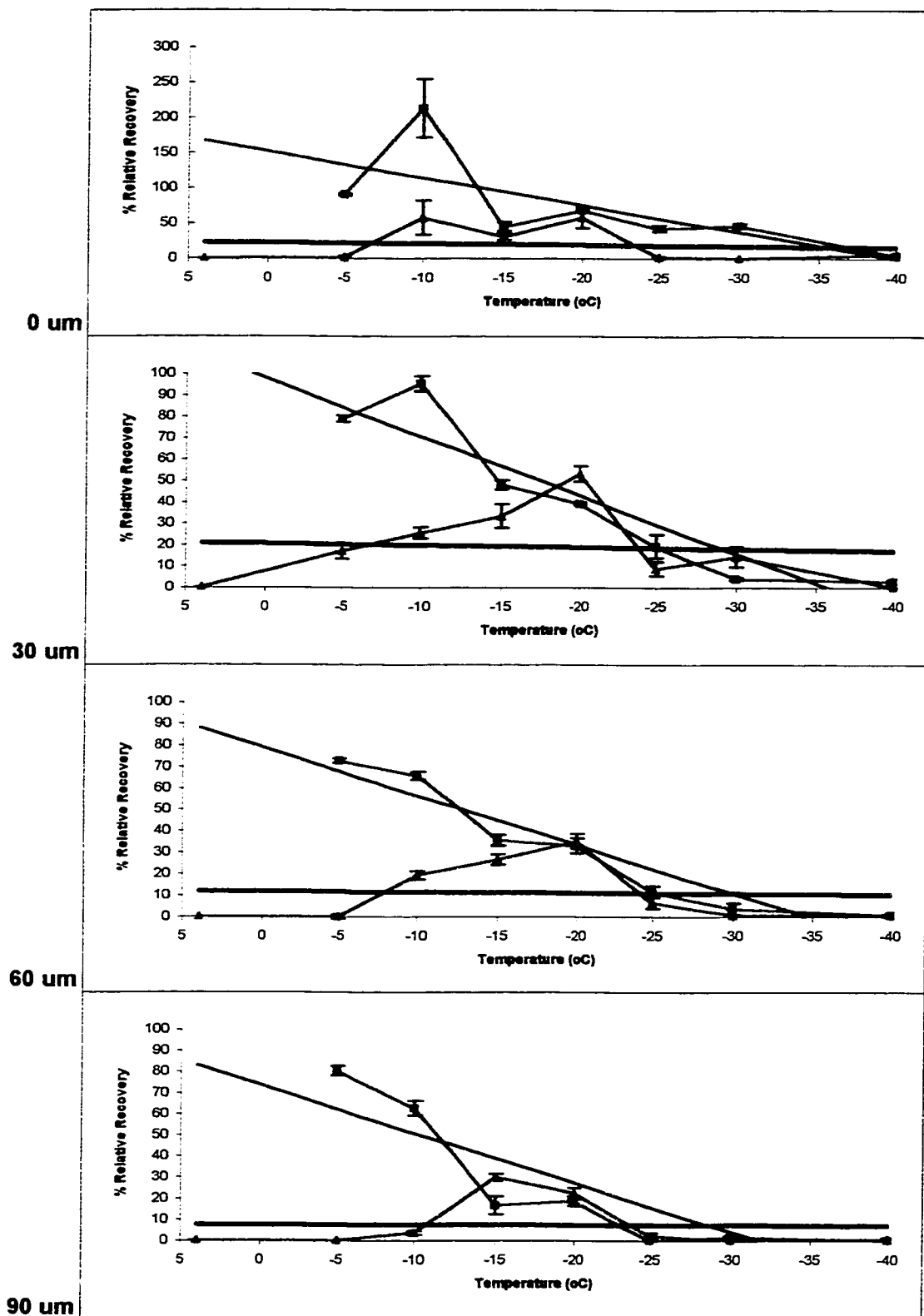
Appendix I.a Graded freezing of intact porcine heart valve leaflets in isotonic PBS.
Relative recoveries determined by confocal microscopy at depths of 0, 30, 60 and 90 um.
Thin black line-trendline for thawed (blue);Thick black line-trendline for plunged (green).
Data points represent mean ± standard error for samples (n = 3).

108

0 um

30 um

60 um

90 um
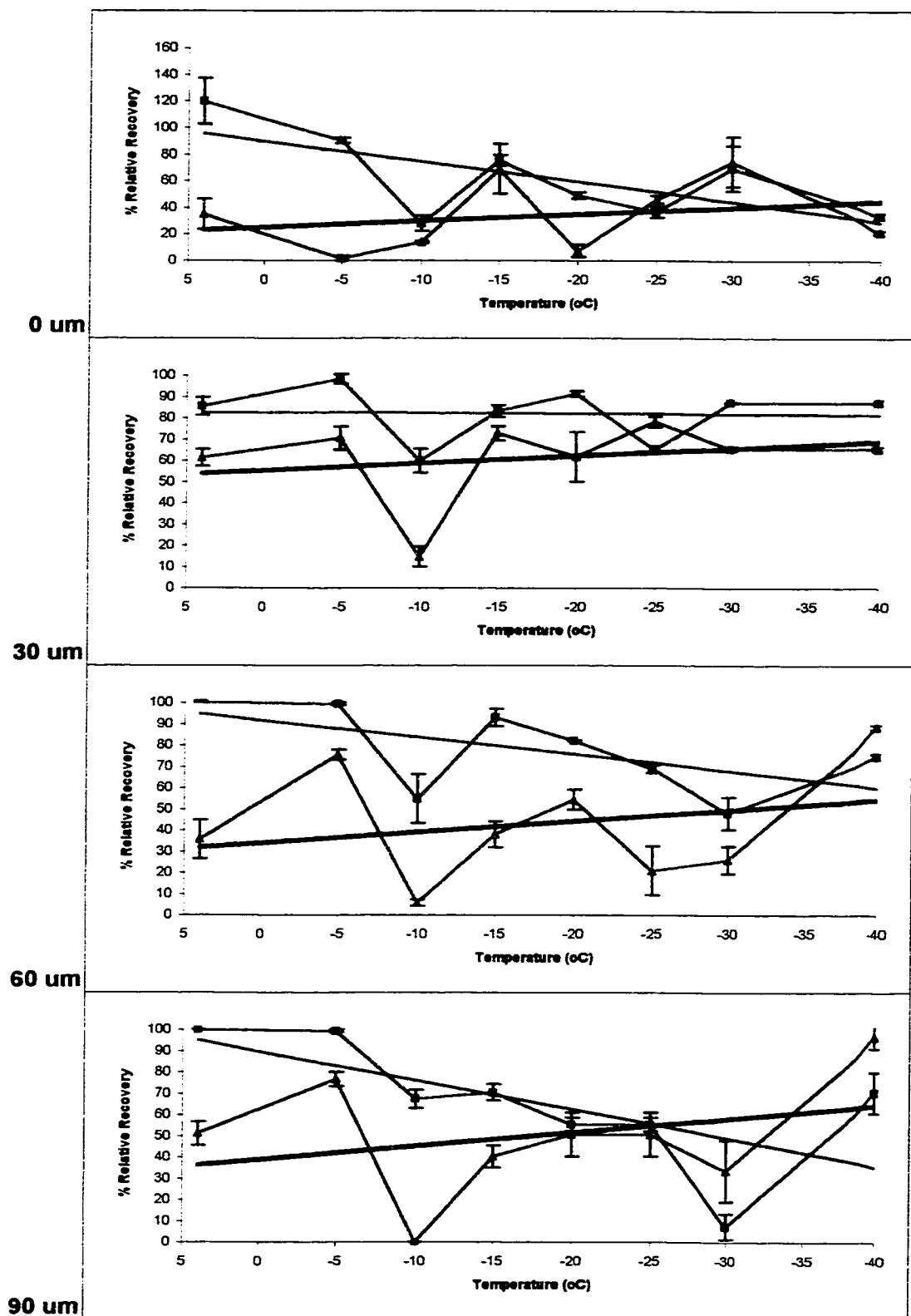
Appendix I.b Graded freezing of intact porcine heart valve leaflets in 1M DMSO.
Relative recoveries determined by confocal microscopy at depths of 0, 30, 60 and 90 um.
Thin black line-trendline for thawed (blue);Thick black line-trendline for plunged (green).
Data points represent mean ± standard error for samples (n = 3).

109

0 um

30 um

60 um

90 um
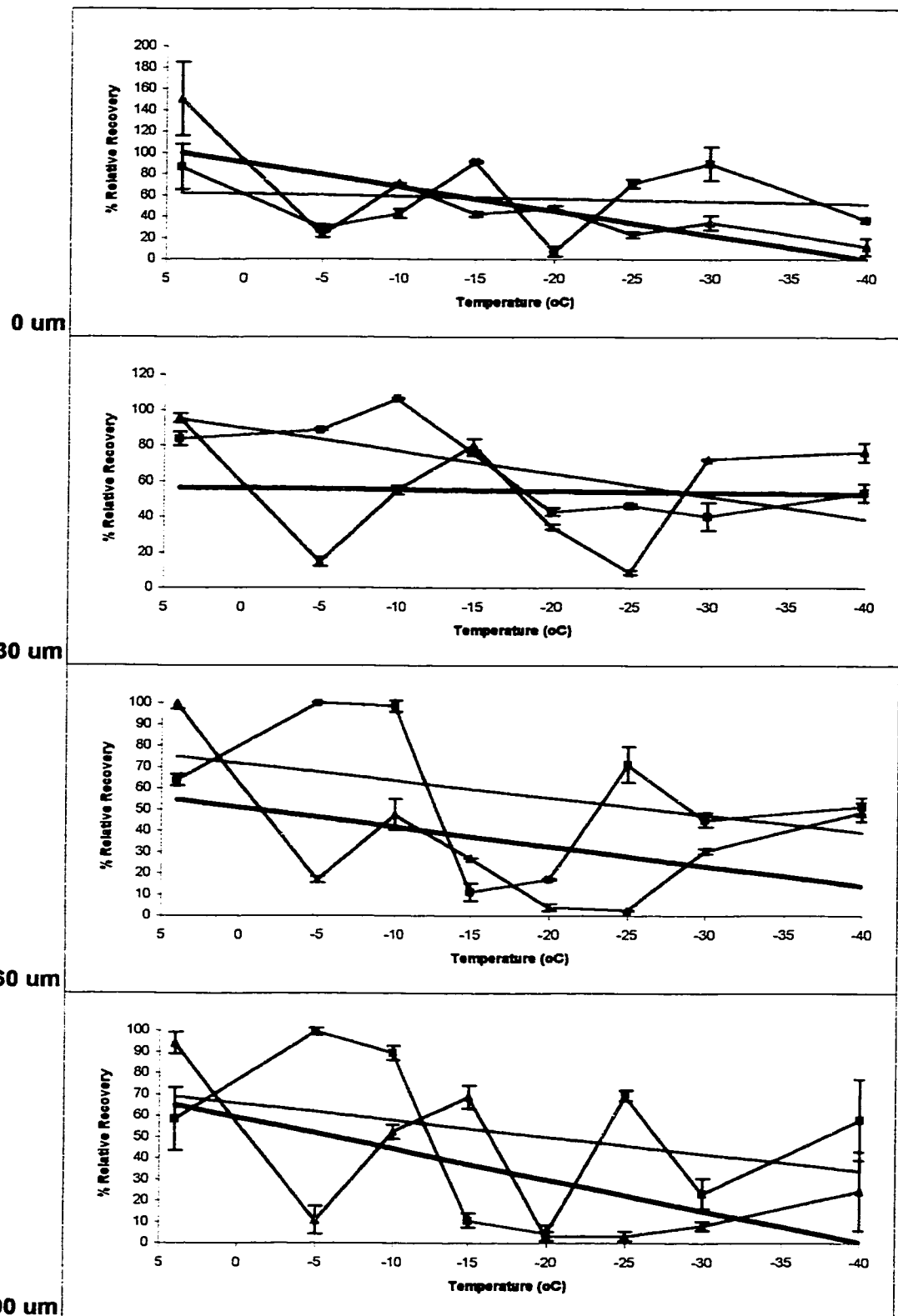
Appendix I.c Graded freezing of intact porcine heart valve leaflets in 2M DMSO.
Relative recoveries determined by confocal microscopy at depths of 0, 30, 60 and 90 um.
Thin black line-trendline for thawed (blue);Thick black line-trendline for plunged (green).
Data points represent mean ± standard error for samples (n = 3).

110

0 um

30 um

60 um

90 um

Appendix I.d Graded freezing of intact porcine heart valve leaflets in 1M PG.
Relative recoveries determined by confocal microscopy at depths of 0, 30, 60 and 90 um.
Thin black line-trendline for thawed (blue);Thick black line-trendline for plunged (green).
Data points represent mean ± standard error for samples (n = 3).

Appendix II. Quadratic function of freezing-point depression curve-fit data. $T_{fp}=Am+Bm^2$; T_{fp} is freezing-point depression in degrees C, A and B are constants, and m is solute molality.

	NaCl	KCl	DMSO	Glycerol	PG	EG
A	3.165	3.239	1.832	2.012	1.700	2.086
B	0.161	0.000	0.159	0.020	0.153	0.007